

# **Association of bacterial respiratory complexes**

Dissertation  
zur Erlangung des Doktorgrades  
der Naturwissenschaften

vorgelegt im Fachbereich  
Biochemie, Chemie und Pharmazie  
der Johann Wolfgang Goethe-Universität  
in Frankfurt am Main

von  
Mohd Khalid Siddiqui  
aus Lucknow, Indien

Frankfurt am Main 2006

(DF1)

vom Fachbereich Biochemie, Chemie und Pharmazie  
der Johann Wolfgang Goethe-Universität als Dissertation angenommen.

Dekan: Prof. Dr. H. Schwalbe

Gutachter: Prof. Dr. B. Ludwig

Prof. Dr. T. Prisner

Datum der Disputation

Diese Doktorarbeit wurde vom 17. Februar 2002 bis zum 28 August 2006 unter Leitung von Prof. Dr. Bernd Ludwig in der Abteilung für Molekulare Genetik, Institut für Biochemie der JW Goethe Universität Frankfurt am Main durchgeführt.

#### Eidesstattliche Erklärung

Hiermit versichere ich, dass ich die vorliegende Arbeit selbständig angefertigt habe und keine weiteren Hilfsmittel und Quellen als die hier aufgeführten verwendet habe.

Mohd Khalid Siddiqui

Frankfurt am Main, den 31. August 2006

## Table of contents

|   |           |
|---|-----------|
| <b>Summary .....</b>  | <b>I</b>  |
| <b>Zusammenfassung .....</b>  | <b>V</b>  |
| <b>1. Introduction .....</b>  | <b>1</b>  |
| 1.1 Oxidative phosphorylation .....                                   | 1         |
| 1.2 Electron transport chain of <i>Paracoccus denitrificans</i> ..... | 2         |
| 1.3 Structures of the respiratory chain complexes .....               | 3         |
| 1.3.1 NADH:ubiquinone oxidoreductase .....                            | 5         |
| 1.3.2 Succinate:ubiquinone oxidoreductase .....                       | 5         |
| 1.3.3 Ubiquinone:cytochrome <i>c</i> oxidoreductase .....             | 6         |
| 1.3.4 Cytochrome <i>c</i> oxidase .....                               | 6         |
| 1.4 Arrangements of the complexes .....                               | 7         |
| 1.4.1 Solid state or supercomplex model .....                         | 8         |
| 1.4.2 Random diffusion model .....                                    | 9         |
| Objectives of this dissertation .....                                 | 12        |
| <b>2. Materials and Methods .....</b>                                 | <b>15</b> |
| 2.1 Suppliers .....   | 15        |
| 2.2 Chemicals .....   | 15        |
| 2.3 Column chromatography .....                                       | 17        |
| 2.4 Proteins .....  | 18        |
| 2.5 Strains .....   | 18        |
| 2.6 Instruments .....   | 18        |
| 2.7. Experimental setup .....   | 19        |
| 2.7.1 FRAP and FCS .....  | 19        |
| 2.7.2 Pulsed EPR .....  | 19        |
| 2.7.3 Flash photolysis .....  | 19        |
| 2.8 Software .....  | 20        |
| 2.9 Solutions .....   | 20        |
| 2.9.1 Growth Medium .....   | 20        |
| 2.9.2 Antibiotics .....   | 22        |
| 2.9.3 Molecular biology .....   | 22        |
| 2.9.4 Protein estimation .....  | 24        |
| 2.9.5 Electrophoresis and Western-blot .....                          | 24        |
| 2.10 Molecular biology methods .....                                  | 32        |
| 2.10.1 Plasmid isolation .....  | 32        |
| 2.10.2 Competent <i>E. coli</i> cells .....                           | 32        |
| 2.10.3 Transformation .....   | 33        |
| 2.11 Growth of <i>P. denitrificans</i> .....                          | 33        |
| 2.12 Membrane preparation .....                                       | 33        |
| 2.12.1 Osmotic pressure method .....                                  | 33        |
| 2.12.2 Sonication method .....  | 34        |
| 2.12.3 Manton-Gaulin Press (MG) method .....                          | 34        |
| 2.12.4 Purification of membrane .....                                 | 35        |

|   |           |
|---|-----------|
| 2.13 Membrane vesicle size measurements.....  | 35        |
| 2.14 Expression and purification of respiratory protein complexes .....                       | 35        |
| 2.14.1 Cu <sub>A</sub> fragment.....  | 35        |
| 2.14.2 Cytochrome <i>c</i> <sub>552</sub> fragment.....                                       | 36        |
| 2.14.3 Cytochrome <i>c</i> <sub>1</sub> fragment .....  | 37        |
| 2.14.4 Cytochrome <i>c</i> <sub>552</sub> from <i>Thermus thermophilus</i> .....              | 37        |
| 2.14.5 Cytochrome <i>c</i> <sub>552</sub> (full length).....                                  | 38        |
| 2.14.6 Purification of cytochrome <i>c</i> oxidase.....                                       | 38        |
| 2.14.7 Isolation of <i>P. denitrificans</i> supercomplex .....                                | 39        |
| 2.15 Horse heart cytochrome <i>c</i> .....  | 39        |
| 2.16. Oxidation of cytochrome <i>c</i> and <i>c</i> <sub>552</sub> .....                      | 39        |
| 2.17 Fv fragment expression .....   | 40        |
| 2.18 Purification and labelling of Fv fragment.....   | 40        |
| 2.18.1 Labelling of Fv antibody fragment .....  | 40        |
| 2.18.2 Fluorescein isothiocyanate (FITC).....   | 41        |
| 2.18.3 Separation of labelled Fv fragment .....   | 41        |
| 2.18.4 Efficiency calculation .....   | 41        |
| 2.18.5 Procedure for labelling with Cy5 dye .....   | 41        |
| 2.18.6 Labelling of membranes.....  | 42        |
| 2.19 Protein quantification .....   | 42        |
| 2.20 Gel electrophoresis .....  | 42        |
| 2.20.1 SDS gel electrophoresis .....  | 42        |
| 2.20.2 Blue-Native (BN) polyacrylamide gel electrophoresis .....                              | 43        |
| 2.21 Reconstitution.....  | 43        |
| 2.21.1 Purification of asolectin .....  | 43        |
| 2.21.2 Bacterial lipid isolation .....  | 43        |
| 2.21.3 Method for reconstitution.....   | 44        |
| 2.22. Membrane fusion.....  | 45        |
| 2.22.1 Electroformation technique.....  | 45        |
| 2.22.2 Ca <sup>++</sup> induced fusion.....   | 45        |
| 2.22.3 Temperature and pH depend fusion .....   | 46        |
| 2.23 Method for negative staining.....  | 46        |
| 2.24 EPR spectroscopy .....   | 47        |
| 2.25 FRAP experiment.....   | 47        |
| 2.26 FCS experiment .....   | 48        |
| 2.27 Flash photolysis method .....  | 48        |
| <b>3. Results.....</b>  | <b>49</b> |
| 3.1 Expression and purification of proteins .....   | 49        |
| 3.1.1 Cu <sub>A</sub> fragment.....   | 49        |
| 3.1.2 Cytochrome <i>c</i> <sub>552</sub> fragment .....                                       | 51        |
| 3.1.3 Horse heart cytochrome <i>c</i> .....   | 51        |
| 3.1.4 Cytochrome <i>c</i> <sub>1</sub> fragment .....   | 52        |
| 3.1.5 <i>Thermus thermophilus</i> cytochrome <i>c</i> <sub>552</sub> .....                    | 53        |
| 3.1.6 Membrane bound cytochrome <i>c</i> <sub>552</sub> .....                                 | 53        |
| 3.1.7 Cytochrome <i>c</i> oxidase.....  | 54        |
| 3.2 EPR experiments .....   | 54        |
| 3.2.1 Relaxation measurement of the Cu <sub>A</sub> fragment with different cytochromes ..... | 54        |
| 3.2.2 Effect of ionic strength of buffer.....   | 57        |

|  |            |
|--|------------|
| 3.2.3 Effect of glycerol .....                                 | 58         |
| 3.2.4 Oxidation of cytochrome $c_{552}$ .....                  | 58         |
| 3.2.5 Concentration effect .....                               | 58         |
| 3.2.6 Temperature dependence .....                             | 59         |
| 3.3 Membrane purification .....                                | 60         |
| 3.4 Reconstitution .....                                       | 60         |
| 3.5 Size of the membrane vesicles .....                        | 61         |
| 3.6 Fusion of membrane .....                                   | 61         |
| 3.6.1 Electrofusion method .....                               | 62         |
| 3.6.2 $Ca^{++}$ induced fusion .....                           | 63         |
| 3.6.3 pH dependent fusion .....                                | 63         |
| 3.7 Deletion mutant .....                                      | 65         |
| 3.8 Translational diffusion experiments .....                  | 65         |
| 3.8.1 Expression and purification of Fv fragment .....         | 65         |
| 3.8.2 Fv fragment labelling by FITC .....                      | 66         |
| 3.8.3 Fv labelling by Cy5 dye .....                            | 68         |
| 3.8.4 Fluorescence Recovery after Photo bleaching (FRAP) ..... | 68         |
| 3.8.5 Fluorescence Correlation Spectroscopy (FCS) .....        | 70         |
| 3.8.6 Flash photolysis experiment .....                        | 72         |
| <b>4 Discussion .....</b>                                      | <b>74</b>  |
| 4.1 Spin relaxation measurements .....                         | 74         |
| 4.2 Reconstitution .....                                       | 78         |
| 4.3 Size of membrane vesicles .....                            | 79         |
| 4.4 Fusion of membrane vesicles .....                          | 80         |
| 4.5 Deletion mutant .....                                      | 81         |
| 4.6 Lateral diffusions experiments .....                       | 83         |
| 4.7 Flash photolysis .....                                     | 86         |
| <b>Outlook .....</b>   | <b>88</b>  |
| <b>Abbreviations .....</b>                                     | <b>89</b>  |
| <b>References .....</b>  | <b>91</b>  |
| <b>Acknowledgements .....</b>                                  | <b>107</b> |
| <b>Curriculum vitae .....</b>                                  | <b>109</b> |

## Summary

The mitochondrial respiratory chain consists of four membrane-embedded redox complexes: NADH:ubiquinone oxidoreductase (Complex I), succinate:ubiquinone reductase (Complex II), ubiquinol:cytochrome *c* oxidoreductase (Complex III), cytochrome *c* oxidase (Complex IV), and cytochrome *c* acting as an electron mediator between the last two complexes. The soil bacterium *Paracoccus denitrificans* has frequently been used in the past as a model system for structure and function of the mitochondrial respiratory chain complexes. In describing the interaction between these redox proteins in the membrane, Hackenbrock *et al.* (1986) presented a model of random diffusion. The first stable supercomplex from *P. denitrificans* was isolated by gel filtration containing Complex III and IV (Berry and Trumpower, 1985). In addition, supercomplexes were isolated from thermophilic bacteria (Sone *et al.*, 1987), yeast, mammalian (Schägger and Pfeiffer, 2001) and plant mitochondria (Eubel *et al.*, 2003). The work of Schägger and co-workers has provided clear evidence for stoichiometric assemblies of individual respiratory complexes in mitochondria by using Blue-Native gel electrophoresis after digitonin solubilization of membranes (Schägger and Pfeiffer, 2001). With this method, they also isolated a supercomplex from *P. denitrificans* containing complexes I, III, and IV with a stoichiometry of 1:4:4 and several copies of cytochrome *c*<sub>552</sub> (Stroh *et al.*, 2004). Based on these findings they suggested a model for the respiratory chain, ‘the respirasome’. Such respiratory supercomplexes may play crucial roles in substrate channelling, catalytic enhancement, protein complex stabilization and in generation of mitochondrial cristae morphology.

Different independent approaches were used to further analyze this situation in a native membrane environment, thus avoiding any perturbation caused by detergent solubilization: measuring the distance and orientation of the different complexes by multi-frequency EPR spectroscopy. We started to analyze the interaction between the Cu<sub>A</sub> fragment derived from *P. denitrificans* and various *c*-type cytochromes by Pulsed X-band (9 GHz) and G-band (180 GHz) EPR. Partner proteins for the Cu<sub>A</sub> (excess negative surface charge) were (i) horse heart cytochrome *c* which contains a large number of positive charges around the heme crevice, (ii) the cytochrome *c*<sub>552</sub> soluble fragment (physiological electron donor and positively charged around heme crevice), and as a control (iii) the cytochrome *c*<sub>1</sub> soluble fragment (negative surface potential, derived from *bc*<sub>1</sub> complex). For the binding studies by Pulsed EPR, longitudinal relaxation T<sub>2</sub> of Cu<sub>A</sub> was measured using a two-pulse echo sequence and recording the signal as a function of time  $\tau$  between the pulses. The Cu<sub>A</sub> fragment was

measured alone and in the presence of different cytochromes, cytochrome  $c_{552}$ , horse heart cytochrome  $c$  and  $c_1$  fragment. The measurements were performed at several magnetic field positions varying temperature between 5 to 25 K.

For orientation studies components of the anisotropic g-tensor can be resolved better using high-field EPR spectroscopy. For  $\text{Cu}_A$ , the  $g_x$  and  $g_y$  spectral components cannot be separated at X-band (9 GHz), but are fully resolved at G-band (180 GHz) frequency. Both measurements show the existence of a strong relaxation enhancement of the  $\text{Cu}_A$  by the specific binding of the *P. denitrificans* cytochrome  $c_{552}$  and horse heart cytochrome  $c$ . This relaxation enhancement is dependent on temperature and provides information about the distance and relative orientation of the two interacting spins within this transient protein complex.

For the first time Pulse EPR techniques have been successfully used for the study of a transient protein complex. The spectral division method provides pure dipolar relaxation traces, which can be analyzed quantitatively to obtain the structure of the protein-protein complex without the necessity of taking the intrinsic relaxation properties of the observed paramagnetic species into account. The structural parameters (distance between the two paramagnetic centers) obtained from fits to experimental data shows two different distances (simulated with two-fixed distance parameter). One distance was in the range of 18-23 Å and a second long distance was found with approximately 40 Å. The smaller distance reflects the specific binding site for biological electron transfer, although we cannot observe the electron transfer between these two proteins due their oxidised condition. The longer distances were ignored in the previous computational docking studies (Flöck and Helms, 2000; Bertini *et al.*, 2005) and the following parameters were taken into consideration: (a) the Fe-Cu distance should not be more than 18 Å for electron transfer, so the authors ignored the larger distance in their simulation (b) the electron was assumed to pass tryptophan (W121) and (c) the distance between the Fe atom and the basic patch of cytochrome  $c$  and the Cu atom and acidic patch on  $\text{Cu}_A$  fragment was considered.

In *P. denitrificans*, both cytochrome  $c_{552}$  and cytochrome  $c$  oxidase are membrane-embedded and integrated in a super-complex together with the  $bc_1$  complex and Complex I (Stroh *et al.*, 2004). Considering that the native cytochrome  $c_{552}$  has a membrane anchoring domain and an additional charged domain, it should be pointed out that these structural elements could further stabilize the supercomplex. The EPR approach for distance determination shows the possibility to apply relaxation methods to protein complexes, when more than two paramagnetic centers are involved. Our preliminary experiments on the complex of



cytochrome *c* with the four subunit detergent solubilised cytochrome *c* oxidase showed that the division method removes all the contributions of heme *a*, *a*<sub>3</sub>, and Cu<sub>B</sub> paramagnetic centers from oxidase to the Cu<sub>A</sub> signal and retains only the dipolar relaxation due to external cytochrome *c*. The next step would be to do this experiment in the presence of lipid membrane (reconstituted system) and larger protein complexes can be analysed to reach the goal of supercomplex like situation.

Alternative approach to prove the existence of supercomplexes in the native membrane is measuring the lateral diffusion of the complexes in the membrane plane by using fluorescence recovery after photo bleaching (FRAP), and fluorescence correlation spectroscopy (FCS). The lateral diffusion coefficients of the different complexes are dependent upon their masses (Reits and Neefjes, 2001). FRAP has been used in the past to determine the diffusion coefficients of the redox components ubiquinone, Complex III, cytochrome *c*, and cytochrome *c* oxidase in the mitochondrial inner membrane (Hochli *et al.*, 1985). The structure of the cytochrome *c* oxidase with the monoclonal antibody Fv fragment was determined by X-ray diffraction and shows the Fv fragment binds to the periplasmic side of cytoplasmic membrane of *P. denitrificans* (Ostermeier *et al.*, 1995; Ribrioux *et al.*, 1995). For the lateral diffusion measurements the labelling of the membrane was done in the two-step procedure; (a) labelling of the Fv fragments by binding of dye (Cy5 or FITC) which have surface exposed lysine residues (b) labelled Fv fragment were mixed with the native membrane and it binds with cytochrome *c* oxidase in the membrane. Therefore, this is an indirect labelling of the complex in membrane to measure the diffusion coefficient. The mass difference between Complex IV and supercomplex is more than 10 fold and FCS can determine its diffusion coefficient. The lateral diffusion should differ for wild type membranes and membranes isolated from deletion mutants lacking either Complex III or I. The initial measurement in a reconstituted system showed promising results. Due to smaller size of native membrane vesicles, it is not possible to do further experiments by FCS. Therefore different methods were tried to fuse native membranes to make giant membranes, such as Ca<sup>++</sup> induced fusion, low pH and electrofusion. After optimisation of different pH and Ca<sup>++</sup> concentration, the membranes were fused in the presence of asolectin at pH 6.0. The diameter of the fused membrane was measured with negative staining electron microscopy, and changed from 150 to 800 nm. Finally, lateral diffusion experiment was performed by FCS in the fused native membranes. Data analysis and calculation of diffusion coefficients are underway.

Further approach to get the quantitative information about respiratory complexes in the membrane by measuring the rotational diffusion of oxidase in the native membrane. Optical absorption spectroscopy at microsecond resolution was used to determine for the translational mobility of oxidase in membrane vesicles (Kawato and Kinoshita, 1981) and carbon monoxide (CO) used as a mobility probe for flash photolysis experiments. Experimental conditions were adjusted to get the optimal signal to monitor the reorientation of oxidase in the membrane plane. CO binds to the cytochrome *c* oxidase under reduced condition to the  $a_3$ -Cu<sub>B</sub> site and the effect was monitored in the Soret region of the spectra. The initial experiments were performed with oxidase in a reconstituted system. The experiment was carried out at different temperatures and varying incubation time of CO with oxidase. The data was analyzed with the method of Chizhov *et al.*, 1996. The rebinding kinetics of CO shows two time constant of 1  $\mu$ s and 20 ms. The 20 ms time will be used for the rotational measurement of oxidase in native membrane. The measurements also performed with the native membrane but due to low amount of oxidase in the membrane, the signal to noise ratio was high. To overcome this problem the cells were grown in methylamine medium and the membranes further purified by sucrose gradient centrifugation to get higher heme contents. After optimization, the next step would be to use non-polarized and polarized light to investigate the rotational mobility of complex organization in native membrane.

## Zusammenfassung

Die mitochondriale Atmungskette besteht aus vier membrangebundenen, redoxaktiven Proteinkomplexen: der NADH:Ubichinon Oxidoreduktase (Komplex I), Succinat:Ubichinon Oxidoreduktase (Komplex II), Ubichinol:Cytochrom *c* Oxidoreduktase (Komplex III) und Cytochrom *c* Oxidase (Komplex IV), sowie Cytochrom *c* als Elektronenüberträger zwischen den beiden letztgenannten Komplexen.

Das Bodenbakterium *Paracoccus denitrificans* wurde bereits in der Vergangenheit häufig als Modellorganismus für Struktur und Funktion der mitochondrialen Atmungskette herangezogen. Die Interaktion zwischen den oben genannten Proteinkomplexen wurde von Hackenbrock *et al.* 1986 mit dem *random diffusion* Modell beschrieben. Ein stabiler Superkomplex bestehend aus Komplex III und IV von *P. denitrificans* konnte erstmals durch Gelfiltration isoliert werden (Berry and Trumpower, 1985). Nachfolgend konnten Superkomplexe auch aus anderen Organismen, wie thermophilen Bakterien (Sone *et al.*, 1987), Hefe- und Säugetiermitochondrien (Schägger und Pfeiffer, 2001) sowie Pflanzenmitochondrien (Eubel *et al.*, 2003) isoliert werden. In den Arbeiten von Schägger *et al.* konnte mittels *blue-native* Gelelektrophorese nach Digitoninsolubilisierung die Assemblierung stöchiometrischer Superkomplexe in Membranen aus Mitochondrien gezeigt werden. Mittels dieser Methode konnte auch ein Superkomplex bestehend aus Komplex I, Komplex III und Komplex IV mit einer Stöchiometrie von 1:4:4 sowie einer unbestimmten Zahl von Cytochrome *c*<sub>552</sub>-Molekülen aufgereinigt werden (Stroh *et al.*, 2004). Aufgrund dieser Ergebnisse wurde das Modell des Respirasoms entwickelt, wobei den respiratorischen Superkomplexen eine wichtige Rolle bei der Stabilität der Einzelkomplexe, Substratkanalisierung und Umsatzsteigerung sowie bei der Bildung der Cristae in Mitochondrien zugeordnet wird.

Untersuchungen der Superkomplexe in nativen Membranen sind notwendig, da dabei der möglicherweise störende Effekt durch die Solubilisierung von Membranen vermieden wird. Diese Überlegungen bilden die Grundlage dieser Arbeit.

Ein Ansatz hierbei ist die Untersuchung der Abstände und Orientierungen zwischen den einzelnen Redoxzentren mittels *multi-frequency* EPR Spektroskopie. Aufgrund der großen Zahl der Redoxzentren in einem Superkomplex wurde zunächst mit einem einfachen System begonnen, wobei die Interaktionen zwischen dem löslichen Cu<sub>A</sub> Fragment der Cytochrom *c* Oxidase aus *P. denitrificans* und verschiedenen *c*-Typ Cytochromen mittels *Pulsed X band* (9 GHz) and G-Band (180 GHz) EPR untersucht wurden. Als Bindungspartner für das Cu<sub>A</sub>

Fragment mit negativer Oberflächenladung wurden (i) Cytochrom *c* aus Pferdeherzmitochondrien, (ii) das lösliche Cytochrom  $c_{552}$  Fragment aus *P. denitrificans* (positive Oberflächenladung) und (iii) als Kontrolle das lösliche Cytochrom  $c_1$  Fragment des Komplex III aus *P. denitrificans* (negative Oberflächenladung) verwendet. Für die Untersuchungen mit *Pulsed EPR* wurde die longitudinale Relaxation  $T_2$  des  $Cu_A$  Fragments gemessen, hierzu wurde eine *two-pulse echo* Sequenz verwendet und das Signal als Funktion der Zeit  $\tau$  zwischen den Impulsen aufgezeichnet. Die Messungen erfolgten mit dem  $Cu_A$  Fragment alleine und sequenziell mit den drei oben genannten Bindungspartnern bei verschiedenen Magnetfeldpositionen und in einem Temperaturbereich zwischen 5 und 25 K. Die Untersuchungen zur Orientierung können besser durch *high-field EPR* Spektroskopie durchgeführt werden, da hier eine höhere Auflösung der Komponenten des anisotropen  $g$ -Tensor möglich ist. Die spektralen Komponenten von  $g_x$  und  $g_y$  des  $Cu_A$  Fragments können nur im G-Band, jedoch nicht im X-Band aufgelöst werden. Messungen in beiden Bereichen zeigen temperaturabhängige Verstärkungen der Relaxation durch Bindung des Cytochrom  $c_{552}$  Fragments und des Cytochrom *c*. Das erhaltene Signal beinhaltet Informationen über den Abstand und die relative Orientierung der beiden im transienten Komplex wechselwirkenden Spins.

In diesen Experimenten konnten erstmals gepulste EPR Messungen von transienten Komplexen beobachtet werden. Die *division method* liefert reine dipolare Relaxationsspektren, die quantitativ ausgewertet werden können und so eine Aussage über die Struktur des Proteinkomplexes ermöglichen, ohne dass intramolekulare Wechselwirkungen der untersuchten paramagnetischen Zentren berücksichtigt werden müssen. Die erhaltenen Daten ergaben nach mathematischer Anpassung zwei unterschiedliche Datensätze für den Abstand zwischen den Zentren. Die Werte hierfür lagen einmal im Bereich zwischen 18-23 Å und um 40 Å. Der kleinere Abstand spiegelt die Situation im nativen Komplex wider bei der Elektronentransfer stattfinden kann, aufgrund der Redoxzustände der beiden Bindungspartner kann hier jedoch kein Elektronentransport beobachtet werden. Der größere Abstand wurde in vorangegangenen Modellrechnungen zur Komplexbildung ignoriert und nur die folgenden Parameter wurden in die Rechnungen mit einbezogen: (a) der Abstand zwischen Eisen und Kupfer, der 18 Å für einen erfolgreichen Elektronenübertrag nicht überschreiten darf, (b) die Rolle des Tryptophan 121 (W121) als Elektroneneintrittspunkt und (c) der Abstand zwischen den Atomen des basischen Bereichs des Cyt *c* und den Seitenketten des sauren Bereichs des  $Cu_A$  Fragments (Flöck and Helms, 2000; Bertini *et al.*, 2005).

Der oben erwähnte Superkomplex aus *P. denitrificans* beinhaltet auch Cytochrom  $c_{552}$ . Natives Cytochrom  $c_{552}$  liegt durch seinen Membrananker ebenfalls in der Membran gebunden vor und besitzt eine weitere geladene Domäne. Diese beiden Elemente tragen wahrscheinlich zur weiteren Stabilisierung des Superkomplexes bei.

Um dieser nativen Form Rechnung zu tragen, sollen weitere Experimente folgen, welche mit der vollständigen, in Lipiden rekonstituierten Oxidase und dem membrangebundenen Cytochrom  $c_{552}$  durchgeführt werden, so dass auch größere Komplexe untersucht werden können. Die oben genannten Experimente und Untersuchungen mit solubilisierter Oxidase haben gezeigt, dass die *division method* alle störenden Signale anderer, integraler, paramagnetischer Zentren entfernen kann. Ergebnisse in einem rekonstituierten System sind derzeit noch in der Durchführung und Auswertung.

Ein weitere Methode zur Untersuchung des Superkomplexes in nativen Membranen ist die laterale Diffusion des Komplexes in der Membranebene mittels *fluorescence recovery after photobleaching* (FRAP) oder *fluorescence correlation spectroscopy* (FCS) zu messen. Reits and Neefjes (2001) konnten zeigen, dass der laterale Diffusionskoeffizient von der Masse abhängig ist. Die Diffusionskoeffizienten von mehreren der Redoxkomponenten der mitochondrialen Atmungskette (Ubichinon, Komplex I, Komplex III, Cytochrom  $c$  und Cytochrom  $c$  Oxidase) konnten bereits mittels FRAP ermittelt werden (Hochli *et. al.*, 1985). Das zur Kristallisation der Cytochrom  $c$  Oxidase aus *P. denitrificans* verwendete Antikörperfragment ( $F_v$ ; Ostermeier *et al.*, 1995; Ribrioux *et al.*, 1995) bindet ebenfalls die in die Membran eingebettete Oxidase, so dass es zur Anfärbung der Oxidase in zwei Schritten wie folgt verwendet werden kann: (a) Ein Fluoreszenzfarbstoff (Cy5 or FITC) der an die Lysinseitengruppen auf der Oberflächens des  $F_v$  kovalent bindet wird mit dem  $F_v$  gemischt. (b) Das gereinigte, angefärbte  $F_v$  wird mit nativen Membranen gemischt und bindet an Komplex IV, wodurch dieser indirekt angefärbt wird. So kann die Diffusionskonstante bestimmt werden, da die Masse des Superkomplexes eine Größenordnung höher sein sollte als die des Komplex IV alleine. Dies soll mittels FCS im Wildtyp und in Deletionsstämmen, die entweder Komplex I oder Komplex III defizient sind, gemessen werden. Die ersten Ergebnisse mit einem rekonstituierten System sind viel versprechend, jedoch ist die Vesikelgröße der nativen Membranen mit 150 nm zu klein. Verschiedene Methoden der Membranfusion, wie Kalziuminduktion, niedriger pH-Wert und niedrige Temperatur oder Elektrofusion wurden im Rahmen der Optimierung durchgeführt. Die Membranfusion unter Zusatz von Asolectin bei pH 6,0 lieferte Vesikel mit einer Größe von 800 nm, wie im Elektronenmikroskop mittels *negative stain* gezeigt werden konnte. Im

Anschluß wurden die Experimente zur Bestimmung des lateralen Diffusionskoeffizienten mittels FCS durchgeführt. Die ermittelten Daten befinden sich momentan noch in der Bearbeitungsphase.

In einem weiteren Ansatz wurde ebenfalls versucht, quantitative Informationen über die Diffusionskonstante der Cytochrom *c* Oxidase in nativen Membranen zu erhalten. Hierzu wurde die Absorptionsspektroskopie genutzt, um mittels Kohlenmonoxid (CO) als Mobilitätssonde für die *flash* Photolyse die laterale Beweglichkeit der Cytochrom *c* Oxidase in Membranvesikeln (Kawato and Kinosita, 1981) zu bestimmen. Während der Optimierungsphase konnte eine Verbesserung der Aufnahme des Signals während der Oxidase Reorientierung erreicht werden. CO bindet an das binukleäre Zentrum der Cytochrom *c* Oxidase im reduzierten Zustand, was anhand der Soret-Bande im Spektrum verfolgt werden kann. Die ersten Versuche wurden mit in Phospholipiden rekonstituierter Cytochrom *c* Oxidase durchgeführt, wobei Temperatur, Kohlenmonoxid- und Dithionitkonzentrationen, welches zur Reduktion des Häm-Liganden dient, variiert wurden. Die erhaltenen Daten wurden wie bei Chizhov *et al.*, 1996 beschrieben analysiert, und die Kinetik der Rückbindung des CO liefert zwei Zeitkonstanten, 1  $\mu$ s und 20 ms. Die zweite wird für die Rotationsmessungen der Cytochrom *c* Oxidase in nativen Membranen verwendet. Diese Messungen wurden ebenfalls mit nativen Membranen wiederholt, jedoch war der Cytochrom *c* Oxidasegehalt zu niedrig, so dass das Hintergrundrauschen eine Auswertung nicht möglich machte. Um dieses Problem zu lösen, wurde *P. denitrificans* auf Methylaminmedium angezogen und die daraus gewonnen Membranen in einem Saccharosegradienten weiter ankonzentriert. Im nächsten Schritt sollen diese nativen Membranen mit polarisiertem Licht untersucht und die Diffusionseigenschaften des Komplexes bestimmt werden, um weitere Aussagen über die Organisationsstruktur treffen zu können.

# 1. Introduction

Two major energy sources are available to living organisms: respiration and photosynthesis. Electron transport chains are biochemical reactions that produce ATP, which is the energy currency of life. The cells of all eukaryotes contain intracellular organelles called mitochondria that produce ATP. Certain bacteria evolved into mitochondria, thus endowing the host cells with aerobic metabolism, a much more efficient way to produce energy than anaerobic glycolysis. Structurally, mitochondria have four compartments: the outer membrane, the inner membrane, the intermembrane space, and the matrix. They perform numerous tasks, such as pyruvate oxidation, the Krebs cycle, and metabolism of amino acids, fatty acids, and steroids, but the most crucial probably is the transduction to generate adenosine triphosphate (ATP), by means of the oxidative phosphorylation system.

## 1.1 Oxidative phosphorylation

The electron transport chain consists of four respiratory enzyme complexes arranged in a specific orientation in the inner mitochondrial or bacterial cytoplasmic membrane. The passage of electrons between these complexes releases energy that is stored in the form of a proton gradient across the membrane and is used by ATP synthase to make ATP from ADP and phosphate (Saraste, 1999; Schultz and Chan, 2001). Bacterial aerobic respiratory systems have greater diversity of electron transfer pathways than mitochondrial respiratory systems (John and Whately, 1975). Biochemical and molecular biological studies have provided ample evidence of a close resemblance between the aerobic respiratory chains of bacteria (e.g. *Paracoccus denitrificans*) and mitochondria with respect to their spectral, compositional, and functional properties. *P. denitrificans* has long been used as a model for the mitochondrial electron transport chain (Stouthamer, 1992). Its respiratory chain consists of NADH:ubiquinone oxidoreductase (Complex I), Succinate:ubiquinone oxidoreductase (Complex II), Ubiquinone:cytochrome *c* oxidoreductase (Complex III) or *bc<sub>1</sub>* complex, Cytochrome *c* oxidase (Complex IV), and F<sub>1</sub>F<sub>0</sub>-ATP synthase (Complex V). Complex I, III and IV serve as proton pumps, using the energy of electron transfer to perform the electrical work of translocating protons from the matrix to the inner mitochondrial space of the mitochondria or the bacterial periplasmic space to generate and sustain an electrochemical gradient across the inner membrane. Under normal physiological conditions, Complex V uses free energy released from the back flow of protons across the membrane to perform the

chemical work of producing ATP from ADP and inorganic phosphate (see Schultz and Chan, 2001).

## 1.2 Electron transport chain of *Paracoccus denitrificans*

Among bacteria, *Paracoccus denitrificans* is widely used to study the electron transport chain. *P. denitrificans*, a gram-negative, denitrifying bacterium present in soil, can grow aerobically in the presence of oxygen or anaerobic on nitrate. It was first isolated in 1908 (Beijerinck, 1910) as *Micrococcus denitrificans*. The original classification of this genus was based upon its ability to convert nitrate into molecular nitrogen. The genus *Paracoccus* is a member of the alpha *Proteobacteria* known as *Rhodobacter* group. It is also closely related to the physiologically well studied photosynthetic *Rhodobacter sphaeroides* and *Rhodobacter capsulatus* (Baker *et al.*, 1998). Most of the molecular biology analyses have been performed on the single strain *P. denitrificans* Pd1222 including a proposed promoter structure and related aspects of gene regulation (Steinrücke and Ludwig, 1991).

The branched respiratory chain of *P. denitrificans* provides an example of flexible electron routing towards oxygen (Figure 1). Under aerobic heterotrophic growth conditions, electrons originating from NADH dehydrogenase and succinate dehydrogenase can follow to three different types of terminal oxidases, two of which are cytochrome *c* oxidases (cytochrome *aa*<sub>3</sub> and cytochrome *cbb*<sub>3</sub>) and third is a quinol oxidase (cytochrome *ba*<sub>3</sub>). There are two branching points; the first is at ubiquinol (QH<sub>2</sub>), where electrons may flow to either the quinol oxidase or cytochrome *bc*<sub>1</sub>; the second is at the level of cytochrome *c*, where the electrons flow to either of the two cytochrome *c* oxidase. For production of ATP, the H<sup>+</sup>-ATPase complex requires an electrochemical proton gradient across the cytoplasmic membrane, which is obtained when charges (protons and electrons) are translocated across the membrane during respiratory electron transfer. The number of protons translocated per electron depends on the route followed by the electrons. Oxidation of the Q-pool via the pathway to cytochrome *aa*<sub>3</sub> results in the highest number of protons translocated per two electron (4H<sup>+</sup>/2e<sup>-</sup>) leading to the highest yield of ATP per reduced molecule of oxygen (Trumpower, 1991), while the other pathway to cytochrome *ba*<sub>3</sub> results in a lower number of protons translocated per two electron (2H<sup>+</sup>/2e<sup>-</sup>), because it bypasses cytochrome *bc*<sub>1</sub> (Puustinen *et al.*, 1989). The third terminal oxidase, cytochrome *cbb*<sub>3</sub>, can also accept electrons from the *bc*<sub>1</sub> complex and electrons flow to oxygen from QH<sub>2</sub> through this enzyme can again be coupled to the translocation of protons per two electrons (4H<sup>+</sup>/2e<sup>-</sup>); although under some conditions lower stoichiometries may occur (De Gier, 1996).



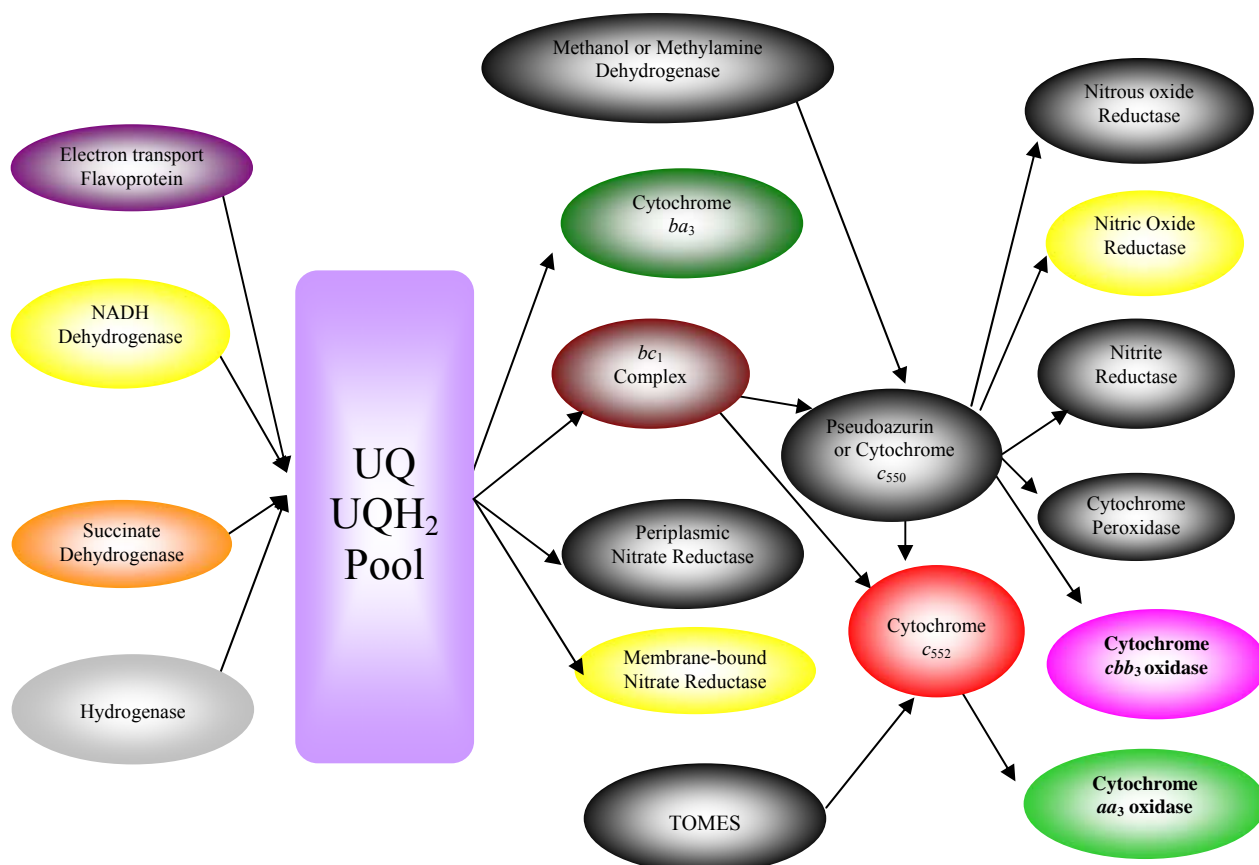


**Figure 1:** Branched electron transport chain of *P. denitrificans*. Enzyme complexes coloured in black show periplasmic location. UQ:ubiquinone, UQH<sub>2</sub>:reduced ubiquinone, TOMES:thiosulphate oxidation multienzyme system (adapted from Baker *et al.*, 1998).

The distribution of the electrons among the different pathways depends partly on the expression levels of the terminal oxidases. Cytochrome *aa*<sub>3</sub> is expressed at atmospheric oxygen tension, while cytochrome *cbb*<sub>3</sub> is expressed predominantly at low oxygen tension and little is known about the induction profile of cytochrome *ba*<sub>3</sub> (see Otten *et al.*, 1999).

### 1. 3 Structures of the respiratory chain complexes

The detailed atomic structures of respiratory complexes by crystallography and NMR spectroscopy along with a vast amount of new information gleaned by other advanced spectroscopic methods, have had a tremendous impact on the understanding of structures and function correlation of these membrane proteins. Only the structures of Complex I and parts of the ATP synthase remain to be elucidated by high-resolution X-ray crystallography of appropriate three-dimensional crystals. The most complex among all the respiratory proteins

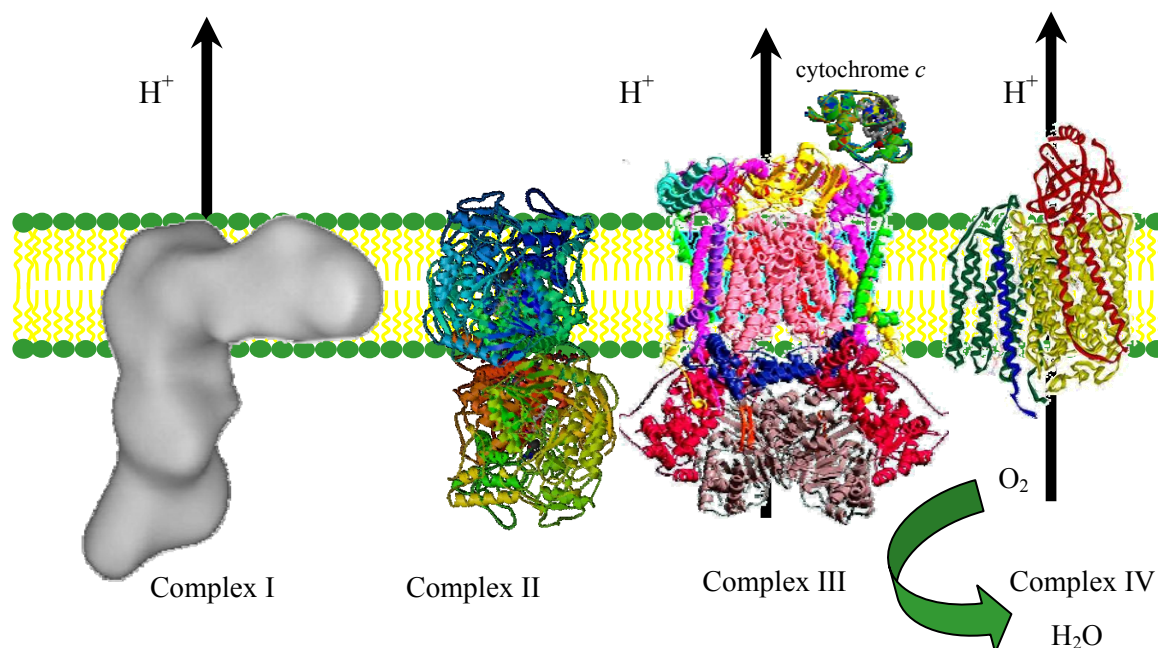


**Figure 2** Structural view of the respiratory complexes in the membrane plane, for Complex I structure analysis and subunit assignment rely on single particle image reconstruction and electron microscopy (Friedrich *et al.*, 2004) structure of Complex II from *Wolinella succinogenes* (pdb entry:1QLA) Complex III structure from chicken heart mitochondria which contain the same functional unit as in *P. denitrificans* (pdb entry:1BCC) the soluble fragment of cytochrome *c*<sub>552</sub> from *P. denitrificans* (pdb entry:1C7M) and four subunit Complex IV from *P. denitrificans* (pdb entry:1QLE).

is Complex I. No crystal structure is available due to its large size and instability of its subunits after detergent solubilisation. Till date only a single molecule reconstruction image and crystal structure of the hydrophobic domain (peripheral arm) of this complex is available (Yagi, 2002; Friedrich, 2004; Sazanov and Hinchliffe, 2006). Complex II is a family of enzymes catalyzing the transfer of electrons between succinate and quinones. This family includes the quinol:fumarate oxidoreductase (QFR) enzymes. Two crystal structures of quinol:fumarate oxidoreductases, from *E. coli* (Iverson *et al.*, 1999) and *Wolinella succinogenes* (Lancaster *et al.*, 1999), have been reported. There are three structures of Complex III from three different sources, bovine heart mitochondria (Iwata *et al.*, 1998), chicken heart mitochondria (Zhang *et al.*, 1998), and from *Saccharomyces cerevisiae* complexed with antibody Fv-fragment (Hunte *et al.*, 2000) solved by X-ray diffraction. All of these structures show that this complex exists in the dimer form required for biological

functions (see Croft, 2004). The structure of Complex IV, a four-subunit and two subunit enzyme complexed with an antibody Fv-fragment from *Paracoccus denitrificans*, (Iwata *et al.*, 1995; Harrenga and Michel, 1999), bovine heart mitochondria (Tsukihara *et al.*, 1996), *Thermus thermophilus* (Soulimane *et al.*, 2000), *Rhodobacter sphaeroides* (Svensson-Ek *et al.*, 2002) and ubiquinol oxidase from *Escherichia coli* (Abramson *et al.*, 2000) were solved by X-ray crystallography. The schematic arrangement of these complexes in the membrane plane is shown in Figure 2.

### 1.3.1 NADH:ubiquinone oxidoreductase

Complex I (NADH:ubiquinone oxidoreductase) is a ubiquitous enzyme present both in the inner membrane of mitochondria and in the cytoplasmic membrane of numerous bacteria. It utilizes NADH formed during glycolysis and the TCA cycle and serves as first proton pump of the respiratory chain. Bovine Complex I is remarkably complicated, with seven mitochondrially encoded subunits, and at least 39 nuclear-encoded subunits (Hirst *et al.*, 2003). However, bacterial homologues of Complex I have only 14 subunits, seven of which are homologues of the mitochondrially encoded subunits and the other seven are homologues of nuclear encoded mammalian subunits (Yagi *et al.*, 2003; Hinchliffe and Sazanov, 2005). These 14 subunits presumably represent a common catalytic core structure. The atomic structure of the complex is not yet solved, only low-resolution structures of the complex have been obtained from electron microscopy images of single particles and two-dimensional arrays. The enzyme from various sources appears to be L-shaped, with presumed membrane-embedded and matrix-located arms (Yagi *et al.*, 2003; Hinchliffe and Sazanov, 2005). However, even this topology has been questioned recently, where an alternative ‘horseshoe’ conformation has been described (Böttcher *et al.*, 2002). Complex I contains non-covalently bound FMN together with several Fe<sub>4</sub>S<sub>4</sub> and Fe<sub>2</sub>S<sub>2</sub> iron–sulphur centres. In the bovine enzyme, six distinct iron–sulphur centres can be distinguished by EPR spectroscopy (Ohnishi, 1998). The electron transfer from NADH to ubiquinone is coupled to the translocation of protons, with accepted proton pumping stoichiometry of 2H<sup>+</sup>/e<sup>-</sup> transferred through the protein (Brandt *et al.*, 2003).

### 1.3.2 Succinate:ubiquinone oxidoreductase

Complex II participates in both the respiratory chain and the TCA cycle, oxidizing succinate to fumarate and transferring the electrons to ubiquinone. Complex II is not a proton pump, but act as a site for regulation of the activity of the TCA cycle. Mammalian SQR is a four-

subunit enzyme, the two largest subunits are extramembranous subunits that face in the matrix space, and a flavoprotein contains a covalently bound flavin adenine dinucleotide (FAD), iron-sulphur protein binds three iron-sulphur clusters: an  $\text{Fe}_2\text{S}_2$  centre, an  $\text{Fe}_4\text{S}_4$  cluster and an  $\text{Fe}_3\text{S}_4$  centre. The two remaining subunits are membrane-bound. These subunits bind a single low-spin *b* heme. The presence of two magnetically interacting ubisemiquinone species has been observed in partially reduced bovine enzyme using EPR spectroscopy. Crystal structures of the QFR enzymes from *E. coli* and *Wolinella succinogenes* have been solved at resolutions of 3.3 Å and 2.2 Å, respectively (Iverson *et al.*, 1999; Lancaster *et al.*, 1999).

### 1.3.3 Ubiquinone:cytochrome *c* oxidoreductase

Complex-III (cytochrome *bc*<sub>1</sub> complex) catalyzes the transfer of electrons from ubiquinol to cytochrome *c*. The reaction is complicated in that both oxidation of ubiquinol (QH<sub>2</sub>) and reduction of ubiquinone (Q) occur during the reaction cycle as part of the proton-translocating cycle. The bovine mitochondrial cytochrome *bc*<sub>1</sub> complex is composed of eleven subunits (Iwata *et al.* 1998), and the bacterial homologue consists of three subunits in *P. denitrificans*. The enzyme contains a cytochrome *b* with two heme moieties *b*<sub>L</sub> and *b*<sub>H</sub>, a subunit liganding a ( $\text{Fe}_2\text{S}_2$ ) center (Rieske protein; ISP) and a cytochrome *c*<sub>1</sub>. It catalyzes electron transfer from ubiquinone to cytochrome *c* via a ubisemiquinone, generating a proton motive force across respiring membranes. It is widely agreed that the electron and proton-transfer pathway occurs essentially by the ‘Q-cycle’ mechanism that was first envisaged by Mitchell in 1962 (Rich, 2003). Ubiquinol oxidation at the ‘Q<sub>o</sub>’ site results in a concerted electron transfer in which the first electron is transferred to the iron–sulphur protein and the second to the low-potential heme *b*, termed *b*<sub>L</sub>. The electron on the iron–sulphur ( $\text{Fe}_2\text{S}_2$ ) protein is passed via cytochrome *c*<sub>1</sub> to the substrate cytochrome *c*. The electron on heme *b*<sub>L</sub> moves across the membrane to reduce the higher potential heme *b*<sub>H</sub> and this in turn reduces ubiquinone to ubiquinol in two steps. This mechanism provides a very efficient means of utilizing the energy of electron transfer to form a proton-motive force across the membrane, resulting overall in two electrogenic proton translocations across the inner mitochondrial membrane for each pair of electrons eventually passed to cytochrome *c* (Croft, 2004).

### 1.3.4 Cytochrome *c* oxidase

The cytochrome *aa*<sub>3</sub> type terminal oxidase accepts electrons from Complex III via the soluble cytochrome *c* in mitochondria while membrane-bound cytochrome *c*<sub>552</sub> in the *P.*

*denitrificans*. It catalyses the transfer of electrons from cytochrome *c* to molecular oxygen. The enzyme is arranged so that cytochrome *c* binds and donates electrons from the intermembrane space. The mammalian mitochondrial cytochrome *c* oxidase is a very large structure that spans the inner mitochondrial membrane and is a dimer, with each monomeric unit being composed of thirteen different subunits (Tsukihara *et al.*, 1996; Yoshikawa *et al.*, 1998). However, sequence comparisons show that there is a wide range of simpler bacterial oxidases that are structurally related to cytochrome oxidase and which form a homologous 'superfamily'. The structure of *P. denitrificans* cytochrome *c* oxidase revealed that the enzyme complex consists of four different subunits (Iwata *et al.*, 1995). It is composed of subunit II which carries the binuclear Cu<sub>A</sub> site that serves as the entry point for electrons donated by cytochrome *c*. Subunit I contains the other redox-active centers: a low-spin heme *a* accepting electrons from the Cu<sub>A</sub> center and transferring them to the binuclear site of oxygen reduction which is formed by one copper atom called Cu<sub>B</sub> and the high-spin heme *a*<sub>3</sub>. Subunit III is equally dispensable, since an enzyme complex consisting only of the subunits I and II has been shown to be catalytically active and completely functional (Ludwig and Schatz, 1980). The fourth subunit a small peptide as was first shown in the crystal structure (Iwata *et al.*, 1995). The function of this very small subunit with only one transmembrane helix remains unclear, as the deletion of its gene had no deleterious effects for assembly or function of the oxidase (Witt and Ludwig, 1997). The two other redox-active atoms calcium and manganese are bound in substoichiometric amounts by specific amino acid residues in the two larger subunits. The importance of these metal ions is not completely understood although some stabilizing role has been implied (Pfitzner *et al.*, 1999).

#### **1.4 Arrangements of the complexes**

The first isolation of the five complexes of oxidative phosphorylation from mammalian mitochondria was achieved about 50 years ago. These respiratory complexes were separated by biochemical procedures and well characterized for several organisms. Two models were proposed for the arrangement of these complexes in the membrane plane. (i) a supercomplex assembly formed by stable associations between these proteins complexes or (ii) random diffusion of individual respiratory complexes.

### 1.4.1 Solid state or supercomplex model

The original idea of a solid state model of complex arrangement was given by Chance *et al.* 1955. There is mounting evidence that *in vivo* respiratory complexes specifically interact forming supermolecular structures called supercomplexes: (i) purification protocols for individual respiratory complexes sometimes lead to the isolation of stoichiometric assemblies of two or more complexes which are functionally active (Hatefi *et al.*, 1961; Hatefi and Rieske, 1967); (ii) stable and enzymatically active supercomplexes can be reconstituted upon mixture of Complex I and III (Fowler and Richardson, 1963; Hatefi, 1978; Ragan and Heron, 1978); (iii) respiratory protein complexes from several bacteria were found to form specific supermolecular structures (Berry and Trumpower, 1985; Sone *et al.*, 1987; Iwasaki *et al.*, 1995; Niebisch and Bott, 2003) ; (iv) inhibitor titration experiments reveal that the respiratory chain of *Saccharomyces cerevisiae* behaves like a single functional unit (Boumans *et al.*, 1998) and (v) flux control experiments indicate specific interactions of respiratory protein complexes (Genova *et al.*, 2003). It was recently proposed that respiratory complexes of mammals are organized as large assemblies constituting a supramolecular network, the so-called “respirasome” consisting of two supercomplexes (I<sub>1</sub>III<sub>2</sub>IV<sub>4</sub> and III<sub>2</sub>IV<sub>4</sub>) as building blocks in a 2:1 ratio (Schägger *et al.*, 2000).

Isolation of supercomplexes by means of protein solubilization using nonionic detergents and separations of solubilised protein complexes by Blue Native (BN)-PAGE were used to investigate the structure of the OXPHOS system of plants and bacteria (Eubel *et al.*, 2003; Krause *et al.*, 2004). Recently with this method all complexes I, III, IV with a stoichiometry of 1:4:4 and several copies of cytochrome *c*<sub>552</sub> were isolated from *Paracoccus denitrificans* (Stroh *et al.*, 2004). A plant mitochondrial and mammalian supercomplex was structurally characterized by electron microscopy (EM) and presents a model for how complexes I and III are spatially organized within the Complex-I+III<sub>2</sub> supercomplex (Dudkina *et al.*, 2005; Schäfer *et al.*, 2006).

Several physiological roles were proposed for these respiratory supercomplexes, like substrate channelling leading to catalytic enhancement, protection of reactive reaction intermediates, and stabilization of individual protein complexes (Schägger and Pfeiffer, 2000; Genova *et al.*, 2003). The major advantage of substrate channelling is the use of localized substrate molecules. This has been shown for mammalian mitochondria quinone and cytochrome *c*, which can react independently of bulk properties of a quinone or cytochrome *c* pool (Gupte and Hackenbrock, 1988). Sequestration of the reactive

intermediate ubisemiquinone, which can react with oxygen to generate superoxide anion radical is essential, since conditions leading to increased levels are involved in the pathogenicity of mitochondrial disorders (Schägger *et al.*, 2004). However, sequestration of ubisemiquinone seems to be a function of individual Complexes I and III. Assembly or stability of complexes III and IV is not adversely affected by the absence of supercomplexes in *P. denitrificans*, *S. cerevisiae*, and human mitochondria (see review Schägger, 2002) However, Complex I from human mitochondria and *P. denitrificans* requires physical association with Complex III for assembly or its stability (Schägger *et al.*, 2004; Stroh *et al.*, 2004).

#### **1.4.2 Random diffusion model**

Membrane-associated biochemical reactions are thought to occur by mechanisms that require lateral diffusion of membrane components. It has been proposed that reactions in the membrane are dependent on random collisions, where diffusion itself is rate limiting. One system in which random collisions have been suggested to be the dominant mode of interaction is the mitochondrial electron-transfer chain. Hackenbrock *et al.*, 1985, postulated the random collision model of mitochondrial electron transport.

The random collision model of mitochondrial electron transport can be summarized as:

##### **1.4.2.1 All the redox components are independent lateral diffusion**

The combined studies of differential calorimetry, freeze fracture electron microscopy showed that the total protein of inner mitochondrial membrane occupies only one third to one half of membrane surface area (Hackenbrock *et al.*, 1985). The lipid bilayer occupied around 50% of the surface area that provides space to the membrane protein to diffuse freely. Antibodies were used as a probe for free lateral diffusion and random collision of redox protein (Höchli *et al.*, 1985). The low pH liposome fusion method showed the kinetically independent diffusion of all sequential electron transfer complexes, cytochrome *c* oxidase and *bc*<sub>1</sub> complex diffuse independently to each other (Schneider *et al.*, 1980). The average distance between the integral membranes proteins is increased due to the liposome fusion to native membrane was showed by freeze fracture technique. Due to increased distance, the electron transfer rates between redox partner decreases proportional to degree of exogenous liposome fusion. The other evidence came from measurement of lateral diffusion of redox component by fluorescence recovery after photo bleaching (FRAP) experiments. The lateral diffusion coefficient of Complex III, IV, cytochrome *c*, ubiquinone

and inner phospholipids were determined by FRAP (Gupte *et al.*, 1984). The recovery data showed that redox component and ubiquinone analogues is greater than 90% recovery in each case and have no significant immobile fraction. It indicates that all the redox component diffuse laterally as a common pool.

#### **1.4.2.1 Cytochrome *c* diffuses primarily in three dimension**

In the inner mitochondrial membrane cytochrome *c* acts as the electron mediator between the  $bc_1$  complex and cytochrome *c* oxidase. Depending on ionic strength cytochrome *c* can diffuse laterally, pseudo-laterally and three-dimensionally with respect to the membrane surface. The three types of diffusion and its strong dependencies on high ionic strength were shown by FRAP. It shows that maximum electron transfer activity of cytochrome *c* occur at physiological (150 mM) ionic strength in isolated inner mitochondrial membranes when cytochrome *c* is in state of three-dimensional diffusion (Gupte *et al.*, 1988).

#### **1.4.2.2 Electron transport is a diffusion-controlled kinetic process**

All the bimolecular redox reactions in the inner mitochondrial membrane are preceded by one or more diffusion-based random collisions between different redox partners (Gupte *et al.*, 1984). This was determined by experimental data from lateral diffusion, effective concentration (ratio of reduced and oxidized) and sum of the radii of the reactive areas of redox components. The collision frequency was calculated with the Hardt equation to compare by experimental maximum turnover number in two-dimensional systems (see reference Hackenbrock *et al.*, 1986). It shows that every redox component undergoes one or more diffusion-based collision with its potential redox partner to yield one turnover. In the data, they never found a turnover number greater than the collision frequency. These findings reveal that a permanent assembly or transient aggregate of redox components is not required for sequential or maximum rate of electron transport.

#### **1.4.2.3 Electron transport is a multicollisional, long-range diffusion process**

Mitochondrial electron transport is on average a long range (>10 nm) diffusional process. The data were interpreted to show that distances between Complex I and III 30 nm, Complex II and III is 27.2 nm, Complex III and IV 19.3 nm (Hackenbrock *et al.*, 1985). These distance were calculated by using the equation  $d = [c_1 + c_2]^{-1/2}$  where  $c_1$  and  $c_2$  are the concentration of individual redox complexes in a two dimensional stationary lattice. Dilution of the inner mitochondrial membrane lipid by phospholipid enrichment method showed the decrease in collision obstruction and increase in the diffusion distances. The diffusion rates



of redox components have a direct influence on the overall kinetic process of electron transfer and can be rate limiting as in diffusion control.

All of the above postulates presented here for the random diffusion model showed that the redox complexes undergo one or more diffusion-based collisions with its potentially reactive redox partner to affect one turnover. Thus electron transport is a diffusional coupled process and diffusion control could be summarized as (i) The diffusion-coupled kinetic process is composed of a diffusion step and chemical reaction step (ii) diffusion control step is defined as when the collision frequency between the reaction partners is equal to the frequency of chemical reaction (iii) when collision frequency between reaction partner exceeds the frequency of chemical reaction, overall kinetic process is diffusion control.

In addition, studies on the rotational mobility of cytochrome *c* oxidase demonstrate that at least half of the oxidase in the native mitochondrial membrane shows free rotational mobility (Kawato *et al.*, 1980). The artificially induced alterations in the distances between electron-transfer components are accompanied by changes in electron-transfer rates. When the distances between redox centers are decreased, the rate of electron transfer from succinate or NADH to oxygen is increased, while an increase in distance decreases the electron-transfer rates (Schneider *et al.*, 1982). These findings led to a proposal that mitochondrial electron transfer occurs by a diffusion-mediated mechanism in which cytochrome *c* and ubiquinone diffuse much faster than the large integral protein complexes. Cytochrome *c* has been suggested to communicate electrons between cytochrome *bc*<sub>1</sub> and *aa*<sub>3</sub>, by rapid diffusion on the negatively charged membrane surface with correct orientation of the mobile carrier maintained by its large dipole moment (Koppenol and Margoliash, 1982). This idea is supported by studies on the effects of chemical modification of cytochrome *c* on its reactivity with its redox partners, indicating that the same residues are involved in the binding of cytochrome *c* to both cytochrome *aa*<sub>3</sub> and cytochrome *bc*<sub>1</sub> (see Hochli *et al.*, 1985). Moreover, when cytochrome *c* is cross-linked to mitochondrial inner membranes, significant rates of electron transfer are retained. This suggests that dissociation of cytochrome *c* from its redox partners may not be required for its activity because of the small size and lipid nature of ubiquinone. However, there is also evidence for direct interaction of cytochrome *bc*<sub>1</sub> with Complex I and with succinate dehydrogenase (Chazotte and Hackenbrock, 1988), raising the possibility that electron transfer by ubiquinone can occur via direct association of the complexes as well as by free diffusion.

## **Objectives of this dissertation**

The aim of my doctoral work was to prove the supercomplex model of respiratory chain complexes in the native bacterial membrane. Here different independent approaches were used to analyze the existence of a supercomplex in a native membrane environment, and to avoid any perturbation caused by detergent solubilization:

- Measuring the distance and orientation of the different complexes by Electron Paramagnetic Resonance (EPR) Spectroscopy: The experiment started with a simple model system and the complexity of the system may be later increased gradually to make the final aim of this approach.
- Lateral diffusion of cytochrome *c* oxidase in the native membrane by using Fluorescence recovery after photobleaching (FRAP), and Fluorescence correlation spectroscopy (FCS): This approach started with a simple system (reconstituted protein in lipid vesicles) and the complexity of the system may be later increased.
- Time resolved photolysis study of the arrangement of different complexes in the membrane by Flash Photolysis method: The experiment started with optimization of CO binding with detergent solubilised and reconstituted cytochrome *c* oxides and may be later performed in the native and complex deleted membranes.

## **Distance and orientation measurements between the different respiratory complexes**

Electron Paramagnetic Resonance EPR, a spectroscopic technique has been applied to investigate both the structure and dynamics of paramagnetic sites in biological systems (Prisner *et al.*, 2001; Eaton and Eaton, 2000). The high sensitivity of electron spins allows studying paramagnetic sites in large macromolecular complexes, and the distance and orientation measurements can provide structural information on these biological systems (Lakshmi and Brudvig, 2002). Time relaxation ( $T_m$ ) distance measurements rely on the enhancement of the spin-relaxation rate of a slow-relaxing spin by a fast-relaxing spin (Eaton and Eaton, 2002).

Due to presence of different paramagnetic centers (hemes, iron-sulphur clusters,  $Cu_A$ ), it is very difficult to assign the EPR signal in a native membrane. Here we started with two simple systems; soluble fragments of cytochrome  $c_{552}$ , containing a single paramagnetic center (Fe) and the soluble domain of subunit II of cytochrome *c* oxidase which contains the binuclear mixed-valence  $Cu_A$  centre. Multi-frequency pulse EPR spectroscopy was applied

to investigate the magnetic dipole-dipole interactions for distance and orientation measurement between these two proteins.

To increase the complexity of the system in terms of paramagnetic centers and size of the protein molecule, we can increase in a 'step by step' manner to measure the distance and orientations between these complexes: (i) cytochrome *c* oxidase and its electron donor soluble or a membrane anchored cytochrome *c*<sub>552</sub> (ii) same component in a reconstituted system mimicking the membrane like situation, (iii) extension of these measurements in the presence of *bc*<sub>1</sub> complex and Complex I the reconstituted system. To compare these distances to native membrane situation three types of deletion mutants could be used, which did not contain Complex I or III or IV. These mutants can be used for the comparison of the distance between the complexes in the natural and reconstituted system. It will confirm whether a supercomplex exists in the native membrane, is not a detergent artefacts and plays a physiological role in electron transport.

### **Lateral mobility of the complex in the native membrane**

An alternative approach to obtain the quantitative information on the lateral diffusion properties of complexes in their native membrane environment could answer the question whether any particular respiratory complex is present as a monomer complex or assembled in a supercomplex form. Two independent techniques, Fluorescence recovery after photo bleaching (FRAP) and fluorescence correlation spectroscopy (FCS) was used. In these experiments, the diffusion of cytochrome *c* oxidase was monitored as it was labelled with monoclonal antibody (Fv fragment) that binds to the periplasmic side of subunit II of oxidase (Iwata *et al.*, 1995). Fv fragment is labelled with the appropriate dye (FITC for FRAP and Cy<sub>5</sub> for FCS), and the labelled Fv fragment is allowed to bind to cytochrome *c* oxidase in the membrane. Therefore, it is an indirect labelling of the complex in the native membrane. Lateral mobility of cytochrome oxidase in membrane plane should answer the question whether the complex moves as an individual entity with a molecular weight of 125 kDa or in supercomplex with 10 fold higher (1900 kDa) molecular weight (Stroh *et al.*, 2004).

### **Flash photolysis method**

In the membrane plane, measurements of rotational motions are particularly important, because of their high sensitivity to the shape and size of the protein or assembly of proteins. A number of membrane proteins permits microsecond and millisecond rotational motions to be plausibly interpreted in terms of specific large-scale motions (see Kawato and Kinoshita,

1981). The measurements of rotational motion will be based on a orientation-dependent photoselection i.e. the selective excitation of molecules on the basis of orientation, and observation of the effects of molecular reorientation during the rebinding of the probe.

The optical absorption spectroscopy will be used for detection of rotational diffusion of oxidase in native membrane. To monitor the reorientation of oxidase in the membrane plane, carbon monoxide (CO) would be used as a probe for this experiment. The CO binds to oxidase in reduced condition at the  $a_3$ -Cu<sub>B</sub> site and the effect will be monitored in the Soret region of the spectra. Non-polarized and polarized light would be used for this measurement. The difference in absorption between horizontally and vertically polarized light will be used for investigate the rotational mobility of respiratory complex in native membrane.

## 2. Materials and Methods

### 2.1 Suppliers

AppliChem GmbH (<http://www.applichem.de>)  
 Amersham Biosciences (<http://www.amershambiosciences.com>)  
 Biomol (<http://www.biomol.de>)  
 Invitrogen (<http://www.invitrogen.com>)  
 Molecular Probes (<http://probes.invitrogen.com>)  
 Merck (<http://www.merck.de>)  
 PeQ lab (<http://www.peqlab.de>)  
 Roth (<http://www.carl-roth.de>)  
 Sigma Aldrich & Fluka (<http://www.sigmaaldrich.com>)

### 2.2 Chemicals

|   |                      |
|---|----------------------|
| 5-Brom-4-Chlor-3-indolyl-phosphate (BCIP) | BTS                  |
| Acetic acid Glacial                       | Carl Roth            |
| Acrylamide 30%                            | AppliChem            |
| Adenosine di-phosphate                    | Calbiochem           |
| Agar-Agar                                 | Carl Roth            |
| Agarose                                   | PeQ lab              |
| Ammonium chloride                         | Carl Roth            |
| Ammonium per sulphate (APS)               | Carl Roth            |
| Ampicillin                                | Carl Roth            |
| Asolectin                                 | Sigma-Aldrich        |
| Avidin                                    | Gerbu                |
| Bacto-trypton                             | Becton and Dickinson |
| Bio-beads Sm-2                            | Bio Rad              |
| Bisacrylamide                             | AppliChem            |
| Bis-Tris                                  | AppliChem            |
| Boric acid                                | Carl Roth            |
| Bovine Serum Albumin (BSA)                | Sigma-Aldrich        |
| Bromophenol blue                          | Biomol               |

|  |                  |
|--|------------------|
| Calcium chloride dihydrate   | Fluka            |
| Chloramphenicol  | Carl Roth        |
| Chloroform   | Carl Roth        |
| Cholic acid-Na salt  | Sigma-Aldrich    |
| Citric acid monohydrate  | Carl Roth        |
| Coomassie-Blue   | Carl Roth        |
| Cupric chloride (CuCl <sub>2</sub> )                               | Fluka            |
| Cy5 dye  | Amersham         |
| Desthiobiotin  | Sigma-Aldrich    |
| Digitonin  | Sigma-Aldrich    |
| Dimethylsulfoxide (DMSO)   | Merck            |
| Di-potassium hydrogen phosphate (K <sub>2</sub> HPO <sub>4</sub> ) | Carl Roth        |
| Dithiothreitol (DTT)   | AppliChem        |
| DNase  | Fluka Chemie     |
| Ethanol  | Carl Roth        |
| Ethidium bromide   | Gibco BRL        |
| Ethylendiamine tetracetic acid (EDTA)                              | Carl Roth        |
| Fluorescein isothiocyanate (FITC)                                  | Molecular probes |
| Folin-Ciocalteu's phenol reagent                                   | Merck            |
| Glycerol   | Carl Roth        |
| Glycine  | Carl Roth        |
| HABA dye   | Sigma –Aldrich   |
| N-2-Hydroxyethylpiperazine-N'-2-ethanesulfonic acid (HEPES) buffer | Carl Roth        |
| Hydrochloric acid (HCl)  | Carl Roth        |
| Hydroxylamine-HCl  | Sigma –Aldrich   |
| Imidazole  | Carl Roth        |
| Isopropanol  | Carl Roth        |
| Isopropyl-β-D-thiogalactopyranoside (IPTG)                         | Fermentas        |
| Kanamycin  | AppliChem        |
| Lysozyme   | Biomol           |

|  |                      |
|--|----------------------|
| Methyl-amine   | Fluka                |
| N,N,N,N-Tetramethylethylenediamine (TEMED)                         | Carl Roth            |
| n-Dodecyl- $\beta$ -D-maltopyranoside (DM)                         | Biomol               |
| Pefabloc SC  | Biomol               |
| Phenylmethylsulphonylfluoride (PMSF)                               | Serva                |
| Ponceau Red S  | Sigma-Aldrich        |
| Potassium chloride (KCl)   | Carl Roth            |
| Potassium cyanide (KCN)  | Riedel-de Haën       |
| Potassium di-hydrogen phosphate (KH <sub>2</sub> PO <sub>4</sub> ) | Carl Roth            |
| Potassium hydroxide (KOH)  | Carl Roth            |
| Proteinase K   | Sigma-Aldrich        |
| Sodium acetate   | Carl Roth            |
| Sodium azide   | Carl Roth            |
| Sodium carbonate (Na <sub>2</sub> CO <sub>3</sub> )                | Carl Roth            |
| Sodium chloride (NaCl)   | Carl Roth            |
| Sodium dithionite  | Fluka                |
| Sodium dodecyl sulphate (SDS)                                      | Carl Roth            |
| Sodium nitrite   | Merck                |
| $\beta$ -Mercapto-ethanol  | Carl Roth            |
| Succinic acid  | Carl Roth            |
| Succinic acid (purity 99.99% , Mn free)                            | Fluka                |
| Sucrose (purity 97.995%)   | Carl Roth            |
| Tris-hydroxymethylaminoethane (Tris)                               | Carl Roth            |
| Urea   | Carl Roth            |
| Yeast extract  | Becton and Dickinson |

### 2.3 Column chromatography

|  |           |
|--|-----------|
| Diethylaminoethyl (DEAE) cellulose       | Pharmacia |
| Diethylaminoethyl (DEAE) sepharose CL-6B | Pharmacia |
| Ni-NTA fast flow                         | Pharmacia |
| Sephacryl S-200                          | Pharmacia |

|                 |               |
|-----------------|---------------|
| Q-Sepharose     | Qiagen        |
| Sepharose-200   | Pharmacia     |
| Sephadex G-25   | Pharmacia     |
| Ultragel AcA-34 | Sepracor      |
| Streptavidin    | IBA Göttingen |

## 2.4 Proteins

|  |                |
|--|----------------|
| Avidin   | Biomol         |
| Horse heart cytochrome <i>c</i>  | Sigma –Aldrich |
| <i>P. denitrificans</i> cytochrome <i>c</i> oxidase  | Prof. Ludwig   |
| Cytochrome <i>bc</i> <sub>1</sub> complex  | Oliver Anderka |
| Cytochrome <i>c</i> <sub>1</sub> fragment  | Julia Janzon   |
| Periplasmic fraction of Fv fragment against subunit II of <i>aa</i> <sub>3</sub> cytochrome <i>c</i> oxidase | Oliver Richter |

## 2.5 Strains

|   | References                             |
|---|--|
| <b>Wild type <i>P. denitrificans</i></b> : Pd1222 (Ri <sup>r</sup> , Sp <sup>r</sup> )                                | DeVries <i>et al.</i> , 1989           |
| <b>Complex III deletion mutant</b> : MK6 (Pd1222, $\Delta fbc::Km^r$ )  | Marcus Korn (1994)                     |
| <b><i>aa</i><sub>3</sub> oxidase deletion mutant</b> : MR31 (Pd1222, $\Delta actaDI::Km^r$ , $\Delta actaDII::Tc^r$ ) | Raitio and Wikström (1994)             |
| <b>Complex I deletion mutant</b>  | M. Finel (1996), Oliver Anderka (2003) |

## 2.6 Instruments

|                           |               |
|---------------------------|---------------|
| Autoclave                 | Schutt        |
| Electrophoresis apparatus | Bio-Rad       |
| Fermentor                 | New Brunswick |
| Heraeus megafuge 1.0R     | Heraeus       |
| Manton-Gaulin Press       | APV Schröder  |
| Biofuge GL                | Heraeus       |



|   |                     |
|---|---------------------|
| pH meter pH40i                            | WTW                 |
| Protein electrophoresis (Mini Protein II) | Bio-Rad             |
| Sonfier 250                               | Branson             |
| Sorvall RC5B, RC3C, RC5                   | Dupont              |
| Spectrophotometer U-3000                  | Hitachi             |
| Spectrophotometer UV IKON                 | Kontron             |
| Speed Vac                                 | Savant              |
| Thermo mixer 5436                         | Eppendroff          |
| Ultracentrifuge L7-65 and L8-70,          | Beckman Instrument  |
| Vortex Reax 2000                          | Heidolph            |
| Zeta sizer Nano ZS                        | Malvern Instruments |

## 2.7. Experimental setup

### 2.7.1 FRAP and FCS

A FRAP setup was described (Knoll *et al.*, 1998) and an initial FCS experiment was done in collaboration with Dr. Ingo Köper, Marcel Friedrich and Dr. Renate Naumann, Material science group Max Planck Institute for Polymer Research Mainz, Germany.

### 2.7.2 Pulsed EPR

EPR spectra were taken in close collaboration of Prof. Dr. T. Prisner at Institut für Physikalische und Theoretische Chemie, J.W.Goethe-Universität, Frankfurt, Germany. Bruker Eleksys-580 X-Band spectrometer equipped with a Bruker MD5-W1 cavity and an Oxford CF935 helium flow cryostat with ITC-5025 temperature controller. The High field EPR experiments were performed on a home-built (Rohrer *et al.*, 2001), 6.4 T, 180 GHz pulse EPR spectrometer. The X band measurements were performed with Sevdalina Lyubenova and high field with Marloes Penning de Vries.

### 2.7.3 Flash photolysis

The laser flash photolysis setup with laser pulse (Nd:YAG, 532 nm, 10 ns, 5 mJ/cm<sup>2</sup>) was used. Two digital oscilloscopes (LeCroy 9361 and 9400A) were used to record the traces in two overlapping time windows. Each data point was properly weighted on the basis of the baseline analysis and the quasilogarithmic data compression, as described by (Chizhov *et al.* 1996). The setup was used with Dr. Igor Chizhov, Institut für Biophysikalische Chemie,

Medizinische Hochschule Hannover. Carbon monoxidase (CO) was purchased from Air liquid.

## 2.8 Software

|                           |   |
|---------------------------|---|
| Clone Manager             | Scientific & Educational Software                                       |
| Zeta particle measurement | Malvern Instruments   |
| Origin software           | <a href="http://www.OriginLab.com">http://www.OriginLab.com</a>         |
| Swiss Pdb viewer          | <a href="http://www.expasy.org/spdbv/">http://www.expasy.org/spdbv/</a> |
| Web lab pdb viewer        | Molecular Simulations Inc   |
| Pymol                     | DeLano Scientific   |

## 2.9 Solutions

### 2.9.1 Growth Medium

#### LB-Medium

|               |             |
|---------------|-------------|
| Peptone       | 1 % (w/v)   |
| Yeast extract | 0.5 % (w/v) |
| NaCl          | 0.5 % (w/v) |

#### TY-Medium

|               |             |
|---------------|-------------|
| Trytone       | 0.8 % (w/v) |
| Yeast Extract | 0.5 % (w/v) |
| NaCl          | 0.5 % (w/v) |

#### Succinate Medium (Ludwig, 1986)

|                        |           |
|------------------------|-----------|
| $K_2HPO_4$             | 50 mM     |
| $NH_4Cl$               | 10 mM     |
| $MgSO_4 \cdot 7 H_2O$  | 1 mM      |
| Citric acid            | 1 mM      |
| Succinic acid          | 40 mM     |
| Trace element solution | 0.2 ml /L |
| pH 6.2 with KOH        |           |

**Trace element solution**

|                                  |        |
|----------------------------------|--------|
| CaCl <sub>2</sub>                | 100 mM |
| CoCl <sub>2</sub>                | 10 mM  |
| CuSO <sub>4</sub>                | 4 mM   |
| FeCl <sub>3</sub>                | 90 mM  |
| H <sub>3</sub> BO <sub>3</sub>   | 5 mM   |
| MnCl <sub>2</sub>                | 50 mM  |
| Na <sub>2</sub> MoO <sub>4</sub> | 10 mM  |
| ZnCl <sub>2</sub>                | 25 mM  |
| in concentrated HCl (37%)        |        |

**Methylamine Medium (Ludwig 2001)**

|                                       |          |
|---------------------------------------|----------|
| Methylamine hydrochloride             | 11 g/L   |
| Citric acid                           | 0.42 g/L |
| K <sub>2</sub> HPO <sub>4</sub>       | 6.0 g/L  |
| KH <sub>2</sub> PO <sub>4</sub>       | 4.0 g/L  |
| MgSO <sub>4</sub> x 7H <sub>2</sub> O | 0.25 g/L |
| Yeast extract                         | 0.1 g/L  |
| Trace solution                        | 1.0 ml/L |
| NaHCO <sub>3</sub>                    | 10 g/L   |

**Trace solution**

|                                       |        |
|---------------------------------------|--------|
| CaCl <sub>2</sub> x 2H <sub>2</sub> O | 300 mM |
| CoCl <sub>2</sub>                     | 10 mM  |
| CuSO <sub>4</sub>                     | 4 mM   |
| FeCl <sub>3</sub>                     | 90 mM  |
| H <sub>3</sub> BO <sub>3</sub>        | 5 mM   |
| MnCl <sub>2</sub>                     | 50 mM  |
| Na <sub>2</sub> MoO <sub>4</sub>      | 10 mM  |
| ZnCl <sub>2</sub>                     | 25 mM  |
| in concentrated HCl (37%)             |        |

### 2.9.2 Antibiotics

| Antibiotic        | Stock concentration       | End concentration |
|-------------------|---------------------------|-------------------|
| Ampicillin (Amp)  | 50 mg/ml in 50 % Glycerin | 50 µg/ml          |
| Streptomycin (Sm) | 25 mg/ml in 50 % Glycerin | 25 µg/ml          |
| Kanamycin (Km)    | 25 mg/ml in 50 % Glycerin | 25 µg/ml          |
| Rifampicin (Rif)  | 30 mg/ml in Methanol      | 60 µg/ml          |

Store at -20 °C.

### 2.9.3 Molecular biology

#### 2.9.3.1 Plasmid isolation (Mini-Prep)

##### Mini I-Solution (TEG pH 8)

|         |       |
|---------|-------|
| Tris    | 25 mM |
| Glucose | 50 mM |
| EDTA    | 10 mM |

##### Mini II-Solution fresh prepared

|      |       |
|------|-------|
| NaOH | 0.2 M |
| SDS  | 1 %   |

##### Mini III-Solution

|                       |         |
|-----------------------|---------|
| 5 M Potassium acetate | 60 ml   |
| Glacial acetic acid   | 11.5 ml |
| H <sub>2</sub> O      | 28.5 ml |

##### TE pH 7.5

|      |       |
|------|-------|
| Tris | 10 mM |
| EDTA | 1 mM  |

Chloroform / Isopropyl alcohol 24 : 1 (v/v)

RNase 2 mg/ml in 50 % Glycerol

**2.9.1.2 Agarose gel electrophoresis**DNA loading buffer

|                         |              |
|-------------------------|--------------|
| Glycerol                | 5 % (v/v)    |
| EDTA                    | 30 mM        |
| Bromophenol blue in TBE | 0.02 % (w/v) |

Ethidium bromide solution

|                  |          |
|------------------|----------|
| Ethidium bromide | 10 mg/ml |
|------------------|----------|

Working concentration 5 µg/ml

TBE (10x) pH 8

|            |       |
|------------|-------|
| Tris       | 1 M   |
| Boric acid | 1 M   |
| EDTA       | 25 mM |

**2.9.1.3 Competent cell preparation**TFB I-Buffer pH 8.5

|                   |            |
|-------------------|------------|
| RbCl              | 100 mM     |
| MnCl <sub>2</sub> | 100 mM     |
| CaCl <sub>2</sub> | 10 mM      |
| Potassium acetate | 30 mM      |
| Glycerol          | 15 % (v/v) |

TFB II-buffer pH 7.0

|                   |            |
|-------------------|------------|
| RbCl              | 10 mM      |
| MOPS              | 10 mM      |
| CaCl <sub>2</sub> | 75 mM      |
| Kac               | 30 mM      |
| Glycerol          | 15 % (v/v) |

All solution were sterilized by filter sterilization

**2.9.4 Protein estimation**Solution A

|                                 |             |
|---------------------------------|-------------|
| Na <sub>2</sub> CO <sub>3</sub> | 2 % (w/v)   |
| NaOH                            | 0.4 % (w/v) |

Solution B

|                                       |           |
|---------------------------------------|-----------|
| CuSO <sub>4</sub> x 5H <sub>2</sub> O | 1 % (w/v) |
|---------------------------------------|-----------|

Solution C

|               |           |
|---------------|-----------|
| K-Na-tartrate | 2 % (w/v) |
|---------------|-----------|

Folin-Ciocalteu's reagent**2.9.5 Electrophoresis and Western-blot****2.9.5.1 SDS-PAGE**Separating gel buffer (4x) pH 8.8 (Laemmli, 1970)

|          |             |
|----------|-------------|
| Tris-HCl | 1.5 M       |
| EDTA     | 8 mM        |
| SDS      | 0.4 % (w/v) |

Stacking gel buffer (4x) pH 6.8 (Laemmli, 1970)

|          |             |
|----------|-------------|
| Tris-HCl | 0.5 M       |
| EDTA     | 8 mM        |
| SDS      | 0.4 % (w/v) |

Acrylamide solution

|               |             |
|---------------|-------------|
| Acrylamide    | 30 % (w/v)  |
| Bisacrylamide | 0.8 % (w/v) |

SDS loading buffer

|                             |         |
|-----------------------------|---------|
| Stacking buffer             | 12.5 ml |
| SDS 20 % (w/v)              | 10.0 ml |
| β-Mercaptoethanol           | 2.0 ml  |
| Glycerol                    | 10.0 ml |
| Bromphenol blue 1 % (w/v)   | 1.0 ml  |
| 50 ml with H <sub>2</sub> O |         |

SDS Running buffer (5x) pH 8.3

|                           |         |
|---------------------------|---------|
| Tris                      | 30 g    |
| SDS (20%)                 | 50 ml   |
| EDTA (500 mM, pH 8.0)     | 4 ml    |
| Glycine                   | 142.5 g |
| 1 L with H <sub>2</sub> O |         |

Coomassie staining solution

|                          |             |
|--------------------------|-------------|
| Coomassie brilliant blue | 0.2 % (w/v) |
| Glacial acetic acid      | 10 % (v/v)  |
| Methanol                 | 20 % (v/v)  |

Coomassie-destaining solution

|                     |            |
|---------------------|------------|
| Glacial acetic acid | 10 % (v/v) |
| Methanol            | 20 % (v/v) |

**2.9.5.2 Western-Blot**Transfer buffer (5x)

|                          |       |
|--------------------------|-------|
| Tris                     | 30 g  |
| SDS (20% w/v)            | 4 ml  |
| Glycine                  | 142 g |
| 1L with H <sub>2</sub> O |       |

Transfer buffer (1x) working solution

|                           |        |
|---------------------------|--------|
| Transfer buffer 5x        | 400 ml |
| Methanol                  | 400 ml |
| 2 L with H <sub>2</sub> O |        |

Ponceau solution

|         |             |
|---------|-------------|
| Ponceau | 0.2 % (w/v) |
| TCA     | 3 % (w/v)   |

TBS pH 7.5

|          |                  |
|----------|------------------|
| Tris     | 50 mM            |
| NaCl     | 150 mM           |
| Tween-20 | 0.1 % (v/v)      |
| NCS      | 5 % in TBS (v/v) |

TNM pH 9.5

|                   |                            |
|-------------------|----------------------------|
| Tris-HCl          | 100 mM                     |
| NaCl              | 100 mM                     |
| MgCl <sub>2</sub> | 50 mM                      |
| BCIP              | 25 mg/ml in DMF            |
| Stored at -20 °C  |                            |
| NBT               | 50 mg/ml in 70 % (v/v) DMF |
| Stored at -20 °C  |                            |

Stop solution, pH 8.0

|      |       |
|------|-------|
| EDTA | 50 mM |
|------|-------|

**2.9.6 Membrane suspension buffer**

|            |        |
|------------|--------|
| Kpi pH 8.0 | 20 mM  |
| NaCl       | 100 mM |
| EDTA       | 1 mM   |

**Sucrose gradient**

|            |                 |
|------------|-----------------|
| Sucrose    | 20 %-60 % (w/w) |
| Kpi pH 8.0 | 20 mM           |
| EDTA       | 1 mM            |

**2.9.8 Purification of respiratory protein complexes**

**2.9.8.1 Cytochrome *c* oxidase**

Buffer for DEAE-sepharose CL6B column

|            |         |
|------------|---------|
| Kpi pH 8.0 | 20 mM   |
| NaCl       | 100 mM  |
| EDTA       | 1 mM    |
| DM         | 0.5 g/L |



Washing buffer with high detergent concentration

|            |         |
|------------|---------|
| Kpi pH 8.0 | 20 mM   |
| NaCl       | 100 mM  |
| EDTA       | 1mM     |
| DM         | 2.0 g/L |

Low salt gradient

|            |         |
|------------|---------|
| Kpi pH 8.0 | 20 mM   |
| NaCl       | 100 mM  |
| EDTA       | 1 mM    |
| DM         | 0.5 g/L |

High salt gradient

|            |         |
|------------|---------|
| Kpi pH 8.0 | 20 mM   |
| NaCl       | 600 mM  |
| EDTA       | 1 mM    |
| DM         | 0.5 g/L |

AcA 34 gel filtration column

|            |         |
|------------|---------|
| Kpi pH 8.0 | 20 mM   |
| NaCl       | 100 mM  |
| EDTA       | 1mM     |
| DM         | 0.2 g/L |

DEAE sepharose CL6B column

|            |         |
|------------|---------|
| Kpi pH 8.0 | 20 mM   |
| NaCl       | 100 mM  |
| EDTA       | 1 mM    |
| DM         | 0.2 g/L |

Low salt gradient

|            |         |
|------------|---------|
| Kpi pH 8.0 | 20 mM   |
| NaCl       | 100 mM  |
| EDTA       | 1 mM    |
| DM         | 0.2 g/L |

High salt gradient

|            |         |
|------------|---------|
| Kpi pH 8.0 | 20 mM   |
| NaCl       | 400 mM  |
| EDTA       | 1 mM    |
| DM         | 0.2 g/L |

**2.9.8.2 Cu<sub>A</sub> fragment purification**Pellet suspension buffer

|                 |       |
|-----------------|-------|
| Tris-HCl pH 8.2 | 20 mM |
|-----------------|-------|

Inclusion body suspension

|                 |       |
|-----------------|-------|
| Tris-HCl pH 8.2 | 20 mM |
|-----------------|-------|

|             |      |
|-------------|------|
| Triton-X100 | 1.5% |
|-------------|------|

Pellet suspension

|                 |       |
|-----------------|-------|
| Tris-HCl pH 8.2 | 20 mM |
|-----------------|-------|

|      |    |
|------|----|
| Urea | 7M |
|------|----|

|      |       |
|------|-------|
| NaCl | 100mM |
|------|-------|

First dialysis buffer

|                 |       |
|-----------------|-------|
| Tris-HCl pH 8.2 | 20 mM |
|-----------------|-------|

|      |     |
|------|-----|
| Urea | 2 M |
|------|-----|

|     |       |
|-----|-------|
| DTT | 0.5mM |
|-----|-------|

Second dialysis

|                 |       |
|-----------------|-------|
| Tris-HCl pH 8.2 | 20 mM |
|-----------------|-------|

|     |        |
|-----|--------|
| DTT | 0.5 mM |
|-----|--------|

Dialysis buffer for overnight

|                 |       |
|-----------------|-------|
| Tris-HCl pH 8.2 | 20 mM |
|-----------------|-------|

|                       |        |
|-----------------------|--------|
| Cu(II)Cl <sub>2</sub> | 300 μM |
|-----------------------|--------|

Q sepharose high performance columnEquilibration buffer

|                 |       |
|-----------------|-------|
| Tris-HCl pH 8.2 | 20 mM |
|-----------------|-------|

|                       |        |
|-----------------------|--------|
| Cu(II)Cl <sub>2</sub> | 300 μM |
|-----------------------|--------|

Gradient

|                 |       |                  |       |
|-----------------|-------|------------------|-------|
| Tris-HCl pH 8.2 | 20 mM | Tris- HCl pH 8.2 | 20 mM |
|-----------------|-------|------------------|-------|

|      |     |      |         |
|------|-----|------|---------|
| NaCl | 100 | NaCl | 1000 mM |
|------|-----|------|---------|

|                       |       |                       |        |
|-----------------------|-------|-----------------------|--------|
| Cu(II)Cl <sub>2</sub> | 300μM | Cu(II)Cl <sub>2</sub> | 300 μM |
|-----------------------|-------|-----------------------|--------|

Gel filtration Sephacryl HR S200 column

|                 |        |
|-----------------|--------|
| Bis-Tris pH 7.0 | 20 mM  |
| NaCl            | 100 mM |

Ni-NTA column

|                 |       |
|-----------------|-------|
| Bis-Tris pH 7.0 | 20 mM |
|-----------------|-------|

**2.9.8.3 Cytochrome  $c_{552}$  fragment purification**Periplasma Buffer

|                 |         |
|-----------------|---------|
| Tris-HCl pH 8.0 | 100 mM  |
| EDTA            | 1 mM    |
| Sucrose         | 5000 mM |

Q-sepharose fast flowEquilibration buffer

|                 |       |
|-----------------|-------|
| Tris-HCl pH 8.0 | 50 mM |
| NaCl            | 50 mM |
| EDTA            | 1 mM  |

Gradient

NaCl (50-150 mM) in equilibration buffer

Gel filtration Sephacryl S-100 column

|                 |        |
|-----------------|--------|
| Tris-HCl pH 7.0 | 20 mM  |
| NaCl            | 150 mM |
| EDTA            | 1 mM   |

**2.9.8.4 Cytochrome  $c_{552}$  from *Thermus thermophilus***CM-Sepharose columnEquilibration buffer

|                 |       |
|-----------------|-------|
| Tris-HCl pH 8.0 | 50 mM |
| EDTA            | 1 mM  |

Gradient

|                 |        |                  |         |
|-----------------|--------|------------------|---------|
| Tris-HCl pH 8.0 | 20 mM  | Tris- HCl pH 8.0 | 20 mM   |
| NaCl            | 100 mM | NaCl             | 1000 mM |

Sephacryl 100 gel filtration

|                 |        |
|-----------------|--------|
| Tris-HCl pH 8.0 | 50 mM  |
| NaCl            | 150 mM |
| EDTA            | 1 mM   |

**2.9.8.5 Membrane bound cytochrome *c*<sub>552</sub>**

Membrane solubilization buffer

|                  |        |
|------------------|--------|
| Kpi pH 8.0       | 50 mM  |
| NaCl             | 150 mM |
| Imidazole        | 20 mM  |
| with NaOH pH 8.0 |        |

Cu-IMAC column

Equilibration buffer

|            |         |
|------------|---------|
| Kpi pH 8.0 | 50 mM   |
| NaCl       | 150 mM  |
| Imidazole  | 20 mM   |
| DM         | 0.2 g/L |

Gradient buffer

|                        |         |
|------------------------|---------|
| Tris- HCl pH 8.2       | 20 mM   |
| NaCl                   | 150 mM  |
| Imidazole <sub>2</sub> | 200 mM  |
| DM                     | 0.2 g/L |

Q sepharose CL6B

|   |         |
|---|---------|
| Kpi pH 8.0                                  | 50 mM   |
| NaCl  | 50 mM   |
| DM  | 0.2 g/L |
| Gradient with 50-600 mM NaCl in same buffer |         |

**2.9.8.6 Reconstitution in liposome**

Reconstitution buffer

|                     |           |
|---------------------|-----------|
| HEPES pH 7.3        | 100 mM    |
| Cholic acid Na salt | 2 % (w/v) |

Dialysis buffer I

|                  |        |
|------------------|--------|
| HEPES-KOH pH 7.3 | 100 mM |
|------------------|--------|

Dialysis buffer II

|                  |         |
|------------------|---------|
| HEPES-KOH pH 7.3 | 10 mM   |
| KCl              | 40.6 mM |
| Sucrose          | 39.6 mM |

**2.9.9 Solutions for spectroscopic methods**Spectra buffer

|              |             |
|--------------|-------------|
| Kpi pH 8.0   | 50 mM       |
| Triton-X-100 | 0.5 % (v/v) |
| EDTA         | 1 mM        |

Oxidase activity buffer

|          |       |
|----------|-------|
| Tris-HCl | 20 mM |
| KCl      | 20 mM |
| EDTA     | 1 mM  |

adjust pH 7.5

**2.9.10 Translational diffusion methods****2.9.10.1 Purification of Fv fragments**Washing buffer (W)

|                 |        |
|-----------------|--------|
| Tris-HCl pH 7.0 | 100 mM |
| NaCl            | 150 mM |
| EDTA            | 1 mM   |

Elution buffer(E)

|                 |        |
|-----------------|--------|
| Tris-HCl pH 7.0 | 100 mM |
| NaCl            | 150 mM |
| EDTA            | 1 mM   |
| Desthiobiotin   | 2.5 mM |

Regeneration buffer(R)

|                 |        |
|-----------------|--------|
| Tris-HCl pH 7.0 | 100 mM |
| NaCl            | 150 mM |
| EDTA            | 1 mM   |
| HABA            | 1 mM   |

**2.9.10.2 Phosphate buffered saline (PBS)**

|                                  |        |
|----------------------------------|--------|
| KH <sub>2</sub> PO <sub>4</sub>  | 0.24 g |
| Na <sub>2</sub> HPO <sub>4</sub> | 1.44 g |
| KCl                              | 0.2 g  |
| NaCl                             | 8 g    |
| per liter                        |        |

**2.9.11. Buffer for EPR experiments**

|                  |      |
|------------------|------|
| HEPES-KOH pH 7.0 | 5 mM |
| Glycerol         | 10 % |

**2.10 Molecular biology methods****2.10.1 Plasmid isolation**

For restriction analysis, the plasmids were prepared by the alkaline lysis method: Cell pellet from a 2 ml overnight culture was suspended in 100 µl Mini-I solution (TEG pH 8.0) followed by gently mixing with 200 µl freshly prepared Mini-II solution (0.2 M NaOH, 1% SDS) for 5 min. After that 150 µl of Mini-III solution (Potassium acetate solution) was slowly added to the mixture. The sample was incubated on ice for 10 min and then centrifuged (13000 rpm, 10 min, Heraeus biofuge). The supernatant was mixed with 800 µl of isopropanol and incubated on ice for 10 min. The sample was then centrifuged at 14000 rpm for 15 min. After removing the supernatant carefully, the pellet was washed once with 70 % ethanol and dried with air. Finally, the pellet was redissolved in 50 µl of sterile water and 5 µl RNase was added, and incubated at 37 °C for 1 hour.

Restriction enzyme digestion was performed in a DNA to enzyme ratio of 1 µg to 10 units under conditions (temperature and buffer) as described by the manufactures (MBI Fermentas). After restriction, the DNA sample was mixed with 20 µl DNA loading buffer. DNA fragments were analyzed in 1% agrose gels in TBE buffer with a horizontal electrophoresis chamber at 100 mV for 1 hour.

**2.10.2 Competent *E. coli* cells**

An overnight culture of *E. coli* K12 strain JM 109 or JM 83 was inoculated in 100 ml LB medium and grown at 37 °C to an OD<sub>600</sub> of 0.5. The culture was cooled down and cells were harvested at 6000 rpm (10 min, 4 °C, Heraeus megafuge). The cell pellet was carefully

suspended in 10 ml ice cooled TFB-I buffer and incubated on ice for 1 hour. After centrifugation the pellet was suspended in 2 ml TFB-II buffer. 100 µl cell aliquots were frozen in liquid nitrogen and stored at -80 °C.

### **2.10.3 Transformation**

100 µl aliquots of competent cells were thawed on ice for 20 min. 1 µl plasmid DNA (10 ng) was mixed with 100 µl of competent cells and incubated on ice for 20 min. The mixture was transferred to 42 °C for 60 sec (heat shock). The cells were regenerated in 1 ml LB medium at 37 °C with slow shaking. The cell suspension was centrifuged (5000 rpm, 5 min, Heraeus biofuge), plated on a pre-warmed (37 °C) agar plate with appropriate antibiotics, and incubated at 37 °C overnight.

### **2.11 Growth of *P. denitrificans***

A single colony of *P. denitrificans* was picked from an LB plate containing appropriate antibiotics (depending upon the strain). It was inoculated in 2 ml LB medium for overnight growth. From this overnight culture, 1 ml was inoculated in 100 ml succinate medium at 32 °C in shaking condition for overnight. 5% of pre-culture was inoculated in 2.5 liter of the medium in 5 liter Erlenmeyer flask at 180 rpm 32 °C room temperature. Same procedure was applied for growth of *P. denitrificans* in methylamine medium. The cells were harvested by centrifugation at 5000 rpm (Sorvall RC3C, 20 min, 4 °C).

### **Mn depleted oxidase**

To avoid any signal from Mn<sup>++</sup> in cytochrome *c* oxidase for EPR experiments, cells were grown in the succinate medium containing 1 µM MnCl<sub>2</sub> instead of 50 µM.

### **2.12 Membrane preparation**

Three different methods were used for the preparation of the cytoplasmic membrane of *P. denitrificans* for different experimental purposes

- Osmotic pressure method
- Sonication method
- French Press (Manton-Gaulin Press) method

#### **2.12.1 Osmotic pressure method**

Frozen cell paste was thawed and diluted to 10 ml/g of cells in buffer (20 mM Kpi, pH 8.0) with Pefabloc SC (100 µM), lysozyme (10 mg/ml) and 0.02 mM MgSO<sub>4</sub> with a small

amount of DNase to reduce viscosity. The suspension was stirred for 15 minutes at room temperature, and then two volume of buffer (20 mM Kpi, pH 8.0, 1 mM EDTA) was added to apply an osmotic shock to cells. All steps were carried out at 4 °C.

### **2.12.2 Sonication method**

Harvested *P. denitrificans* cells were dissolved in buffer (20 mM Kpi, pH 7.0, 10 mM EDTA), Pefabloc SC (0.5 mg/ml) and mixed with homogenizer for 5 min. Lysozyme (10 mg/ml) was added in the concentration of 1 ml per 100 ml of the cell solution. For lysozyme activity cells were incubated for 1 hour in ice. Thereafter cells were stored at -80 °C for 30 min. After thawing, the cell wall and genomic DNA were destroyed by sonication (Branson Sonifier 250, 40% output, max 40% duty cycle for 5 min), and membranes collected by ultracentrifugation (Beckman L-70, rotor 45Ti, 40,000 rpm, 1 h, 4 °C).

### **2.12.3 Manton-Gaulin Press (MG) method**

In this method membranes were prepared by rupture of the cell wall at a pressure of 400 bar with Manton-Gaulin Press (APV Schröder, Lübeck, Germany). Frozen cells were thawed in buffer (20 mM Kpi, pH 8.0, 1 mM EDTA), homogenized and Pefabloc SC was added in final concentration of 100 µM. The suspension was put in the MG Press; first pumped for 5 min, then 400 bar pressure applied for 5 min. All steps were carried out in cold room (8 °C).

In all three cases, unbroken material was first centrifuged at 5000 rpm (Sovrvall RC3 10 min 4 °C). The supernatant was centrifuged at (12,000 rpm, Sorvall GSA rotor, 4 °C, overnight).

In different methods used for cell breakage after first centrifugation, pellets consisted of a chalky grey lower layer and a very soft, reddish brown upper layer. The soft reddish layer was suspended in buffer (20 mM Kpi, pH 8.0, 1 mM EDTA). The suspended pellet was ultracentrifuged (Beckman L-70, rotor 45Ti, 35,000 rpm, 1 h, 4 °C). Pellet containing reddish brown layer was suspended in small amount of buffer (20 mM Kpi, pH 8.0, 1 mM EDTA) and stored at -80 °C.

Membrane quality was checked by recording absorption spectra (500-650 nm) of the reduced minus oxidized forms of the heme groups contained in the respiratory chain complexes. The solubilized membrane was reduced by addition of dithionite and oxidized by addition of ferricyanide.



#### 2.12.4 Purification of membrane

The membrane was further purified by the sucrose gradient method using 0-60% (w/v) sucrose in buffer (20 mM Kpi, 1 mM EDTA, pH 8.0). Reddish brown membranes were placed on the top of the gradient and centrifugation was carried out (Beckman L-70, 25,000 rpm, 18 h, 4 °C) using swing bucket rotor 'Sw28'. After centrifugation, different bands were visible. The dark reddish brown layer was appeared at the 35% sucrose gradient. This reddish brown layer was collected with the help of long bended needle. Thereafter the pellet was diluted five fold with buffer (20 mM Kpi, pH 8.0, 1 mM EDTA) and membranes were collected by ultracentrifugation (Beckman L-70, rotor 65Ti, 50,000 rpm, 1 h, 4 °C). The pellet was suspended in a small amount of buffer and stored at -80 °C for further use.

#### 2.13 Membrane vesicle size measurements

The size of membrane vesicles were measured by Zeta sizer Nano ZS (Malvern Instruments UK) at 25 °C. Size measurements were made on the gradient purified native membrane samples obtain by the three different types of membrane preparations. The samples were diluted in PBS. The size and shape of the membrane vesicles prepared by different method was checked by electron microscopy

#### 2.14 Expression and purification of respiratory protein complexes

##### 2.14.1 Cu<sub>A</sub> fragment

The soluble Cu<sub>A</sub> fragment of cytochrome *c* oxidase from *P. denitrificans* contains amino acid residues 130-280 of subunit II crystal structure (see Iwata *et al.*, 1995). This construct was used to express the subunit II domain of oxidase in *E. coli* JM 109 cells. A his-tagged version of Cu<sub>A</sub> fragment was described previously (Lappalainen *et al.*, 1993) but the His tag is not used for purification, nor is its presence in the protein desirable, it was cleaved off *in vivo* by

TEV-protease. This method used for the expression for Cu<sub>A</sub> soluble fragment described by Maneg *et al.*, 2003. The harvested *E. coli* cells were suspended in 20 mM Tris-HCl (pH 8.2) containing 100 μM pefabloc SC (serine protease inhibitor). Cells were broken with small pulses of sonication (Branson Sonifier 250, 40% output, max 40% duty cycle for 1 min). The suspension was centrifuged (Beckman L-70, rotor 45Ti, 40,000 rpm, 1 h, 4 °C). The pellet was washed with 20 mM Tris-HCl (pH 8.2) buffer containing 3% (w/v) Triton X-100. After

that it was dissolved in 7M urea, 20 mM Tris-HCl (pH 8.2). The dissolved protein was first dialyzed for 4 h against (20 mM Tris-HCl pH 8.2, 100 mM NaCl, 2 M urea, 0.5 mM DTT), then another 4 h against (20 mM Tris-HCl, pH 8.2, 100 mM NaCl, 0.5 mM DTT) and overnight against (20 mM Tris-HCl, pH 8.2, 300  $\mu$ M Cu(II)Cl<sub>2</sub>). The final dialysis was done against (20 mM Tris-HCl, pH 8.2, 300  $\mu$ M Cu(II)Cl<sub>2</sub>) for 4 h. Dialysis was carried out at 4 °C in a 3.5-kDa cut-off dialysis tubing. The supernatant was applied to Q-Sepharose fast flow anion exchange column equilibrated with (20 mM Tris-HCl, pH 8.2, 300  $\mu$ M Cu(II)Cl<sub>2</sub>). The purple colour peak fractions containing the Cu<sub>A</sub> fragment were pooled, concentrated in a Vivaspin concentrator (10,000 MWCO) to small volume and loaded to Sephacryl HR S200 which had been equilibrated with (20 mM Bis-Tris pH 7.0, 300  $\mu$ M CuCl<sub>2</sub>). An additional purification step on a nickel-nitrilotriacetic acid (Ni-NTA) column in (20 mM Bis-Tris, pH 7.0) buffer was done to remove residual His-tagged material. The purity was checked with SDS-PAGE and concentration was determined by absorbance spectra at 480 nm using an extinction coefficient of 3.0 mM<sup>-1</sup> cm<sup>-1</sup> (Maneg *et al.*, 2003).

#### 2.14.2 Cytochrome *c*<sub>552</sub> fragment

The soluble fragment of cytochrome *c*<sub>552</sub> from *P. denitrificans* is a 10.5-kDa protein. It lacks the helical 30-residue membrane anchor as well as the acidic 40-residue linker segment, and was expressed in the *E. coli* DH5K (Reincke *et al.*, 1999). The bacteria were grown aerobically at 37 °C in LB medium with appropriate antibiotics. For expression, IPTG was added to a concentration of 1 mM at a cell density of OD<sub>600nm</sub> = 0.5. Cells were harvested and suspended in 100 ml of periplasmic buffer (100 mM Tris-HCl, pH 8.0, 500 mM sucrose, 1 mM EDTA). The suspension was stirred for 30 min at 4 °C with lysozyme (100  $\mu$ l/ml) and ultracentrifuge (Beckman L-70, rotor 45Ti, 40,000 rpm, 1 h, 4 °C) to get periplasmic fraction. Soluble fragments were purified from periplasma by column chromatography in different steps: (i) ion exchange chromatography on Q-Sepharose in 50 mM Tris-HCl, 1 mM EDTA, pH 8.0, and eluted by a salt gradient of 0-350 mM NaCl in the same buffer (ii) fractions with the highest specific heme content red in color were pooled and separated further by gel filtration on Sephacryl S-200, (iii) pooled fractions were loaded in Q-Sepharose and eluted with a salt gradient of 0-300 mM NaCl. All red fractions containing cytochrome *c*<sub>552</sub> were pooled and concentrated by a concentrator (Viaspin 5,000 MWCO).

### 2.14.3 Cytochrome $c_1$ fragment

A soluble fragment cytochrome  $c_1$  was derived from the  $bc_1$  complex, containing 125 amino acid residues was expressed in *E. coli* (Eichhorn, PhD dissertation, 2004). The cells were grown aerobically at 37 °C and over grown cells were transferred in the 2.5 liter of LB medium in a 5 liter Erlenmeyer flask and expression was induced by 1 mM IPTG at 16 °C. The cells were harvested and periplasmic fraction was prepared with using 50 mM Tris-HCl, pH 8.0, 500 mM sucrose, 1 mM EDTA and adding PMSF, lysozyme in concentration of 0.1 mM and 80 µg/ml respectively. The suspension was kept on ice for 30 min. The spheroplast was removed by ultracentrifugation (Beckman L-70, rotor 45Ti, 45000 rpm, 30 min, 4 °C). After ultracentrifugation, this fraction was purified by ion-exchanger chromatography equilibrated with (50 mM Tris-HCl, pH 8.2, 100 mM NaCl, 1 mM EDTA) and eluted by a 300-600 mM NaCl gradient in the same buffer. The red fractions were collected and further purified by gel filtration Sepharose-200. The red fractions were pooled and concentrated

### 2.14.4 Cytochrome $c_{552}$ from *Thermus thermophilus*

Cytochrome  $c_{552}$  from *T. thermophilus* was expressed in *E. coli*. The freeze culture was inoculated in LB medium containing ampicillin (50 µg/ml) and chloramphenicol (30 µg/ml) and grown at 37 °C with shaking. The pre-culture was inoculated in five liter Erlenmeyer flasks containing 2.5 liter LB medium with appropriate concentrations of antibiotics (Overnight, 180 rpm). *E. coli* cells were harvested by centrifugation (Sorvall RC3C, 5000 rpm, 4 °C, 20 min). The periplasmic fraction was prepared of harvested cell and suspended in the periplasma buffer (100 mM Tris-HCl, pH 8.0, 5 mM EDTA, 500 mM sucrose) with lysozyme (100 µg/ml), Pefabloc SC (10 µg/ml) and kept on ice for 30 min. The spheroplast was removed by ultracentrifugation (Beckman L-70, 35000 rpm, 30 min, 4 °C). Thereafter, the periplasma was stirred for 30 min at 4 °C and genomic DNA was destroyed with small pulse of sonicator (Branson Sonifier 250, 20% output, 10% duty cycle for 1 min). Afterwards the supernatant was collected by ultracentrifugation (Beckman L70, rotor 65Ti, 45000 rpm, 1 h, 4 °C). The pH of supernatant was checked before applying to the column. The cytochrome  $c_{552}$  in the supernatant was purified by column chromatography in two steps: (i) ion exchange chromatography on CM-Sepharose fast flow (50 mM Tris-HCl, pH 8.0, 1 mM EDTA) and eluted by a salt gradient of 0-300 mM NaCl in the same buffer (ii) then further purified by gel filtration on Sephacryl S100 (50 mM Tris-HCl, pH 8.0, 150 mM

NaCl, 1 mM EDTA). All red fractions were collected, pooled, checked with redox spectra, and analyzed with SDS PAGE, before further use (Maneg, PhD dissertation, 2003).

#### 2.14.5 Cytochrome *c*<sub>552</sub> (full length)

The membrane-bound (full-length) cytochrome *c*<sub>552</sub> contains 178 amino acid residues. His-tagged version of this protein was expressed in *E. coli* (Drosou *et al.*, 2002). The cells were grown at 37 °C in LB medium with ampicillin (50 µg/ml) and chloromphenicol (30 µg/ml) to an OD<sub>600</sub> of 3.0 without induction by IPTG. Cells were harvested and suspended in buffer (50 mM Kpi, pH 8.0, 150 mM NaCl) and broken by Manton-Gaulin press at 400 bar. After ultracentrifugation (Beckman L-70, rotor 45Ti, 35000 rpm, 1 h, 4 °C), membranes were suspended in 50 mM Kpi, pH 8.0, 150 mM NaCl. The membrane was solubilised with DM, with a ratio of 1.5 g of detergent per gram of membrane protein. For separation of supernatant centrifugation was done (Beckman L-70, rotor 45Ti, 35000 rpm, 1 h, 4 °C). The supernatant was applied on Cu-IMAC metal affinity column. It was equilibrated with (50 mM Kpi, pH 8.0, 20 mM imidazole, 150 mM NaCl, and 0.5 g/L DM) and eluted with a linear gradient of 20 to 200 mM imidazole in same buffer. Reddish fractions were pooled and loaded on a Q-Sepharose column equilibrated with (50 mM Kpi, pH 8.0, 50 mM NaCl, and 0.2 g/L DM) eluted with a linear gradient of 50 to 600 mM NaCl. The red fractions were collected and analyzed by redox spectra and SDS-PAGE. The heme concentration was determined by recording redox difference spectra employing an extinction coefficient  $\epsilon_{\text{red-ox}}=19.4 \text{ mM}^{-1} \text{ cm}^{-1}$

#### 2.14.6 Purification of cytochrome *c* oxidase

*P. denitrificans* cells were grown in a Mn depleted medium. The *aa*<sub>3</sub> type cytochrome *c* oxidase was purified after solubilization of membranes by dodecyl maltoside (DM) (Hendler *et al.*, 1991). Membranes were solubilised at a protein to detergent ratio of 1:1.5 (30 min, 4°C). Solubilised material was separated by ultracentrifugation (Beckman L-70, rotor 45Ti 35000 rpm, 1 h, 4°C). The supernatant was applied to a first column, an anion exchanger DEAE-sepharose CL6B equilibrated with 20 mM Kpi, pH 8.0, 100 mM NaCl, 1 mM EDTA, DM 0.5 g/L and washed (20 mM Kpi, pH 8.0, 100 mM NaCl, 1 mM EDTA, DM 2.0 g/L). Elution of green fraction was achieved by a gradient of 100 mM to 600 mM NaCl in the same buffer. It was collected, and concentrated in minimal volume (Vivaspin 50,000 MWCO). There after, concentrated green sample was applied to a AcA 34 gel filtration column. It was equilibrated and eluted with (20 mM Kpi, pH 8.0, 100 mM NaCl, 1 mM

EDTA, DM 0.5 g/L). After elution, the sample was applied to a third column, an anion exchanger DEAE sepharose CL6B equilibrated with (20 mM Kpi, pH 8.0, 100 mM NaCl, 1 mM EDTA, DM 0.5 g/L) and eluted by a gradient of 100 – 400 mM NaCl containing 20 mM Kpi, pH 8.0, 100 mM NaCl, 1 mM EDTA, 0.2 g/L DM. The concentration was determined by recording redox difference spectra of *a*-type heme employing an extinction coefficient  $\epsilon_{603-630}=11.7 \text{ mM}^{-1} \text{ cm}^{-1}$  for single heme and for heme  $a+a_3$   $23.4 \text{ mM}^{-1} \text{ cm}^{-1}$  (Ludwig and Schatz, 1980).

#### 2.14.7 Isolation of *P. denitrificans* supercomplex

*P. denitrificans* strain (Pd1222) was used for the isolation of a supercomplex (Stroh *et al*, 2004). The cells were grown in methylamine medium and membranes isolated. 200 mg proteins (20 mg/ml) were suspended in 2 mM 6-aminohexanoic acid, 150 mM NaCl, 1 mM EDTA, 150 mM imidazole-HCl, pH 7.0. Membranes were solubilised by adding 3 g of digitonin per gram of protein at constant stirring at room temperature. Ultracentrifugation (Beckman L-70, rotor 60Ti, 35000 rpm, 30 min, 4°C) was done before application to a hydroxylapatite column, which was equilibrated with 20 mM sodium phosphate, pH 7.2. Following washing at room temperature with 2 column volumes of 0.1 % digitonin, 150 mM sodium phosphate, pH 7.2, individual respiratory chain complexes and supercomplexes were eluted by 0.05 % Triton X-100, 150 mM sodium phosphate, pH 7.2. The elute was concentrated approximately 5-fold to obtain a volume of 2.5 ml (Vivaspin 100,000 MWCO) and applied to a Sepharose CL-6B column (equilibrated with 0.05 % digitonin, 100 mM NaCl, 5 mM 6-aminohexanoic acid, 1 mM EDTA, 20 mM Na-MOPS, pH 7.3; run at 4 °C). After gel filtration, the supercomplex was checked by Blue native (BN) PAGE, and the protein concentration was determined by the Lowry method.

#### 2.15 Horse heart cytochrome *c*

The solid cytochrome (Sigma) was dissolve in buffer (20 mM HEPES-KOH pH 7.0). The ionic strength of the buffer is gradually changed to 20 mM to 5 mM. There after it was oxidized with a tiny amount of cytochrome *c* oxidase and purified by gel filtration chromatography (5mM HEPES–KOH pH 7.0, 10% glycerol).

#### 2.16. Oxidation of cytochrome *c* and *c*<sub>552</sub>

To fully oxidize the horse heart cytochrome *c* and *P. denitrificans* cytochrome *c*<sub>552</sub> for EPR experiments these fragments were incubated with a tiny amount of cytochrome *c* oxidase

from *P. denitrificans* for 30 min, and purified by gel filtration using (5 mM HEPES-KOH pH 7.0, 10% glycerol) buffer.

Concentrations of different cytochromes (*c*,  $c_{552}$  and  $c_1$ ) were determined by recording redox difference spectra employing an extinction coefficient for horse heart cytochrome *c*  $\epsilon_{550-535} = 21.0$ ,  $c_{552}$   $\epsilon_{550-540} = 19.4$ ,  $c_1$   $\epsilon_{553-540} = 19.4 \text{ mM}^{-1} \text{ cm}^{-1}$

### 2.17 Fv fragment expression

The Fv fragment for  $aa_3$  cytochrome *c* oxidase was cloned and expressed as described by Kleymann *et al.* 1995. The Fv fragment encoded by plasmid pASK68 was produced using *E.coli* K12 strain JM83. Cells were grown at room temperature (21 °C) in the LB medium containing ampicillin (100 µg/ml) to OD<sub>600</sub> of 0.5. Expression was induced by 0.1 mM IPTG. After 3 h, induced cells were harvest by centrifugation. The preparation of periplasmic fraction of harvested cell was performed with using 50 mM Tris-HCl, pH 8.0, 500 mM sucrose, 1 mM EDTA and lysozyme (10µg/ml) kept on ice for 30 min. The spheroplast was removed by ultracentrifugation (Beckman L-70, rotor 60Ti, 35000 rpm, 1 h, 4 °C). The supernatant was taken and pass through a sterile filter 0.2µm. Avidin was added in final concentration of 40 µg/ml before applying to streptavidin column in order to protect from the binding of endogenous biotin groups.

### 2.18 Purification and labelling of Fv fragment

1 ml spin column matrix streptavidin (IBA GmbH) binds up to 4 nmole recombinant *Strep-tag* fusion protein (corresponding to 120 µg of a 28 kDa protein (Fv-*Strep-tag* , IBA protocol)). Before applying the purified periplasmic fraction, the column was equilibrated with 100 mM Tris-HCl, pH 8.0, 150 mM NaCl, 1 mM EDTA. After applying the sample, the column was washed with 5 volumes of buffer and eluted with 100 mM Tris-HCl, pH 8.0, 150 mM NaCl, 1 mM EDTA, 2 mM desthiobiotin. The column was regenerated with 100 mM Tris-HCl, pH 8.0, 150 mM NaCl, 1 mM EDTA, 1 mM HABA buffer. After regeneration, colour of column was changed from yellow to red. All these steps were performed in cold room. 10 µl samples of each fraction were used for SDS-PAGE analysis.

#### 2.18.1 Labelling of Fv antibody fragment

Before labelling, the buffer of the purified Fv fragment (Tris-HCl, pH 7.3) was exchanged to reaction buffer (sodium carbonate, pH 9.5). Fv concentration was determined by measuring absorbance at 280 nm with extinction coefficient of  $50,400 \text{ cm}^{-1} \text{ M}^{-1}$  (Ribrious *et al.*, 1996).

### 2.18.2 Fluorescein isothiocyanate (FITC)

FITC is covalently coupled to primary amines (lysines) of the Fv fragment. 10 mg of FITC were dissolved in 1 ml anhydrous DMSO. The Fv fragment and dye was mixed in a ratio of 1:10. All steps were carried out in dark condition. Reaction was stopped with 10  $\mu$ l of 1.5 M freshly prepared hydroxylamine-HCl. Unreacted FITC dye was removed by gel filtration or by dialysis.

### 2.18.3 Separation of labelled Fv fragment

Two methods were used for separation of Fv fragment from excess dye.

*Gel filtration method:* The labelled Fv fragment was applied to a gel filtration column (Sephadex G-25), eluted with phosphate buffered saline (PBS), and collected in small fractions (500  $\mu$ l). Two peaks appeared, the first peak contained the labelled Fv and second one the excess dye.

*Dialysis methods:* The reaction mixture was placed in a dialysis tube (3.5 kDa MWCO) against phosphate buffered saline (PBS) for overnight dialysis. The buffer was exchanged twice.

### 2.18.4 Efficiency calculation

The labelling efficiency was calculated as number of dye molecule per protein according protocol provided by Molecular Probes. The absorbance was measured at 280 nm to determine the protein concentration, and at 494 nm the dye absorbance. The extinction coefficient used for the FITC dye was 68,000  $\text{cm}^{-1}\text{M}^{-1}$

### 2.18.5 Procedure for labelling with Cy5 dye

1 mg of Cy5 (Amersham) was dissolved in anhydrous DMSO immediately, at a concentration of 1 mg/ml. Fv fragment and dye was added in reaction buffer (sodium carbonate, pH 9.5). For the FCS experiments the optimal ratio between Fv and dye should be one (one dye molecule per Fv) so different ratios were used to find optimal conditions. After mixing, the solution was incubated at room temperature for 1 hour with stirring. Reaction was stopped with 10  $\mu$ l of 1.5 M freshly prepared hydroxylamine-HCl. Untreated Cy5 dye was removed by gel filtration or by dialysis (in both cases result and efficiency were identical).

### 2.18.6 Labelling of membranes

For lateral diffusion experiments, three different types of membrane preparation (osmotic pressure, sonication and Manton-Gaulin method) was mixed with labelled Fv fragment in a ratio of 1:10 (ratio determined with concentration of oxidase in membrane). After mixing, the suspension was incubated for 30 min at room temperature then separated by ultracentrifugation (Beckman L-70, rotor 60Ti, 55000 rpm, 1 h, 4 °C). After centrifugation pellet was washed with PBS then centrifuged again and this process was repeated twice to get rid of excess Fv. Finally, the pellet was dissolved in minimum volume of PBS.

### 2.19 Protein quantification

Protein concentration in the membrane was performed by the procedure of Lowry *et al.*, 1951, as modified by Helenius and Simons, 1972. The standard used for the determination of concentration with the known amount of bovine serum albumin (BSA) in the dilution range of 0.1-2.0 mg/ml

### 2.20 Gel electrophoresis

#### 2.20.1 SDS gel electrophoresis

SDS PAGE was used for checking purity of isolated cytochrome *c* oxidase, cytochrome *c*<sub>1</sub>, cytochrome *c*<sub>552</sub>, Cu<sub>A</sub> fragment, and monoclonal Fv fragment. The stacking gel buffer and separating gel buffer with freshly prepared 10 % APS solution were mixed according the table for casting of gel.

| <b>Solution</b>       | <b>Staking gel</b> | <b>Separating gel<br/>12%</b> | <b>Separating gel<br/>15%</b> |
|-----------------------|--------------------|-------------------------------|-------------------------------|
| Acrylamide solution   | 700 µl             | 3.6 ml                        | 4.5 ml                        |
| Stacking gel buffer   | 1.0 ml             | ---                           | ----                          |
| Separating gel buffer | -----              | 2.25 ml                       | 2.25 ml                       |
| H <sub>2</sub> O      | 2.35 ml            | 3.0 ml                        | 2.1 ml                        |
| 10% APS               | 75 µl              | 75 µl                         | 75 µl                         |
| TEMED                 | 15 µl              | 15 µl                         | 15 µl                         |

The protein sample was mixed with loading buffer and loaded into the wells. Ideally, the glycerol in a sample causes it to sink neatly to the bottom of the well, and allows a sample volume of 20 µl. The gel was run at 200 volts for 43 min. The staining of the gel for



detection of proteins in polyacrylamide gels was performed with staining solution for 20 min at 65 °C with agitation. Excess dye was washed out by ‘destaining’ with acetic acid/methanol with agitation.

### **2.20.2 Blue-Native (BN) polyacrylamide gel electrophoresis**

For the confirmation of supercomplex isolation, Blue-native polyacrylamide gel electrophoresis (BN-PAGE) was performed in the lab of Prof. H. Schägger, Biochemie I, Zentrum der Biologischen Chemie, Universitäts klinikum Frankfurt.

## **2.21 Reconstitution**

### **2.21.1 Purification of asolectin**

For reconstitution of membrane protein generally asolectin from ‘soybean’ (Sigma-Aldrich) was used. It contains mixture of (phosphatidylcholine 40%, phosphatidyl ethanolamine 40%, and other phospholipids 20%) and purified before incorporation of different respiratory complexes.

25 g of asolectin was mixed with 500 ml acetone and stirred for 48 hours at room temperature to extract impurities. The insoluble material was washed again with 200 ml acetone. The phospholipids mixture was dissolved in the 200 ml of diethylether and phospholipids precipitated by slowly adding acetone. The same procedure was repeated twice and this transferred into a round-bottom flask for evaporation. The light yellowish layer was collected and stored at -20 °C.

### **2.21.2 Bacterial lipid isolation**

Bacterial lipid was extracted from the membrane of *P. denitrificans* by the Bligh-Dyer lipid extraction method (Bligh-Dyer, 1955). 1.5 ml of CHCl<sub>3</sub>/MeOH (1:2) and 0.4 ml bacterial membrane (20 mg/ml protein concentration) were vortexed to dissolve the membrane. After mixing, 0.5 ml CHCl<sub>3</sub> was added and the mixture vortexed once again. After vigorous mixing 0.5 ml of H<sub>2</sub>O was added. Two phases formed which were separate by centrifugation at 3000 rpm (Heraeus Biofuge, 10 min). The organic (lower) layer was transferred to a new tube and the solvent evaporated in a Speed Vac (Mid mode, 1 h). The white layer in the tube was collected and used for the reconstitution experiments.

### 2.21.3 Method for reconstitution

Different strategies have been applied for the membrane protein incorporation (Rigaud *et al.*, 1995). The “step-by-step” reconstitution method proved a powerful reconstitution procedure for mitochondrial and bacterial respiratory complexes. In this method the phospholipids and detergent were mixed and micelles were formed. Thereafter, protein was added in the preformed micelles. Detergent was removed with dialysis. The advantages of this method, fairly distribution of membrane protein and a functional unidirectional orientation in proteoliposome.

#### 2.21.3.1 Oxidase reconstitution (Darley-Usmar Method)

Cytochrome *c* oxidase was purified by the method described earlier in this section (2.15.7). 50 mg/ml of purified asolectin was dissolved in the 100 mM HEPES-KOH, pH7.3, containing 25 mM of cholic acid in the final volume. The pH was adjusted with KOH and suspension stirred at 4 °C for 60 min. The opalescent suspension was sonicated using probe type Branson Sonifier 250 setting the vibration power (30 sec cycle duration with 1 min cooling interval, 40% output). The sonication was continued until the opalescent solution become transparent and clarified. Then cytochrome *c* oxidase was added in a concentration of 5-100  $\mu$ M depending upon the type of experiment (EPR, FCS, FRAP and flash photolysis). Thereafter, dialysis was done in the three steps for removal of detergent and incorporation of oxidase into the liposomes. First dialysis was performed in 1 liter (100 mM HEPES-KOH, pH 7.3) for 4 hours, second in the (10 mM HEPES-KOH, pH 7.3, 39.6 mM sucrose, 40.6 mM KCl) with two changes 4 hours and overnight. After dialysis the solution was centrifuged (6000 rpm, Heraeus megafuge, 30 min) and pellet (contain large lipid aggregates and titanium from sonic probe) was discarded.

#### 2.21.3.2 Oxidase and cytochrome *c*

The same procedure (2.19.2.1) was used for the reconstitution of cytochrome *c* oxidase and cytochrome *c*<sub>552</sub> for distance and orientation studies by EPR. Cytochrome *c* oxidase and cytochrome *c* concentration was used in 1:1 ratio (heme concentration).

#### 2.21.3.3 Reconstitution of supercomplex (asolectin and lipid from *P. denitrificans*)

The supercomplex was reconstituted in the purified asolectin as described by Darley-Usmar method (2.19.3.1) with modifications. Cholic acid concentration was reduced from 25 mM to 10 mM final concentration. The detergent was removed by Bio-Beads to avoid any harsh

detergent treatment and long exposure for the supercomplex. The supercomplex was also reconstituted in bacterial lipid using same procedure.

#### **2.21.3.4 Bio-Beads SM adsorption**

1 g of bio-beads was used for every 5 ml of detergent solution. Prior to use of the dry bead, they were degassed in HEPES-KOH, pH 7.3 buffer under vacuum to avoid any air in the pores. The detergent was effectively removed by continuous mixing with a magnetic stirrer for 1 hour at 4 °C. The beads were removed by centrifugation (6000 rpm, Heraeus megafuge, 30 min) and it was regenerated with 100% methanol for further use.

### **2.22. Membrane fusion**

#### **2.22.1 Electroformation technique**

Native membrane fusion to obtain giant unilamellar vesicles (GUV) was tried by electroformation technique (Angelova and Dimitrov, 1986). With this approach, GUV are produced varying in size from 10 to 100  $\mu\text{m}$ . The homogeneity of the size distribution depends on the lipid composition and buffer conditions. The chamber for vesicle preparation was composed of two microscope slides, each coated with a thin layer of indium tin oxide, which made them optically transparent and electrically conductive. The native membranes in PBS were deposited on the indium tin oxide glass plates and the solvent was evaporated over saturated NaCl with in a desiccators. The sealant paste Sigillum wax of 1-mm thickness was used as a spacer between the two plates. After adding the buffer (MOPS and sucrose) into the chamber (3 ml), a voltage of 1.1 V at 10 Hz frequency applied for 2 to 3 h through thin metal electrodes, sealed on the glass plates. This experiment was conducted with help of Prof. Dr. Klaus Fendler, Max Planck Institute of Biophysics Frankfurt.

#### **2.22.2 $\text{Ca}^{++}$ induced fusion**

$\text{Ca}^{++}$  induced fusion was performed by the method of Miller and Racker 1976 with some modifications. The purified membrane was diluted to 1 mg/ml of protein with buffer. After warming to room temperature, 1 M  $\text{CaCl}_2$  was added to a final concentration of 5 to 20 mM to check the optimal concentration of  $\text{Ca}^{++}$  for fusion.. The solution was vortexed and left for 30 min. The  $\text{Ca}^{++}$ -induced fusion was stopped by the addition of 0.5 M K-EGTA to a final concentration of 1.5 times of concentration of  $\text{Ca}^{++}$ . The pH of the EGTA solution was 8.0 in order to prevent acidification of the resulting solution by protons displaced by calcium ions. The fused vesicles were centrifuged in a bench centrifuge (6000 rpm, Heraeus

megafuge, 30 min for 5 min). The mixture applied for velocity run as described in the previous section. In order to facilitate complete removal of free  $\text{Ca}^{++}$  which might be trapped in interlamellar spaces of fused membrane vesicles, it was washed and further purified with sucrose gradient.

### **2.22.3 Temperature and pH depend fusion**

The sucrose gradient purified membrane from *P. denitrificans* was used for the fusion experiments. The fusion was performed at 32°C with constant stirring; 5.0 ml of bacterial membrane (10 mg of protein/ml) were placed in a 50 ml glass beaker. The asolectin vesicles were prepared by 50 mg/ml by Branson Sonifier 250 setting the vibration power (30 sec cycle duration with 1 min cooling interval, 40% output). The sonication was performed until the suspension become transparent. A 2.5 ml of sonicated phospholipids vesicle was added in the membrane solution and pH was immediately adjusted to pH 6.0 with HCl and kept constant. After 30 min, another 2.5 ml of phospholipids vesicles were added and the pH was readjusted to 6.0. After a total of 1 h, the pH was adjusted to 8.0 with KOH and mixture was placed on ice. The fused vesicle suspension was applied on sucrose density gradient at aliquots of 5 ml per tube (30 ml) and centrifuged for velocity run (Beckman L-70, rotor Sw 28, 25000 rpm, 1 h, 4 °C). The bulk of the phospholipids liposome remained at the top of the gradient, whereas the membranes separated into the lower layer of fractions. Sucrose was removed from different fraction by washing with HEPES-KOH buffer and fused membrane was collected by centrifugation (Beckman L-70, rotor 60Ti, 55000 rpm, 1 h, 4 °C).

### **2.23 Method for negative staining**

A droplet of the sample (fused membrane in HEPES-KOH buffer pH 7.5) solution (1:100 diluted) was placed on Formvar® coated; glow discharged copper grids for adsorption. After about one minute the sample was almost sucked off leaving only a small layer of fluid left. After that a drop of “stain” (1% uranyl acetate in water) was put on the sample in the grid and sucked off after some seconds and this procedure was repeated for three times for complete removal of stain. After completely drying the grid it was viewed in an electron microscope (EM208S, FEI company). Images were taken with a TVIPS 1K x 1K slow scan CCD camera (Tietz, Munich, Germany). This experiment was conducted with help of Dr. Winfried Haase, department of structural biology, Max Planck Institute of Biophysics Frankfurt.

### 2.24 EPR spectroscopy

Electron spin echo decay measurements were performed with Sevdalina Lyubenova in the group of Prof. Prisner at Institut für Physikalische und Theoretische Chemie, using a Bruker Elexsys-580 X-Band spectrometer equipped with a Bruker MD5-W1 cavity and an Oxford CF935 helium flow cryostat with ITC-5025 temperature controller. A  $\pi/2$ - $\tau$ - $\pi$  Hahn echo sequence was used to measure the echo decay experiments on the maximum of the  $\text{Cu}_A$  signal, in the temperature range 10-25 K. The samples were transferred into standard quartz EPR tubes and subsequently frozen in liquid nitrogen. The sample typically contained 100  $\mu\text{M}$  fully oxidized  $\text{Cu}_A$  fragment and varying ratios of fully oxidized cytochromes in 5 mM HEPES–KOH pH 7.0, 10 % glycerol buffer. For cytochrome *c* oxidase measurement 50  $\mu\text{M}$  fully oxidized enzyme and different cytochrome *c* were mixed in the different ratios for relaxation experiment.

G-band Pulse EPR spectroscopy: Marloes Penning de Vries performed the measurements and spectral analysis in the department of Prof. Dr. T. Prisner at Institut für Physikalische und Theoretische Chemie, J.W.Goethe-Universität. A two-pulse echo sequence as described for X band was used for all measurements, with typical  $\pi/2$  pulse lengths of 40-60 ns and a minimum  $\tau$  value of 200 ns. The relaxation measurements were performed at the signal maximum corresponding to the  $g_{yy} = 2.02$  position. The temperature was set to 15 K and measured by a temperature sensor at the sample position with an estimated relative error of less than 1 K. Due to the strongly increased spectral width of the  $\text{Cu}_A$  spectra at G-band frequencies the typical sample concentration was set to 200  $\mu\text{M}$  fully oxidized  $\text{Cu}_A$  fragment and varying ratios of fully oxidized cytochromes in 5 mM HEPES –KOH pH 7.0, 10% glycerol. The samples were transferred into standard quartz capillary tubes and subsequently frozen in liquid nitrogen.

### 2.25 FRAP experiment

FRAP experiments were carried out under conditions of constant incident light intensity and uniform disk illumination in an epifluorescence microscope equipped with a conventional mercury arc lamp and a correct combination of a dichroic mirror and optical filters for the FITC fluorophore. Both the apparatus and the experimental procedure have been described (2.8.1). Experiments were performed at room temperature ( $\sim 20^\circ\text{C}$ ), with a bleaching time not exceeding 10% of the characteristic diffusion time. 20 recoveries were recorded at different locations in the sample under study. For this experiment membrane were fixed with

planar supported lipid bilayers. It was formed on cleaned cover slips mounted on a small tank adapted to the microscope stage. The cleaning procedure of the cover slips was of great importance with respect to the formation of the bilayer. Cover slips were first sonicated in ethanol for 5 min, dried in an oven for 15 min at 110 °C, immersed in Millipore water for 1 h and then rinsed extensively with water (15 times in a large volume of water). These clean cover slips were kept in water. Just before use, a cover slip was taken out of water and placed on the top of the sample cell.

### 2.26 FCS experiment

Fluorescence correlation spectroscopy (FCS) were performed with Chayan Nandi in the department of Prof. Dr. B. Brutschy at Institut für Physikalische und Theoretische Chemie, using on a commercial Confo-2 combination system (Carl Zeiss). All FCS measurements were performed in Cy5-labelled Fv fragment with native bacterial membranes. Dilutions were carried out in phosphate buffered saline (PBS)

### 2.27 Flash photolysis method

Chizhov *et al.* 1996 in (2.8.3) describe the flash photolysis apparatus used for rotational diffusion measurements in detail. Cytochrome *c* oxidase (*aa<sub>3</sub>* type) was purified from membranes of *P. denitrificans* according to (2.16.7). The final preparation of this *aa<sub>3</sub>* type of oxidase was made in the 20 mM Kpi 1 mM EDTA pH 8.0, 0.2 % DM. The fully reduced enzyme was prepared by the addition of a small excess of dithionite to a deoxygenated enzyme solution. It was exposed to CO for 15 min to form the fully reduced CO complex. The formation of the CO complex was confirmed by its Soret (441 nm) and visible (605 nm) spectral change in shape and shift of wavelength. The oxidation states and reduction state were determined by size and position of the Soret band and visible band at 605 nm and 441 nm respectively. Absorbance changes due to photolysis of the heme *a<sub>3</sub>*-CO complex were measured at 446 nm.

## 3. Results

### 3.1 Expression and purification of proteins

#### 3.1.1 Cu<sub>A</sub> fragment

The Cu<sub>A</sub> domain of subunit II of cytochrome *c* oxidase from *P. denitrificans* is a 16.6 kDa protein containing a binuclear Cu center with slow relaxing spin density ( $S=1/2$ ). The highest amount of Cu<sub>A</sub> binding domain was expressed in *E. coli* with a construct containing a His tag that was cleaved by TEV protease as described (Maneg *et al.*, 2003). The Cu<sub>A</sub> fragment was produced with a characteristic purple copper by refolding the denatured protein of inclusion bodies by removal of urea (2.15.1). For high-field EPR experiments, the protein was further purified by Ni-NTA column chromatography to remove any extra copper that is bound to the His tag. Mutational studies show an extensive area of exposed acidic residues on subunit II which are involved in the initial docking and its give a negative surface charge to the Cu<sub>A</sub> fragment (figure 4). In the Cu<sub>A</sub> fragment the main residues involved in the interaction are D135, D59, E126, E140, E142, D146, N160, Q120, and D178 resulting in a net negative charge on the surface (Drosou *et al.*, 2002).

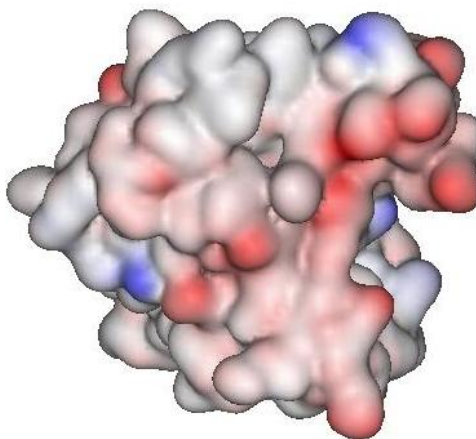


**Figure 4** The Cu<sub>A</sub> fragment, a set of acidic residues on the presumed docking site showed red in colour (Maneg *et al.*, 2003; pdb entry:1QLE)

The optical spectra were recorded at room temperature and field swap EPR spectra were measured at 15 K at X-band frequency (9 GHz) and G-band frequency (180 GHz) at 5 K in buffer (5 mM HEPES–KOH, pH 7.0, 10% glycerol) are shown in figure 6. The effective g tensor in specially arranged Cu in the Cu<sub>A</sub> fragment is shown in figure 5

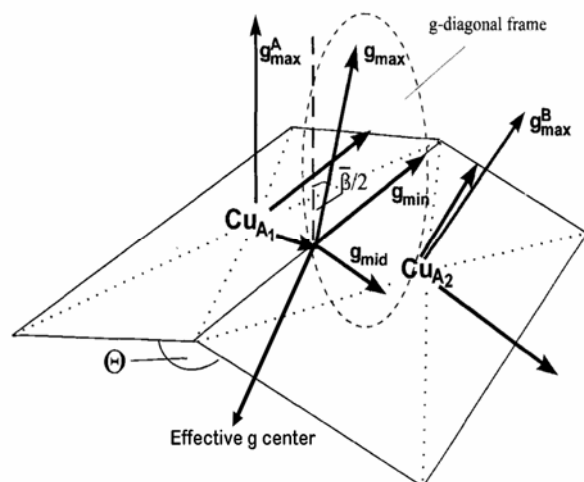


**Figure 5** The schematic construction of the  $g$ -tensor in a delocalized mixed-valence  $Cu_A$ . The effective  $g$  tensor between two  $Cu$  centers where the distance was calculated (modified Beinert 1997)

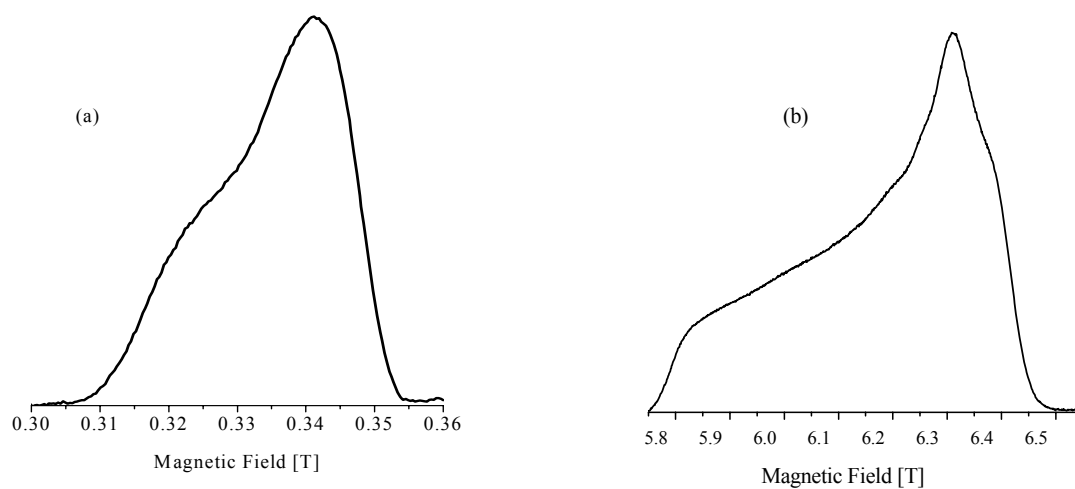


**Figure 6** Field swept echo detected EPR spectra of the  $Cu_A$  centre in the soluble  $Cu_A$  fragment

(a) X-band frequency (9 GHz),  $100 \mu M$   
 $Cu_A$ ,  $T=15 K$

(b) G-band frequency (180 GHz),  
 $3 mM Cu_A$ ,  $T=5 K$



### 3.1.2 Cytochrome $c_{552}$ fragment

The soluble fragment of cytochrome  $c_{552}$  from *P. denitrificans* was expressed in *E. coli* and its purification and biochemical characterization was performed according the protocol (Reincke *et al.*, 1999). The buffer of purified  $c_{552}$  fragment was changed with gradual decreasing of ionic strength of the buffer for the better adaptation of the soluble protein in low ionic buffer condition. The high resolution structure of soluble fragment of cytochrome  $c_{552}$  from *P. denitrificans* has been determined in both redox states at low salt concentrations by X-ray diffraction and NMR spectroscopy (Harrenga *et al.*, 2000; Reincke, *et al.*, 2001). Under the experimental conditions no significant redox coupled conformational changes can be observed.

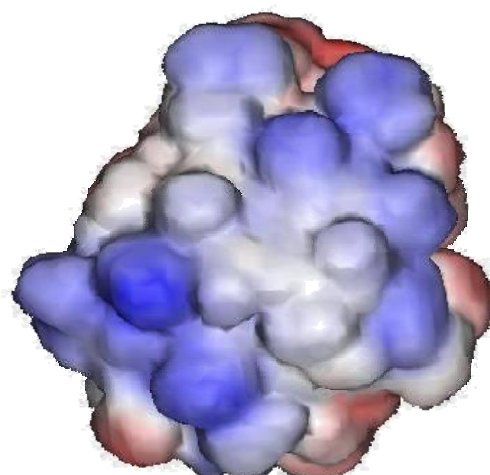


**Figure 7** *P. denitrificans* cytochrome  $c_{552}$  the positive charge on the surface due to presence of lysine residues showed in blue (Reincke *et al.*, 1999; pdb entry:IC7M).

The soluble fragment of cytochrome  $c_{552}$  possesses twelve strongly acidic residues and eleven strongly basic ones. The distribution of these charged residues is highly asymmetrical. As shown in figure 7, most of the basic residues are clustered around the solvent exposed heme edge. The surface around the exposed part of the heme is positively and the surface of the opposite side strongly negatively charged.

### 3.1.3 Horse heart cytochrome $c$

The structure of horse heart cytochrome  $c$  has been determined at 1.3 Å resolution (Bushnell *et al.*, 1990). The electrostatic surface potential of the eukaryotic cytochromes  $c$  looks qualitatively similar to *P. denitrificans* cytochrome  $c_{552}$ . Their surface is even more positively charged around the exposed part of the heme and their opposite side is less negatively charged (figure 8).

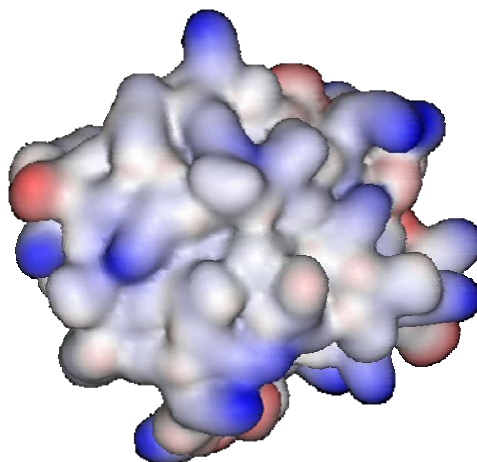


**Figure 8** Horse heart cytochrome *c*, positive charges shown in blue (Bushnell *et al.*, 1990; *pdb* entry:1HRC).

Lysine residues surrounding the exposed heme edge are believed to be important for a proper orientation and interaction with the redox enzymes (see review Banci *et al.*, 1999). Due to this nature, it is presumed that it has a higher binding constant for the Cu<sub>A</sub> fragment interaction.

### 3.1.4 Cytochrome *c*<sub>1</sub> fragment

The soluble *c*<sub>1</sub> fragment of the *bc*<sub>1</sub> complex has a molecular weight of 23.8 kDa. It was expressed in *E. coli* at 16°C. The purification was performed with two column chromatography according to the protocol provided by Julia Janzon (see also Eichhorn PhD dissertation 2003). For the EPR experiments, the fragment was used as a negative control and its structure shown in figure 9 is based on the yeast *bc*<sub>1</sub> complex coordinates (Hunte *et al.*, 2000).

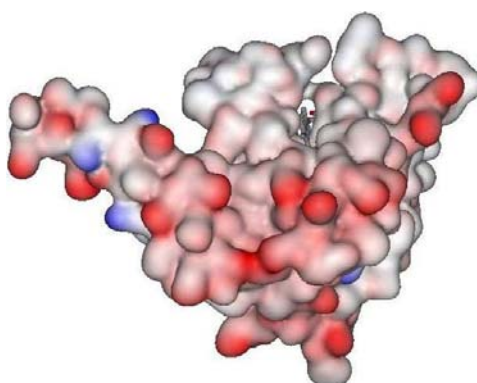


**Figure 9** Cytochrome *c*<sub>1</sub> a soluble fragment derived from *bc*<sub>1</sub> complex. The structure shown by alignment calculated on the basis of the yeast *bc*<sub>1</sub> complex and negative charges shown in red (Hunte *et al.*, 2000; *pdb* entry:1EZV).

### 3.1.5 *Thermus thermophilus* cytochrome *c*<sub>552</sub>

*T. thermophilus* cytochrome *c*<sub>552</sub> is a soluble class I *c* type cytochrome with a molecular mass of 14.2 kDa (131 amino acid residues). The structure was determined at 1.3 Å resolution by Soulimane *et al.*, 1997. It was expressed in *E. coli* and purified according to a procedure described by Maneg *et al.*, 2003. *T. thermophilus* cytochrome *c*<sub>552</sub> was used as a negative control to the binding interaction studies between the Cu<sub>A</sub> and cytochrome *c*<sub>552</sub> from *P. denitrificans*. The surface potential between the *T. thermophilus* cytochrome *c*<sub>552</sub> and *P. denitrificans* cytochrome *c*<sub>552</sub> reveals significant differences in the charge distribution. The structure shows mostly uncharged residues around the exposed heme edge. The positive potential at heme proximity due to results from the strong positive charge of iron. The different charge distribution of residues results from its hydrophobic nature (Figure 10)

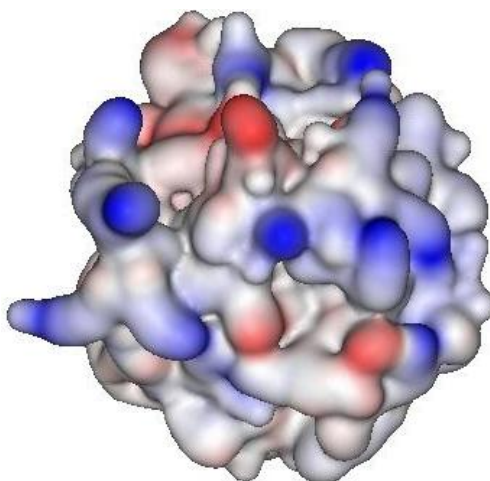


**Figure 10** Cytochrome *c*<sub>552</sub> from *Thermus thermophilus*, different surface charges due to its hydrophobic nature (Soulimane *et al.*, 2000; pdb entry:1C52).

### 3.1.6 Membrane bound cytochrome *c*<sub>552</sub>

The native cytochrome *c*<sub>552</sub> (full length), a 18 kDa protein, contains three functional domains: an N-terminal helical membrane anchor, a negatively charged spacer region, and a typical class I *c*-type heme domain. This membrane-anchored cytochrome *c*<sub>552</sub> is believed to be the main electron transfer shuttle protein between the *bc*<sub>1</sub> complex and *aa*<sub>3</sub> oxidase in native membranes of *P. denitrificans*. A kinetic interaction study of full-length cytochrome *c*<sub>552</sub> and cytochrome *c* oxidase from this organism has been reported (Drosou *et al.*, 2002).

### 3.1.7 Cytochrome *c* oxidase

The four subunit cytochrome *c* oxidase was purified with the method described (2.15.7). After purification buffer was changed from (20 mM KPi, pH 8.0, 0.2 % DM) to EPR buffer. For reconstitution experiment, the buffer of purified oxidase was changed in 10 mM HEPS-KOH, pH 7.3, 0.02% DM buffer.

## 3.2 EPR experiments

### 3.2.1 Relaxation measurement of the Cu<sub>A</sub> fragment with different cytochromes

The relaxation experiments were started with a model system (one paramagnetic centre and soluble nature) to measure the distance and orientation of these two interacting partners. The spectrum was taken with Sevdalina Lyubenova. The Cu<sub>A</sub> domain of cytochrome *c* oxidase acts as a slowly relaxing spin (3.2.2). The other reaction partner cytochrome, with the *c* type heme (Fe) in its low spin ( $S=1/2$ ) acts as a fast relaxing spin (3.2.3). In electron spin echo decay experiments the intensity of a Hahn echo is recorded as a function of separation time  $\tau$  between the two pulses. The Hahn echo sequence ( $\pi/2-\tau-\pi$ ) was used to measure both the field-swept EPR spectra (Figure 6a) and the echo decay traces. The X-band two-pulse echo decay experiments were performed in the temperature range 10-25 K and taken at a field position corresponding to the maximum of the Cu<sub>A</sub> signal (corresponding to the  $g_{\perp}$  position). The G-Band Pulse EPR experiments were performed with a two-pulse echo sequence with typical  $\pi/2$ -pulse lengths of 35-40 ns and a minimum  $\tau$  value of 200 ns. The relaxation measurements were mainly performed between the signal maximum and the high-field edge (Figure 6b), corresponding to the  $g_{yy}$  and  $g_{xx}$  positions respectively, in a temperature range of 5-15 K. Here we started to analyze the distance and orientation between different cytochromes *c* and the Cu<sub>A</sub> fragment by X-band and G-band pulsed EPR spectroscopy. It is a model system for method development for measurement of distance and orientation before going to the supercomplex like environment where more paramagnetic centers will be present. The kinetics of the electron transfer reaction between the different cytochromes and a soluble Cu<sub>A</sub> fragment from *P. denitrificans* have also been studied by stopped flow experiments and its interaction by chemical shift change by NMR spectroscopy (Maneg *et al.*, 2003; Wienk *et al.*, 2003).

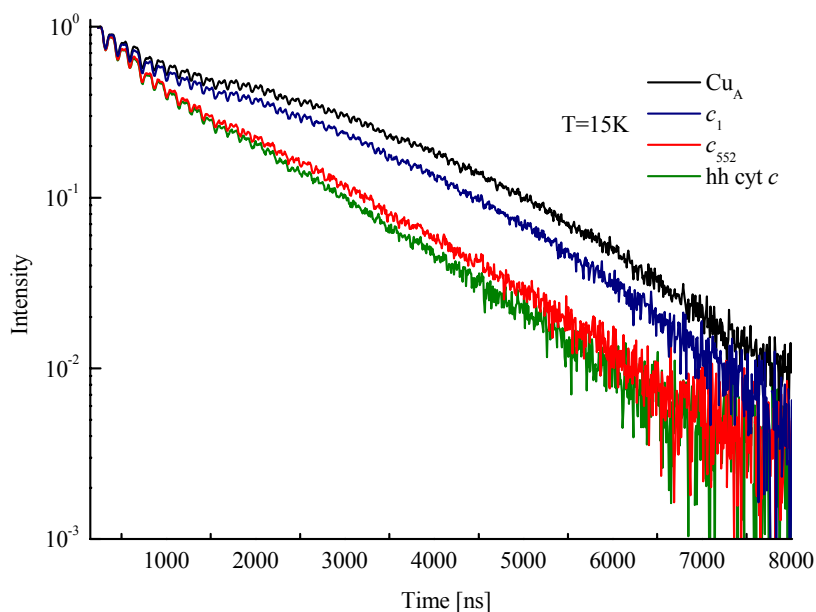


**Figure 11** The two-pulse echo decay traces of the  $Cu_A$  fragment alone or in the presence of cytochrome  $c_{552}$ , horse heart cytochrome  $c$ , and cytochrome  $c_1$ , were measured under the same conditions (temperature 15 K, field position corresponding to  $g_{\perp}$  of the  $Cu_A$  signal).

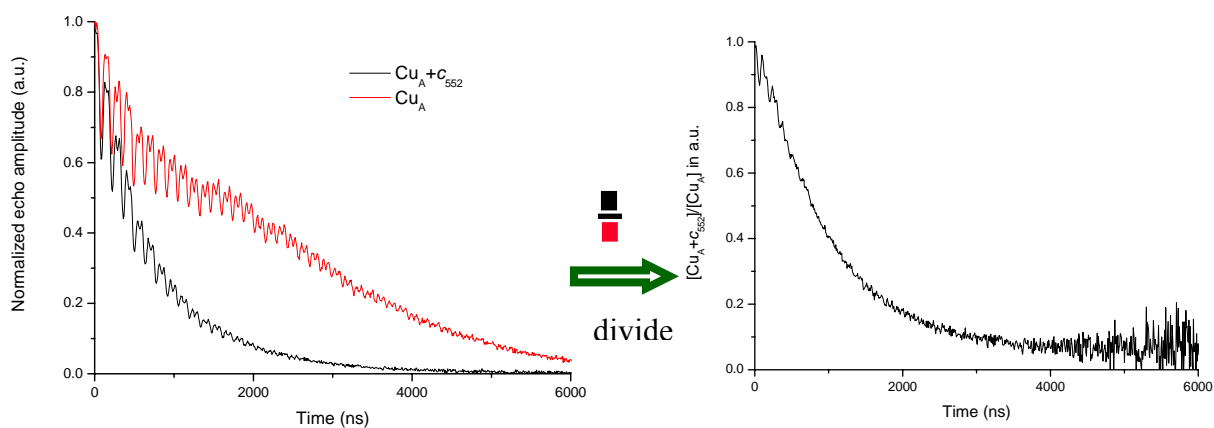


**Figure 12** Division method for dipolar coupling: Electron spin-echo decay traces of:  $100 \mu M Cu_A$  fragment alone and in a  $100 \mu M : 100 \mu M$  mixture with cytochrome  $c_{552}$  ( $Cu_A + c_{552}$ ). The division of these two time traces ( $Cu_A + c_{552}$ )/ $Cu_A$  yield the pure dipolar relaxation.

The two-pulse echo decay experiments were performed with the Cu<sub>A</sub> fragment and several partner proteins: (i) a soluble domain of cytochrome *c*<sub>552</sub>, is similar to the mitochondrial cytochrome *c* and mediates electron transfer between the *bc*<sub>1</sub> complex and *aa*<sub>3</sub> oxidase (ii) horse heart cytochrome *c* having similar binding affinity to Cu<sub>A</sub> as cytochrome *c*<sub>552</sub> (iii) cytochrome *c*<sub>1</sub> fragment derived from *bc*<sub>1</sub> complex which contains negative charges on the surface like Cu<sub>A</sub> fragment was used as negative control. The qualitative effect of the relaxation behaviour with the Cu<sub>A</sub> fragment and different cytochromes is shown in Figure 11.

The decay of the slow-relaxing species (Cu<sub>A</sub>) shown in the Figure 11, is not only caused by dipolar relaxation ( $\phi^{\text{dip}}$ ), but also by the intrinsic Cu<sub>A</sub> relaxation,  $\phi^{\text{CuA}}$ . We measure the product of these signals. At X-band, the signal is additionally modulated by the hyperfine coupling ( $\phi^{\text{mod}}$ ) of protons and nitrogen to Cu<sub>A</sub>.

This gives a total echo signal:

$$\begin{aligned}\phi^{\text{obs}} &= \phi^{\text{CuA}} \phi^{\text{mod}} \quad \text{Cu}_A \\ \phi^{\text{obs}} &= \phi^{\text{dip}} \phi^{\text{CuA}} \phi^{\text{mod}} \quad \text{Cu}_A + c_{552}\end{aligned}$$

The division of these two spectra provides the pure dipolar relaxation trace shown in figure 12. The division method removes all intrinsic relaxation and hyperfine modulation of the Cu<sub>A</sub> paramagnetic center and allows the extraction of pure dipolar coupling between the two interacting partners. The distances and orientation between these two proteins were calculated as follows:

$$D \sim \frac{g_{\text{eff}}^s g_{\text{eff}}^f}{r^3} (3 \cos^2(\theta_D) - 1)$$

The relaxation enhancement depends on the dipolar coupling, (D), which depends strongly on orientation and length (r) of the dipolar vector between the two paramagnetic centers, and on the angle ( $\theta_D$ ) of this vector with respect to external magnetic field (f and s superscripts denoting the fast relaxing (heme) and slow relaxing species (Cu<sub>A</sub>)). Data clearly show the relaxation enhancement of Cu<sub>A</sub> upon addition of the *P. denitrificans* cytochrome *c*<sub>552</sub>. The pure dipolar relaxation traces (divided by Cu<sub>A</sub> traces) of Cu<sub>A</sub> with these three different cytochromes are shown in figure 13. As can be seen, the dipolar relaxation traces for the Cu<sub>A</sub> fragment in the presence of either of the specifically binding cytochromes, horse heart cytochrome *c* and *P. denitrificans* *c*<sub>552</sub> are very similar to each other and their decay is much faster than non-binding cytochrome *c*<sub>1</sub>.

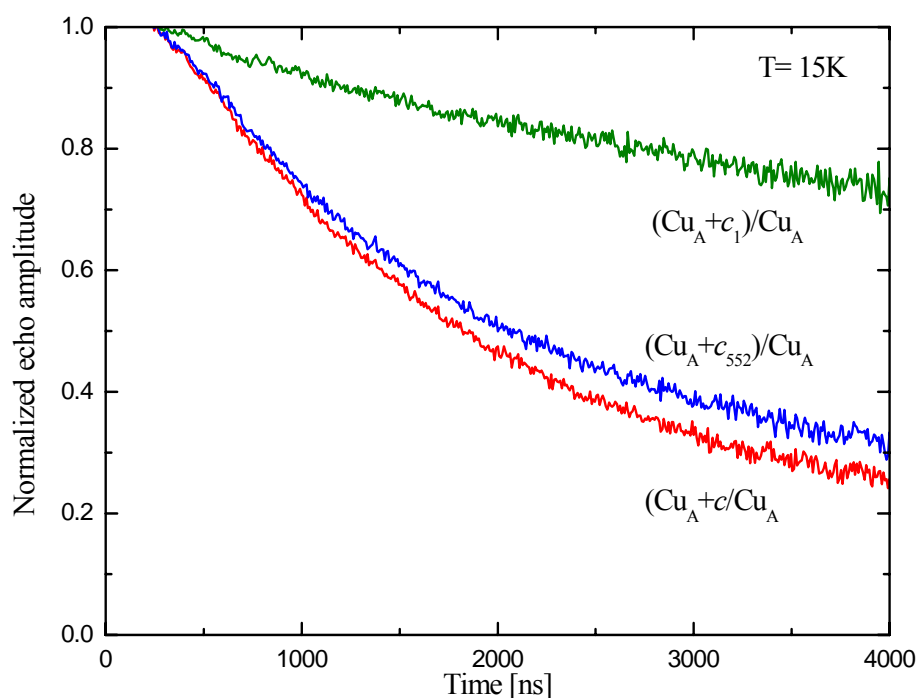


**Figure 13** Dipolar relaxation traces of 100  $\mu\text{M}$ :100  $\mu\text{M}$  mixtures of  $\text{Cu}_A$  with horse heart cytochrome  $c$  ( $(\text{Cu}_A+c)/\text{Cu}_A$ ), cytochromet  $c_{552}$  ( $(\text{Cu}_A+c_{552})/\text{Cu}_A$ ) and cytochrome  $c_1$  ( $(\text{Cu}_A+c_1)/\text{Cu}_A$ ) measured at the same experimental conditions as given in fig 11 (temperature 15K)

### 3.2.2 Effect of ionic strength of buffer

The  $\text{Cu}_A$  fragment and the different cytochromes were isolated in the different buffer conditions. For EPR measurements HEPES-KOH (pH 7.0) was chosen as buffer due to its higher buffering capacity and lower pH drift compared to other buffers like Bis-Tris and phosphate buffer at lower temperature. All EPR experiments were performed at 4 to 25 K temperatures. The ionic strength of the buffer plays an important role for the complex formation (see review Maneg *et al.*, 2003). The strong ionic strength dependence on the complex formation and mutagenesis studies (Witt *et al.*, 1999) a two-step model has been proposed for the interaction of cytochrome  $c$  oxidase with its substrate cytochrome  $c$ . In the first step, the orientation is mediated by long-range electrostatic forces, followed by the fine-tuning of the interaction by hydrophobic patches within the docking site of the two-partner proteins. For EPR experiments, the relaxation of the two proteins was not changed when the ionic strength of the buffer was changed from 1 mM to 5 mM. Higher ionic strength leads to dissociation of the complex formation but increasing the ionic strength from 1 to 5 mM does not affect binding and it increases buffering capacity and prevents unspecific binding of the two soluble proteins.

### 3.2.3 Effect of glycerol

Glycerol has been used for many years to stabilize the activity of enzymes and the native structure of recombinant proteins, since glycerol decreases the surface tension of water to stabilize the protein (Kornblatt *et al.*, 1992). The two soluble proteins which have molecular weights of 10.5 kDa (cytochrome  $c_{552}$ ) and 16.0 kDa ( $Cu_A$ ) have a strong tendency to self associate at lower buffer concentration. To avoid aggregation, decrease unspecific interaction and stabilize the interaction between the two proteins all the experiments were performed in buffer containing 10% glycerol. The low amount of glycerol does not have any effect on the binding of the two proteins and shows consistent results with all the soluble proteins used for EPR experiment.

### 3.2.4 Oxidation of cytochrome $c_{552}$

The cytochrome  $c_{552}$  and horse heart cytochrome  $c$  were oxidised with  $K_3Fe(CN)_6$ , because the heme (Fe) is paramagnetic in oxidised state. But relaxation measurement showed that  $K_3Fe(CN)_6$  binds to the heme and influence the relaxation behaviour of the  $Cu_A$ -cytochrome  $c$  transient complex. Due to binding of  $K_3Fe(CN)_6$  to cytochrome, it was oxidize with the small amount of cytochrome  $c$  oxidase. The oxidase accepts electron from the cytochrome  $c$  and forms  $Fe^{+3}$  (oxidation state). The oxidation state was checked by optical spectroscopy. Oxidized sample was purified by gel filtration and used for EPR measurements.

### 3.2.5 Concentration effect

For relaxation measurements, the  $Cu_A$  fragment and the various cytochromes were started with an equal molar ratio. The experiment was performed with different ratios to get the transient complex in the 1:1 ratio because due to higher concentration and unspecific binding the following scenario were possible: (i) the  $Cu_A$  see more than one cytochrome (ii) the unspecific binding of cytochrome to the  $Cu_A$  site (iii) and 1:1 complex formation.

The effect of higher concentrations of cytochrome  $c_1$  in the mixture (100  $\mu$ M  $Cu_A$ : with varying amount of  $c_1$ ) lead to a linear concentration dependence of the decay traces. Much stronger relaxation effect was observed in the case of two specific binding cytochromes. Similar results have been obtained at G-Band (180 GHz) frequency. The binding cytochromes show faster dipolar relaxation traces compared to the non-binding cytochrome  $c_1$ . The difference shows less pronounced effect compared to the X-band EPR results



because higher protein concentration (200  $\mu\text{M}$ ) had to be used at this frequency for sensitivity reasons.

### 3.2.6 Temperature dependence

Due to the strong temperature dependence of the longitudinal relaxation time ( $T_1$ ) of cytochrome *c* the dipolar relaxation traces should have a strong temperature dependence as predicted by theory (Eaton and Eaton, 2000; Lyubenova *et al.*, submitted). The dipolar relaxation traces in the temperature range 12-23 K of the complex of  $\text{Cu}_A$  fragment with horse heart cytochrome *c* and  $c_{552}$  is shown with simulation (Figure 13). Both complexes show indeed a pronounced minimum in dipolar relaxation at a temperature of about 15 K. The temperature dependence of the echo decay traces for the cytochrome  $c_1$  mixture is very different and shows different temperature dependence. Not only is the strength of the dipolar relaxation much weaker in this case, but the decay curves are monoexponential at all temperatures and do not show a pronounced minimum in dipolar relaxation. It is in agreement with our assumption that cytochrome  $c_1$  does not build a specific protein complex with  $\text{Cu}_A$  fragment.

### 3.3.7 Simulation of pure dipolar coupling

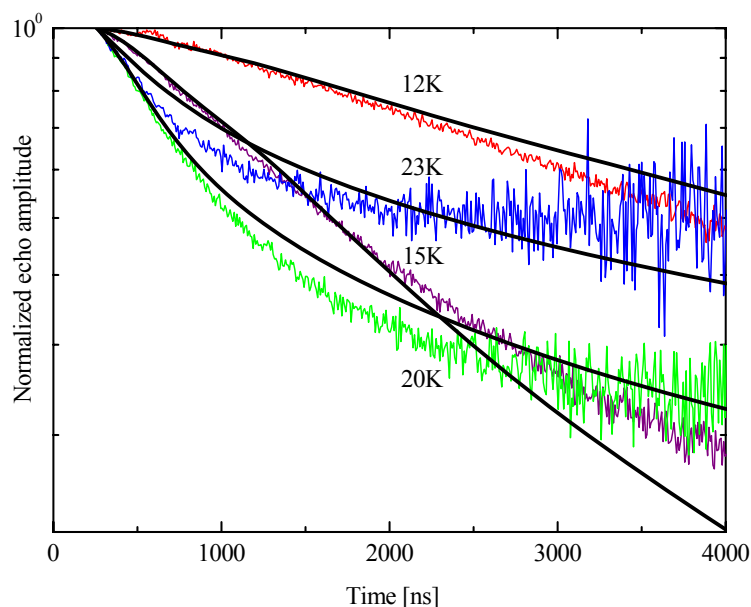


**Figure 14** Experimental X-band relaxation traces of 100  $\mu\text{M}$  : 100  $\mu\text{M}$  mixtures of the  $\text{Cu}_A$  fragment with horse heart cytochrome *c*, measured at different temperatures with simulations (black lines). The fit parameters are: dipolar angles:  $\theta_D=54^\circ$ ,  $\phi\Delta=11^\circ$ , distance Fe to center Cu-Cu:  $R_1=23 \text{ \AA}$ ,  $R_2=40 \text{ \AA}$ , Euler angles: set1=(27,6,29) $^\circ$ , set 2=(90,57,12) $^\circ$ , relative amplitudes of both structures :  $A_1=1.2$ ,  $A_2=1$ , unbound  $\text{Cu}_A$  fragment =11%. Experimental parameters as in Figure 13 described in section 3.3.7 (simulation work is done in the group of Prof. Prisner).

A home written simulation program (SIMPLEX algorithm, MatLab ) was used by Sevdalina Lyubenova to simulate the temperature dependence of the dipolar relaxation time traces for the transient complex between Cu<sub>A</sub> and cytochromes. The simulation was performed with the known values for both g-tensors and the T<sub>1</sub> value for the cytochrome *c* taken from the literature (Scholes *et al.*, 1984; Brautigan *et al.*, 1977) and the g-tensor values for cytochrome *c*<sub>552</sub> were obtained from X-Band measurements. The fit parameters are: the distance between the two paramagnetic centers R; the polar angles ( $\theta_D$  and  $\varphi_D$ ) describing the orientation of the R vector with respect to the Cu<sub>A</sub> g-tensor axis system; the Euler angles ( $\alpha$ ,  $\beta$ ,  $\gamma$ ) describing the orientation of the cytochrome *c* g-tensor axis system (and therefore the orientation of the cytochrome *c*) within the frame of the Cu<sub>A</sub> g-tensor axis system. These values were reproduced in simultaneous SIMPLEX fits of the dipolar decay traces at all temperatures for random starting values.

### 3.3 Membrane purification

*P. denitrificans* cells grown in methylamine medium have a higher heme to protein ratio compared to cells grown in succinate medium. The inner cytoplasmic membrane contains all respiratory complexes is isolated by three different methods (2.13) to get large size of membrane vesicle. Membranes were further purified by sucrose gradient centrifugation (2.13.4) to get high purity of respiratory complexes. The purified dark brown coloured membranes were used for different experimental setup.

### 3.4 Reconstitution

Different strategies have been described for membrane protein incorporation in lipid membranes (Rigaud *et al.*, 1995; Rigaud and Levy, 2003). The “step-by-step” reconstitution method proved a powerful reconstitution procedure for mitochondrial and bacterial respiratory complexes. In this method, the phospholipids and detergent were mixed and micelles were formed. Thereafter, protein was added to the preformed micelles. Detergent was removed with dialysis or bio-beads method (Rigaud *et al.*, 1997).

Here, cytochrome *c* oxidase was reconstituted in asolectin, and detergent was removed by dialysis. The reconstitution process had to be examined more precisely, which was done using strategies described by Rigaud *et al.*, 1988. Since membrane reconstitution is dependent on the type of detergent used, lipid to protein ratios, and the physical state of the lipid-detergent mixture, these parameters were studied in detail by Draley-Usmar method

(Draley-Usamr *et al.* 1987). Proteoliposomes were reconstituted of oxidase: asolectin in a ratio of 1:80 (w/w) and were formed by detergent solubilisation described in the method section.

These strategies for reconstitution were used for oxidase and asolectin for different type of experiment. For EPR experiments the ratio was used 1:1 (heme ratio) between the oxidase and membrane bound cytochrome *c*<sub>552</sub>. In the lateral diffusion experiment, it was reconstituted as in ratio of bacterial membrane protein to lipid (1:80 w/w).

The isolated supercomplex was reconstituted in the purified lipid from asolectin and *Parracocus* lipid with a ratio of protein and lipid 1:40, 1:80, and 1:120 (w/w). The detergent was removed by Bio-bead method for quick removal of detergent from the lipid mixture. The reconstitution of supercomplex in the liposome vesicles was checked by BN PAGE.

### 3.5 Size of the membrane vesicles

The size of membrane vesicles was measured with Zeta sizer Nano ZS (Malvern Instruments UK) at 25 °C. The zeta sizer is based on the principle of Photon Correlation Spectroscopy (PCS) and its measures particles in the sub micron region. For small particle, size the only one major competing technique is electron microscopy. PCS measures Brownian motion and relates this to the size of particles. Three independent methods were used for membrane vesicles preparation. The size of membrane vesicles were measured on the gradient purified native membranes diluted in PBS. The data demonstrate the three different types of methods used for vesicle preparation yield three different size distributions. The size of the membrane vesicle were averaged and calculated by automated software programme (Malvern Instruments UK).

| Method of membrane preparation | Diameter of membrane vesicle |
|--------------------------------|------------------------------|
| Osmotic shock                  | 300 nm                       |
| Sonication                     | 180 nm                       |
| Manton-Gaulin Press            | 200 nm                       |

### 3.6 Fusion of membrane

Several methods to produce large vesicles have been developed and reported in the literature. One of the methods that have been applied successfully to produce large proteoliposomes is based on a dehydration-rehydration procedure described by Criado and Keller (1987). Such a method consists of the dehydration of biological membranes or

performed proteoliposomes in the presence of added exogenous lipids followed by a rehydration process in the desired buffer (Ajouz *et al.*, 2000). As a variant of this method, the rehydration of thin dried films

obtained after the evaporation of the solvent from lipid-protein complexes solubilised in organic solvents has been used to produce giant proteoliposomes (Darszon *et al.*, 1980). The main disadvantage of this dehydration-rehydration method is that the supercomplex may become inactive and disturb the native membrane environment.

### 3.6.1 Electrofusion method

The native membranes were tried to fuse with a new method based on a procedure for the reconstitution of transmembrane proteins into GUVs (Doeven *et al.*, 2005). This method involves partial dehydration of native membrane on conductive glass surfaces; and controlled rehydration in the presence of an alternating electric field to form giant vesicles (Angelova *et al.*, 1992). The dehydrated native membrane was made on electro conductive glass slides. The native membrane was not completely dehydrated to avoid the biological activity of the protein inside the native membrane. Thus, it is essential to perform a partial dehydration of native membrane under controlled humidity, i.e., under saturated solution of NaCl. In the next step of the fusion, process is a rehydration step in the presence of an AC electric field. Growing of large GUVs from the rehydrated lipid-protein film was promoted with an AC electric field with increments from 20 mV to 1.1 V at 12 Hz frequency. Once the GUVs were formed, the AC frequency was lowered to 4 Hz and the voltage raised to 2 V for 30 min. This helped the mature giant vesicles to adopt a spherical shape and to separate them from the glass slides.

It is important to stress that the buffer composition used for the preparation of native membrane and for the rehydration step is crucial, considering that low ionic strengths impede the formation of giant vesicles by electroformation. The composition of the buffers used for the preparation of the preformed liposomes and for the rehydration buffer is very important since the process of GUV formation by electroformation requires low ionic strengths (Angelova, 2000). The initial experiment was performed with Prof. Klaus Fendler Max Planck Institute and the optimization condition was tried with Dr. Kirsten Bacia Institute of Biophysics, Biotechnologisches Zentrum der TU Dresden for the fusion of native membrane . Due to different complexity in the native membrane, no fusion was observed by this method.

### 3.6.2 Ca<sup>++</sup> induced fusion

In the case of Ca<sup>++</sup> induced fusion the ion concentrations plays an important role (Miller and Racker 1976). Figure 16 shows that no fusion occurred in the presence of 20 mM Ca<sup>++</sup>, membranes only gets aggregated and the shape of the membrane changes. At pH 6.0, in the presence of Ca<sup>++</sup> and asolectin small fused bacterial membrane vesicles were observed in close apposition with the bacterial membrane, indicative of the fusion process. As expected with membrane fusion, an average increase in membrane surface area occurred progressively from Ca<sup>++</sup> ion addition in the presence of asolectin. However, the relative; distribution of the size in this method remained unchanged (Figure 17). In the presence of lower concentrations of Ca<sup>++</sup> and asolectin, the fusion occurred but it was not good enough.

### 3.6.3 pH dependent fusion

The pH dependent fusion procedure in the presence of added asolectin was done at 32 °C. The condition was optimised for the membrane and fused membrane was separated by velocity gradient centrifugation. After centrifugation, it separated in two distinct zones. These fractions were designated as upper cream colour zone and lower light brown colour zone. An additional band, which did not penetrate into the gradient, contained free asolectin. The procedure was optimised with all conditions held constant except for incubation time, which was used to control the percentage yield of each membrane fraction: shorter incubations produced more non-fused membrane zone and less fused one, whereas longer incubations produced more fused and less unfused. After fusion, negative staining assessed the ultra structural details of fused membranes. The non-fused wild type gradient purified membrane is shown in figure 15. It reveals that the average size of the vesicles is in the range of 100-150 nm.

If fusion occurs between the membranes, lipid-to-membrane protein ratio must increase. Furthermore, it is important to determine that such an increase does not occur because of loss of membrane protein during the fusion process. The protein concentration was determined in the fused membrane (Lowry *et al.*, 1951). After the pH induced fusion in the presence of asolectin, the separation on velocity gradient shows the difference in the band size compared to native membrane due to changed buoyant density. Cytochrome *c* oxidase was quantified in order to assess the possibility of membrane protein loss during the fusion process. As cytochrome *c* oxidase, a heme *a*-containing, redox protein is completely membrane-

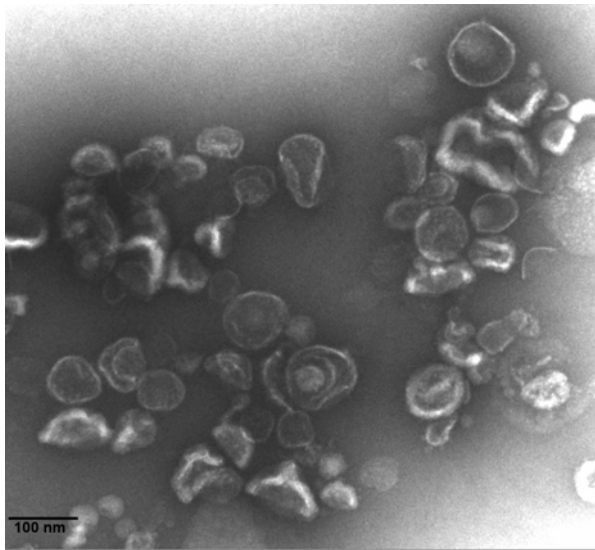


**Figure 15** Gradient purified cytoplasmic membrane of *P. denitrificans*; bar = 100 nm.

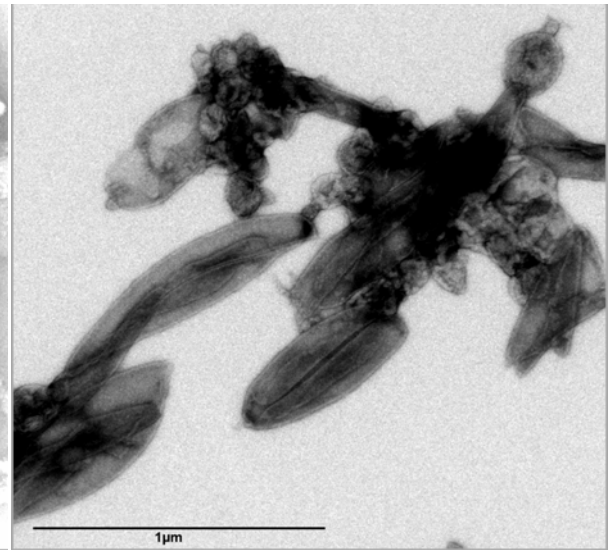


**Figure 16** High concentration of  $\text{Ca}^{++}$  shows the changes in the shape and aggregation of membrane; bar = 1  $\mu\text{m}$ .

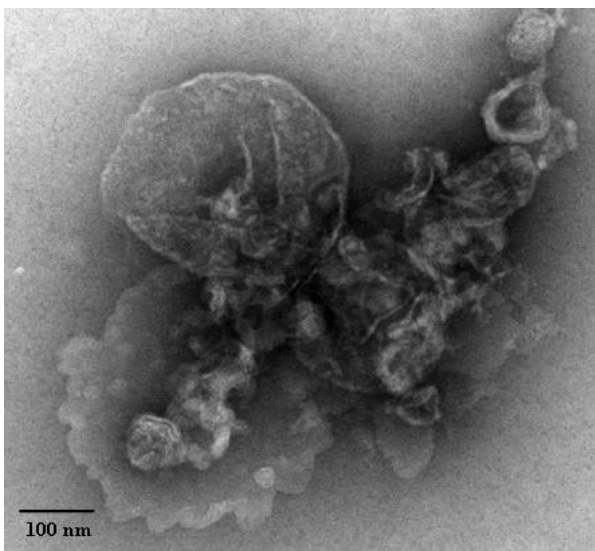


**Figure 17**  $\text{Ca}^{++}$  induced fusion in the presence of externally added asolectin; bar = 100 nm

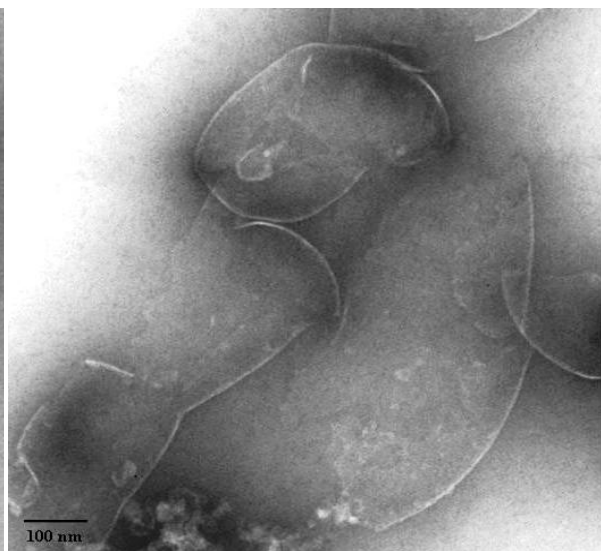


**Figure 18** pH induced fusion of membrane in the presence of externally added asolectin; bar = 100 nm

imbedded it can be quantified by the difference spectra. Heme content per mg of total membrane protein remained constant in sucrose density fractions indicating that loss of membrane protein did not occur during lipid addition of the inner membrane.

The fusion of inner mitochondrial membrane described that the distribution of the inner membrane particles decreased in density but remained random and membrane became increasingly enriched with phospholipids indicated that integral proteins can diffuse independently of one another in the plane of the inner membrane (Schneider *et al.*, 1980). Here in the case of the bacterial membrane, the asolectin only facilitate their fusion and it is not added in a large excess. After membrane fusion, the extra lipid would not affect the architecture of the native membrane and supercomplex composition. To prove this, we would do the FCS experiment in the native membrane to examine the supercomplex.

### 3.7 Deletion mutant

The parental strain wild type *P. denitrificans* Pd1222 was used in this study (De Vries *et al.*, 1989). The wild type membranes of this contain all the complexes in the supercomplex 'respirasome'. In strain MK6, the complex III is replaced by a kanamycin resistance cassette introduced via homologous recombination (Korn *et al.*, 1994). The different complex deletion mutant was used for the lateral diffusion experiment to compare the supercomplex formation in native membrane. The complex IV deletion mutant MR31 was used in the flash photolysis experiment to check the specificity of carbon monoxide (CO) binding to oxidase in the native membrane that no other complex interfere with the binding of CO at observation wavelength.

### 3.8 Translational diffusion experiments

#### 3.8.1 Expression and purification of Fv fragment

Fv fragment is the smallest unit of the antibody that retains the binding characteristic and specificity of the whole antibody molecule. The Fv fragment is a non-covalently associated heterodimer of the variable domains of the antibody heavy chain and light chain. It was expressed in *E. coli* and purified with one step purification method. The Fv fragment had been used for crystallization of membrane proteins (Ostermeier *et al.*, 1995). The cytochrome *c* oxidase from *P. denitrificans* co-crystallised with Fv fragment (Iwata *et al.*, 1995) is shown in figure 20. The Fv fragment contains surface exposed lysine residues where the dye molecule binds. A schematic diagram with dye is shown in figure 19. The Fv

fragment coupled directly to fluorescence and nanogold particles was shown with immunoelectron and immunofluorescence microscopy (Ribrioux *et al.*, 1996). The Fv fragment recognizes an epitope on subunit II of the cytochrome *c* oxidase which is localized on the periplasmic surface of the inner membrane of *P. denitrificans*. This was determined by immunoelectron microscopy and X-ray crystallography (Kleymann *et al.*, 1995; Ostermeier *et al.*, 1997).

### 3.8.2 Fv fragment labelling by FITC

Proteins can be covalently modified in many ways to suit the purpose of a particular assay. The most common target for protein labelling is primary amines like lysine residues. The lysine residues are abundant, widely distributed and easily modified because of their reactivity and their location on the surface of proteins.

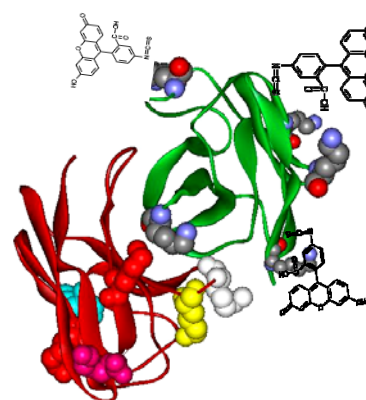


**Figure 19** Presence of lysine residues in the Fv fragment only three residues were surface accessible for dye binding

Fv antibody fragment was labelled with a number of different fluorescent probes currently available from commercial sources. Each probe has its own characteristic spectral signals of excitation (or absorption) and emission (or fluorescence). Fluorescein (the reactive isothiocyanate form, FITC) is currently the most commonly used fluorescent dye. FITC is a small organic molecule, and is typically conjugated to proteins via primary amines (i.e., lysine). Usually, between 2 to 4 FITC molecules are conjugated to each Fv fragment (Ribrioux *et al.*, 1996). Thus, an antibody will usually be conjugated in several parallel reactions to different amounts of FITC to choose the optimal conjugation ratio. The 488 nm line of an argon laser typically excites fluorescein, and emission was collected at 530 nm. The extents of FITC conjugation to the antibody depend on the concentration of antibody and dye in solution. Before the conjugation of dye, the buffer of Fv fragment was exchange by dialysis or a concentrator to reaction buffer. Optical spectroscopic method was used for calculation of concentration of Fv fragment and degree of labelling. Under these condition, 2-3 dye molecules were conjugated with Fv fragment.





**Figure 20** Ribbon structure of four subunit cytochrome c oxidase with Fv fragment yellow subunit I; red subunit II; dark green subunit III, blue subunit IV); and light and heavy chain of Fv fragment are shown in light green and red in colours (Iwata et al., 1995; pdb entry:1QLE)

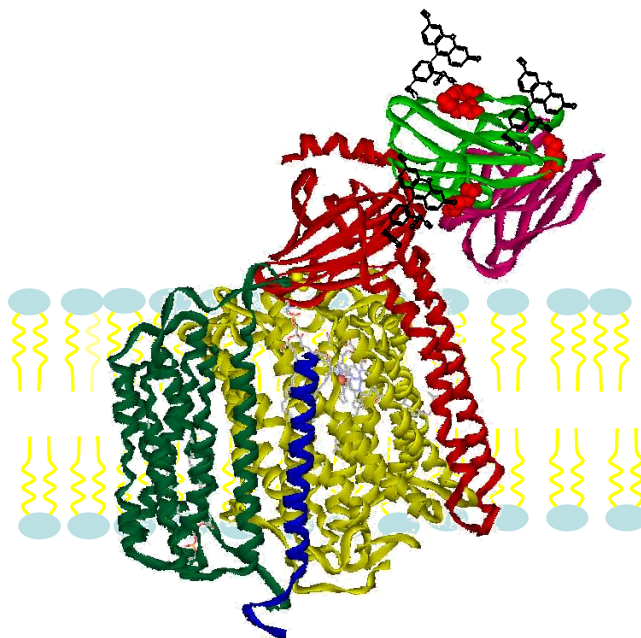


**Figure 21** Schematic representation of binding of labelled Fv fragment to cytochrome c oxidase in membrane plane based on our experimental observation and Ribrioux et al., 1996

### 3.8.3 Fv labelling by Cy5 dye

Cy5 dye, a small organic molecule is typically conjugated to proteins via primary amines (lysines). Usually, between 2 to 3, Cy5 molecules are conjugated to each antibody and higher conjugations can result in solubility problems as well as internal quenching. The 633 nm line of He-Ne laser typically excites Cy5, and emission was collected at 680 nm. The entire conjugation was performed according to method (2.17.8). The extent of Cy5 conjugation to the antibody depends on the concentration of antibody and dye in solution. An absorbance spectrum was taken at every step for the efficiency calculation and it shows that 2-3 dye Cy5 molecule conjugate with Fv fragment.

### 3.8.4 Fluorescence Recovery after Photo bleaching (FRAP)

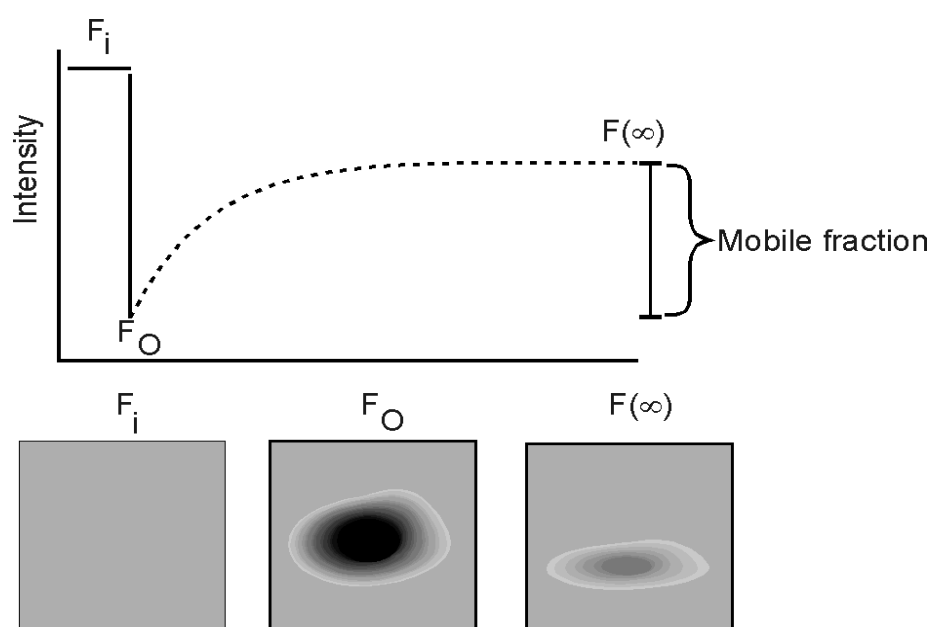


**Figure 22** Principle of FRAP: a region in the fluorescent area is bleached at time  $t_0$  the fluorescence decreases from the initial fluorescence  $F_i$  to  $F_0$ . The fluorescence recovers over time by diffusion until it has fully recovered ( $F_\infty$ ). The mobile fraction can be calculated by comparing the fluorescence in the bleached region after full recovery ( $F_\infty$ ) with that before bleaching ( $F_i$ ) and just after bleaching ( $F_0$ ) (<http://www-cellbio.med.unc.edu/facilities/frap.htm>)

FRAP describes the fluorescence redistribution after photo bleaching. FRAP experiments provide information about the mobility of a fluorescent molecule in a defined area (Axelrod *et al.*, 1976). Two parameters can be deduced from FRAP: the mobile fraction of fluorescent molecules and the rate of mobility, which is related to the characteristic diffusion time,  $t_D$ . Figure 22 shows a typical fluorescence recovery curve, allowing the determination of the

two parameters. The mobile fraction can be determined by comparing the fluorescence in the bleached region after full recovery ( $F_{\infty}$ ) with the fluorescence before bleaching ( $F_i$ ) and just after bleaching ( $F_0$ ). The mobile fraction  $R$  is defined as

$$R = (F_{\infty} - F_0)/(F_i - F_0)$$

When a molecule is assumed to be a sphere with a volume proportional to its molecular mass, the diffusion coefficient is proportional to the inverse of the cube root of molecular mass ( $D \sim M^{-1/3}$ ).

Native biological membranes are far from being homogeneous mixtures of their lipid and protein components. In fact, most of the FRAP data reported so far for lipids and proteins in biological membranes show the existence of an immobile fraction which can be considered as a strong indication that the membrane is structured laterally (Tocanne *et al.*, 1994). However, for proteins it has been shown that the detection of an immobile fraction may reflect not only a micro-compartmentation of the diffusion area but possibly an anomalous translational diffusion of the molecules (Feder *et al.* 1996). Because the FRAP technique is based on the long-range translational motion of both proteins and lipid can be the differentiated with diffusion of the large molecular mass and freely movable protein.

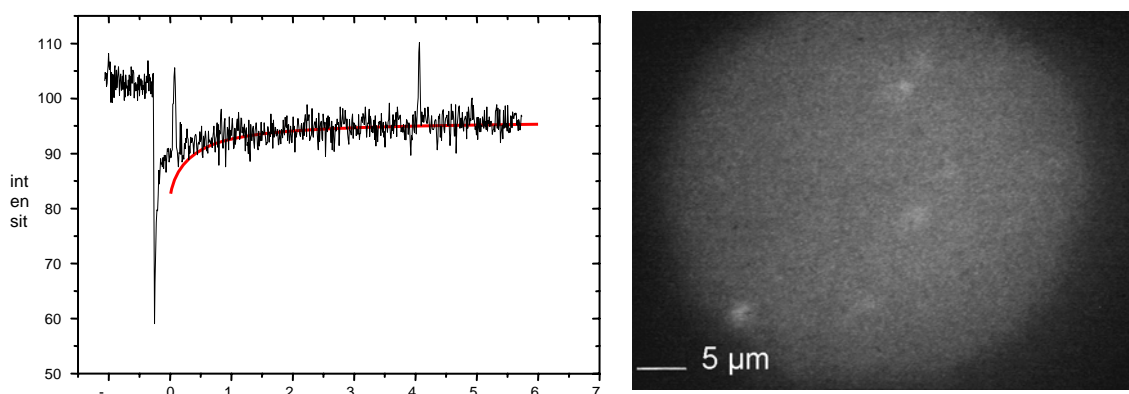


**Figure 23** FRAP experiment: The initial experiment was performed with supercomplex in the reconstituted system. The measurements were performed with Ingo Köper, Material science group Max Planck institute of polymer research Mainz Germany.

The FRAP was performed by using the edge bleach technique developed by Koppel (Koppel, 1979; Koppel *et al.*, 1980) in the inner mitochondrial membrane. The supercomplex was reconstituted in the asolectin and *Paracoccus* lipid to perform the initial experiment. First result is shown in figure 23. The diffusion recovery curve shows that the experiment could be performed in the native bacterial membrane. The experimental setup

shows that the bleaching area should be in the range of 5  $\mu\text{m}$  to perform the experiment and bleach the complexes inside the membrane. Due to the small vesicles, size of less than a micrometer it not possible to do the experiments. This is also a reason we did not get a consistent diffusion coefficient in the different type of membrane. To overcome this problem we started to do the experiment in the Fluorescence Correlation spectroscopy (FCS).

### 3.8.5 Fluorescence Correlation Spectroscopy (FCS)



**Figure 24** The schematic diagram shows the optically defined observation volume ( $250 \text{ nm}^3$ ) for labelled molecule (Haustein and Schwille, 2004)

The biological function of molecules not only depends on their structure, but also on their mobility and dynamic properties, which are strongly influenced by the environment. The single molecule-based technique fluorescence correlation spectroscopy (FCS) allows inherent averaging over a large number of single-molecule passages through the measurement volume (Figure 24). Laser light focused by a high numerical aperture objective defines the excitation volume. At thermal equilibrium, fluorescent molecules diffusing through the focus volume to give rise to minute signal fluctuations which are analyzed by FCS (Haustein and Schwille, 2004). This characteristic clearly distinguishes FCS from the technically related method FRAP. The FRAP method was widely used for determining diffusion characteristics in solutions and on membranes (Axelrod *et al.*, 1976). In this method the concentrations are micromoles or higher, so that thousands of particles in the measurement volume are contributing to the signal at any time. The information derived from conventional applications of FRAP on membranes includes diffusion coefficients, reaction rates and a quantity due to incomplete recovery called ‘immobile fraction’. This

technique has been applied to detect single diffusing fluorophores on artificial supported lipid films (Schmidt *et al.*, 1996). Therefore, FCS was used in the molecular binding and aggregation experiment. The individual diffusion characteristics would allow determining the diffusion constant for the supercomplex in the native membrane. The investigation of the diffusion of fluorescently labelled Fv molecules shows consistent auto correlation function. However, the sensitivity of autocorrelation analysis is restricted because the diffusion coefficient depends on the molecule's hydrodynamic radius and thus on the cubic root of the molecular mass for particles. The initial experiment was performed with the labelled Fv fragment in the solution. It shows the good time correlations with signal (fluctuation) curve for the determination of the diffusion coefficient. In the next step, the experiment was performed with labelled native membrane. Due to the focus volume  $250 \text{ nm}^2$  and vesicles size in the same range, we cannot focus inside the vesicles to do the correlation experiment. The measurement was based upon mobility of cytochrome *c* oxidase in the native membrane, which was investigated by using fluorescently labelled Fv monoclonal antibodies prepared and purified (2.17). To avoid the excess dye labelling to oxidase in the membrane. It was incubated with a fixed amount of labelled Fv fragment and washed three times to remove any non-specifically bound dye.

FCS experiments were started with measurements of diffusion time of labelled oxidase in detergent and in the reconstituted system. Cytochrome *c* oxidase was incorporated into phospholipids as described by Darley-Usmar (2.19.3.1) and then fused to increase the vesicles size (see 3.6.3). The labelling of oxidase was performed with a monoclonal antibody fragment derived against subunit II of oxidase (Fv), or a polyclonal antibody against cytochrome *c* oxidase (IgG). These antibodies were labelled with mono-functional Cy5 dye as described (see section 2.19.6). The three different types of fused native membranes derived from (i) wild type (WT) bacterial strain, (ii) a Complex I deletion strain, or (iii) a Complex III deletion strain, were decorated with monoclonal antibody (Fv-Cy5), or polyclonal antibody (IgG-Cy5). The diffusion time was measured in these native membranes. For a further control, the molecular mass of Fv-Cy5 labelled oxidase in native membrane was increased by addition of polyclonal antibody against oxidase. All FCS experiments were performed in a collaboration with Chayan Nandi in the group of Prof. Brutschy at Institut für Physikalische und Theoretische Chemie, Frankfurt University. The analysis of data and calculation of diffusion coefficients are underway.

### 3.8.6 Flash photolysis experiment

For the quantitative information on the translational diffusion of respiratory complex in the native membrane, the flash photolysis experiment was started in collaboration. The initial experiment was performed with reconstituted cytochrome *c* oxidase in lipid vesicles. In the native membrane the cytochrome *c* oxidase, react with CO and form mixed valance state with heme. It was known that no detectable decay of flash-induced linear dichroism of the cytochrome oxidase-CO complex in mitochondria for times up to 5 ms. Taking into account subsequent studies of the orientation of the heme  $a_3$ -CO complex and data shown by Kawato and co-workers imply that both mobile and relatively immobile populations of cytochrome oxidase are present in the mitochondrial inner membrane. Cytochrome oxidase maintains a fixed orientation with respect to the membrane plane, implying that rotation occurs around the normal to the plane of the membrane. A theoretical treatment of this case was described for heme proteins of the rotational relaxation time about the membrane normal axis of a single rotating species and when different rotating species of cytochrome oxidase such as monomer, dimer, or supercomplex (theoretical description of rotational mobility in membrane Kawato and Kinoshita, 1981). The CO-bound enzyme complexes were photolyzed with laser flash photolysis setup with laser pulse (Nd:YAG, 532 nm, 10 ns, 5 mJ/cm<sup>2</sup>). Two digital oscilloscopes (LeCroy 9361 and 9400A) were used to record the traces in two overlapping time windows. Each data point was properly weighted on the basis of the baseline analysis as described by (Chizhov *et al.* 1996). Figure 25 shows the transient difference spectra following the photolysis of CO bound to the fully reduced enzyme. The residual spectra obtained assuming one and two processes are compared in figure 25, respectively. Further bleaching of the peak and the trough on a millisecond time scale follows the microsecond changes, which are attributed to CO recombining with cytochrome  $a_3$ . The residuals represent the difference between the transient data and the global fit (Chizhov *et al.* 1996). The residuals based on a single process ( $T \sim 20$  ms) shows a significant positive absorbance on an early microsecond time scale, which disappears when two exponentials are assumed. The apparent lifetimes of the two processes were 1  $\mu$ s and 20 ms. We conclude from the analysis that the photo-dissociation cycle of the fully reduced CO-bound complex can be described by at least two kinetic processes.

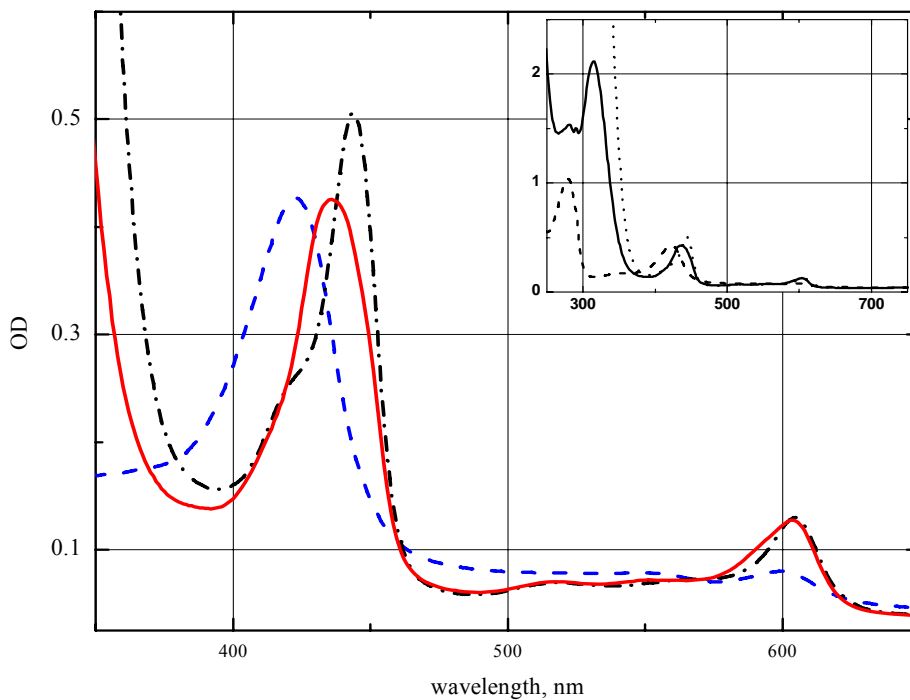


**Figure 25** Absorption spectra of three major states of cytochrome c oxidase): oxidised enzyme as prepared (dashed line), fully reduced state (dotted line), and CO bound reduced state (solid line).

The two apparent lifetimes of 1  $\mu$ s and 20 ms are in agreement with previous studies in which the photolysis of CO bound to the fully reduced mitochondrial oxidase was followed at a few selected wavelengths in the visible region (Einarsdottir *et al.*, 1993). These optimization measurements were performed in detergent solubilised oxidase.

## 4 Discussion

### 4.1 Spin relaxation measurements

Pulsed Electron Paramagnetic Resonance (EPR) spectroscopy is an important technique to measure the distance and orientation of two interacting proteins (Eaton and Eaton, 2000), based on the relaxation enhancement that a fast relaxing spin exerts on a nearby slow relaxing one. For the binding studies by Pulsed EPR, longitudinal relaxation  $T_2$  of  $\text{Cu}_A$  was measured using a two-pulse echo sequence and recording the signal as a function of time  $\tau$  between the pulses. Significant relaxation enhancement of the  $\text{Cu}_A$  centre in the presence of cytochrome  $c_{552}$  and horse heart cytochrome  $c$  was observed by pulse EPR experiments. These results confirm the previous results shown by chemical shift method of NMR spectroscopy (Wienk *et al.*, 2003). Complex formation takes place due to surface charges because both partner proteins were in oxidised condition (oxidised form shows the paramagnetic nature of metal centre) and no electron can be transferred due to the oxidized condition of both proteins. The qualitative result shown in Figure 11 proved that the interaction between the  $\text{Cu}_A$  fragment and binding cytochrome  $c$  and non binding can be easily distinguished with this method. The traces show that the relaxation enhancement is dependent upon presence of surface charge. In the case of horse heart cytochrome the enhancement is higher in comparison to cytochrome  $c_{552}$ . The negative control using cytochrome  $c_1$  showed very less enhancement due to the presence of same surface charge as for the  $\text{Cu}_A$  fragment.

The possibility to measure the  $\text{Cu}_A$  fragment alone and the transient complex with cytochrome  $c$  allowed to extract the dipolar contributions to the relaxation traces by a simple division of the experimental traces. It allows us to distinguish specific binding from non-specific interactions. The extraction of dipolar relaxation allows for simulation of the experimental decay traces, to obtain quantitative information about the distance and the relative orientation in the complex.

For quantitative analysis of the transient complex between  $\text{Cu}_A$  fragment and horse heart cytochrome  $c$  the variation of most of the fit parameters is very small. The experimental dipolar relaxation traces for the complex of  $\text{Cu}_A$  fragment and cytochromes at different temperatures were simultaneously fitted via either a SIMPLEX or a sequential quadratic programming algorithm. The following fit parameters for a single binding geometry was: the distance  $R$ ; the polar angles of the dipolar vector with respect to the  $\text{Cu}_A$  g-tensor frame ( $\theta_D$ ,



$\varphi_D$ ); the Euler angles ( $\alpha, \beta, \gamma$ ) of the cytochrome g-tensor with respect to the  $\text{Cu}_A$  g-tensor frame; the exchange coupling  $J$ ; an offset to account for unbound  $\text{Cu}_A$  fragment. Therefore simultaneous fit with distribution of at least two fixed distances were conform the dipolar decay traces of X-band could be satisfactory fulfilled. The structural parameters (particularly the distance  $R$  between the two paramagnetic centers) obtained from this fits shows one distance in the range of 18-23 Å and a second long distance was found with approximately 40 Å. The distance was calculated from computational docking studies to take the following parameter into consideration: (a) the Fe-Cu distance should not be more than 18 Å for electron transfer, so they ignore the larger distance in simulation parameter (b) consideration of tryptophan (W121) residue in the calculation and electron pass through this residue and (c) the distance between the atoms of the residues in the basic patch of cytochrome was considered and the residues in the acidic patch on  $\text{Cu}_A$  fragment (Flöck and Helms, 2000; Bertini *et al.*, 2005). The differences in the experimental decay curves for both binding cytochromes clearly point to structural differences in specific binding. The mode of interaction proposed here for the cytochrome  $c_{552}$ - $\text{Cu}_A$  fragment transient complex bears some similarities to other electron transfer complexes involving cytochrome  $c$  of known X-ray structure. These structures include the complex between cytochrome  $c_2$  and the photosynthetic reaction centre from *Rhodobacter sphaeroides* (Axelrod *et al.*, 2002), between cytochrome  $c$  and the  $bc_1$  complex from *Saccharomyces cerevisiae* (Hunte *et al.*, 2002), and between first crystal complex cytochrome  $c$  and cytochrome  $c$  peroxidase from the same *S. cerevisiae* (Pelletier *et al.*, 1992). The structure of the transient complex of spinach plastocyanin (Pc), a protein of 10.5 kDa with a type-I copper site, and the water-soluble fragment of turnip cytochrome  $f$  has been determined by NMR spectroscopy employing the paramagnetism of the heme (Ubbink *et al.*, 1998). The structure of the complex shows that spinach Pc binds to cytochrome  $f$  with both its acidic patches and the hydrophobic patch involved. Residues in the acidic patches of Pc interact with residues of the basic patch of cytochrome  $f$ . The observed distance of 11.2 Å between the heme iron and the copper center allows for fast electron transfer (Lange *et al.*, 2005). The co-complex between cytochrome  $c$  and cytochrome  $bc_1$  complex structure reveals that the architecture of the complex exhibits an edge-to-edge distance of the two  $c$  type heme groups of 9.4 Å (Hunte *et al.*, 2002). The structure of the co-complex clearly argues for electron transfer from cytochrome  $c_1$  to cytochrome  $c$  by direct heme-to-heme transfer. However, in the yeast co-complex the hydrophobic patches of both cytochromes do not seem to be tightly sealed, water molecules that are not resolved at the given resolution might be present in the close

environment of donor and acceptor and might take part in such a structural pathway. All of these structures showed the presence of compact interaction site, where hydrophobic interactions are largely prevalent among short-range contacts and define the optimal interface arrangement to allow electron transfer.

All previous data of oxidase and cytochrome were analyzed by different docking methods. Nevertheless, for the first time the experimental data were simulated for the distance and orientation measurements. The two observed states with distances of 20 and 40 Å may represent the two states of a transient protein-protein complex as proposed in the two-step model of complex formation between electron transfer proteins. A two-step model was proposed to describe the docking of the membrane-embedded cytochrome *c* oxidase with its soluble substrate cytochrome *c* (Witt *et al.*, 1998). The first step of interaction is governed by long-range electrostatic interaction mediated by oppositely charged surfaces on either protein, and a preorientation of both redox partners is obtained. In a second step is followed by a fine-tuning mediated by hydrophobic surfaces to acquire a docking conformation for optimal electron transfer (see Maneg *et al.*, 2004). A strong, positive surface potential for the mitochondrial or bacterial electron donor, cytochrome *c* or *c*<sub>552</sub>, is evident, while several acidic residues have been suggested to participate in docking on a negatively charged patch located mostly on Cu<sub>A</sub> fragment. Under the electron transfer conditions, an optimal salt concentration results from a compromise of the association and the dissociation rates for cytochrome *c*. Mutations in exposed residues in the relevant area above the Cu<sub>A</sub> site were analysed, to estimate the extent of the acidic region responsible for cytochrome *c* docking (Drosou *et al.*, 2002).

The dynamic model of Bertini *et al.* for the interaction between cytochrome *c*<sub>552</sub> and cytochrome *c* oxidase, the four solutions obtained through this procedure are characterized by different networks of intermolecular interactions, which correspond to a substantial diversity in the orientations of the partner proteins within the complex. The observation that the restraints derived from the experimental data are satisfied only partially, suggests that the cytochrome *c*<sub>552</sub>-cytochrome *c* oxidase complex may have considerable dynamic features, and that the ensemble of the docking solutions. So they represent an overall description of the diverse orientations assumed by the partner proteins during interactions compatible with our data (due to orientation difference and its not fixed with one orientation like horse heart cytochrome *c*) and the two-step docking mechanism (Witt *et al.*, 1999). In our case, we are observing only the first stage, with no electron transfer between these two complexes because both the partners were in oxidized state. The long-range nature of the electrostatic

forces causes the initial encounter adduct to be not specific, resulting in many different orientations with approximately the same energy, whereas van -der-Waals forces, acting at short distances. In the kinetic studies (stopped flow) on Cu<sub>A</sub> fragment and cytochrome *c*<sub>552</sub> showed that their interaction involves two to three effective charges on each protein, according to the ionic strength dependence of the electron transfer rate (Maneg *et al.*, 2003). A previously proposed computational model for the complex (Flöck and Helms, 2000), cytochrome *c*<sub>552</sub> was found in two different orientations depending on whether it was docked against two subunits and four subunit cytochrome *c* oxidase. Furthermore, given this interpretation, the single docking structures should be regarded as accurate pictures of specific adduct conformations between Cu<sub>A</sub> fragment and horse heart cytochrome *c*. The docking scenario for complex between cytochrome *c*<sub>552</sub> and Cu<sub>A</sub> to rotate and slightly slide on the surface of Cu<sub>A</sub> fragment, maintaining a central contact area that involves hydrophobic residues. Similar to what is found in our work, a role of salt bridges in complex formation was inferred also by an analogous calculation performed on beef heart oxidase and horse heart cytochrome *c* (Roberts and Pique, 1999). A general docking feature emerging from the experimental data and the present model is that oppositely charged surfaces on the two proteins are used to direct the relatively mobile cytochrome *c* molecule on the surface of its redox partner in a pseudo-specific way, supporting the concept of pseudo-specific docking for electron transfer proteins (Williams *et al.*, 1995). This concept explains that different combination and orientations should be possible between redox partner through hydrophobic surface patches and electrostatic interaction.

In photosynthesis, the experimental data from plastocyanin and cytochrome *f* of spinach indicated the supercomplex formation and the structural data on the overlapping docking sites of Pc-cyt *f* and Pc-PS I complexes (Musiani *et al.*, 2005). In the case of bacterial respiratory chain, the kinetic argument proved that the cytochrome *c*<sub>552</sub> protein is the favoured electron donor for the *aa*<sub>3</sub> cytochrome *c* oxidase from *P. denitrificans* (Maneg *et al.*, 2003). It is also supported in native membrane of *P. denitrificans*, both cytochrome *c*<sub>552</sub> and cytochrome *c* oxidases are membrane embedded and integrated in a super-complex together with the *bc*<sub>1</sub> and Complex I (Stroh *et al.*, 2004). Considering that the native cytochrome *c*<sub>552</sub> has a membrane anchoring domain and an additional charged domain, it should be pointed out that these structural elements could further stabilize a supercomplex and may even allow higher electron transfer rates, without the constraints imposed by three-dimensional diffusion of the electron mediator. This organisation promotes frequent encounters between the redox partners, which are not all necessarily productive for electron

transfer. In fact, the orientational freedom of cytochrome  $c_{552}$  should be quite large in spite of the membrane anchor and the supramolecular association, because it is likely to act like a pendulum for the interaction with both the  $bc_1$  complex and the oxidase.

Finally, it is possible to apply relaxation method to protein complexes, where more than two paramagnetic centers are involved. Our preliminary experiments on the complex of cytochrome  $c$  with the four subunit detergent solubilised cytochrome  $c$  oxidase (four paramagnetic centers  $Cu_A$ , heme  $a$ ,  $a_3$ , and  $Cu_B$ ) showed that the division method removes all the contributions of the other internal paramagnetic centers from oxidase to the  $Cu_A$  signal and retains only the dipolar relaxation due to external cytochrome  $c$ . The next step would be to do this experiment in the presence of a lipid membrane (reconstituted system) and larger protein complexes to reach the goal of a supercomplex-like situation.

## 4.2 Reconstitution

Cytochrome  $c$  oxidase was reconstituted into lipid vesicles. From the analysis of the abundant literature concerning the insertion of membrane proteins into liposomes, four basic strategies have been outlined: mechanical means, freeze-thaw, organic solvents, and detergents. These reconstitution strategies have proven to be very useful to prepare pure proteoliposome vesicles (Rigaud *et al.*, 1995). To preserve protein activity, many criteria have to be considered to fully optimize the reconstitution of a membrane protein: the dispersion of protein insertion, the final orientation of the protein, the morphology and the size of the reconstituted proteoliposomes, as well as their residual permeability (Rigaud and Lévy, 2002).

Thus, the vast majority of membrane protein reconstitution procedures are those involving the use of detergents. Indeed, due to their amphiphilic character, most membrane proteins require detergents, not only as a means of disintegrating the structure of native membranes in the initial step of their solubilization, but also as a means of keeping the protein in a non-denaturing environment during further purification (Lemaire *et al.*, 2000). The standard procedure used to reconstitute a purified membrane protein involves comicellization of the protein in an excess of phospholipids and appropriate detergent, to form a solution of mixed lipid-protein-detergent and lipid-detergent micelles. Next, the detergent is removed from the micellar solutions, resulting in the progressive formation of closed lipid bilayers into which the proteins eventually incorporate. All the detergent-mediated reconstitutions described in the literature rely on this standard procedure but differ essentially in the techniques used to remove the detergent, which can be dialysis, gel chromatography, dilution, or hydrophobic

adsorption onto polystyrene beads. Reconstitutions from detergent micellar mixtures have yielded proteoliposomes of different sizes and compositions depending on the nature of the detergent, the particular procedure to remove it, as well as the nature of the protein and the lipid composition.

Therefore, each membrane protein responded differently to the various reconstitution procedures and the approach has long been studied (Rigaud *et al.*, 1995; Lichtenberg 1985, Silvius 1992). The original information about the mechanisms of lipid-protein association in the presence of detergent, this “step-by-step” reconstitution strategy proved to be a powerful reconstitution procedure, more suitable than the other methods (Rigaud *et al.*, 2000). In particular, it should be stressed that reconstitution of a membrane protein into detergent saturated preformed liposomes ensured a unidirectional insertion of the protein in the membrane and generally produced the most efficient proteoliposomes. An additional advantage of new reconstitution strategy for supercomplex relied on the use of Bio-Beads SM2 to remove the detergent. Indeed, the fast removal of detergent from reconstituted proteoliposomes was an absolute necessity since residual detergent might disturb the association of supercomplex.

### 4.3 Size of membrane vesicles

An instrument based on the principle of Photon Correlation Spectroscopy (PCS) was used for measurement of membrane vesicles size. Usually PCS is concerned with measurement of particles suspended within a liquid. The major difference between a PCS experiment and a diffraction experiment is that the light intensities in PCS are so low that a photo multiplier was used in order to count individual photons of light. For many systems, measurement at a single angle (usually 90°) is sufficient for interpretation of the size distribution. However, certain sizes of particle, e.g. 480 nm spheres will have a scattering intensity minimum at 90° and the reduced signal to background ratio will increase the measurement error. In these cases, measurement at another angle will improve the results. In PCS experiment use of the maxima and minima in the intensity versus angle diagram to enhance the detection of selected sizes of particles.

The size of membrane vesicles were measured on the purified native membrane. Three independent methods were used for membrane vesicles preparation and data demonstrate the different methods used for vesicle preparation have different sizes. The primary purpose of this study was to determine the size of membrane vesicles to do FRAP or FCS experiment for the lateral diffusion of the respiratory complexes in the membrane. The osmotically

prepared membrane vesicles have bigger size as compared to other membrane preparation as we expect the different type of methods lead to different size of membrane vesicles. However, these vesicles were not sufficiently big for the FCS or FRAP experiment.

#### 4.4 Fusion of membrane vesicles

Giant unilamellar vesicles with sizes ranging from 10 to 100  $\mu\text{m}$  are potentially attractive model system and are becoming objects of intense scrutiny in diverse areas focusing on biological functions such as adhesion, fusion and fission, or motility (Angelova and Dimitrov, 1986; Luisi and Walde, 2000). However, the fragility and protein-hostile preparation procedures of these large vesicles have so far precluded their use in membrane reconstitution. Several methods to produce giant vesicles have been developed and reported in the literature. One of the methods that have been applied successfully to produce large proteoliposomes amenable to patch-clamp recording and electrophysiological measurements is based on a dehydration-rehydration procedure (Criado and Keller, 1987). Such a method consists of the dehydration of biological membranes or preformed proteoliposomes in the presence of added exogenous lipids followed by a rehydration process in the desired buffer (Ajouz *et al.*, 2000). The rehydration of thin dried films obtained after the evaporation of the solvent from lipid-protein complexes in organic solvents has been used to produce giant proteoliposomes (Darszon *et al.*, 1980). The main disadvantage of this dehydration-rehydration method is that the supercomplex may be destroyed in their composition.

In this native membrane fusion, I tried a new method based on reconstitution of transmembrane proteins into GUVs (Doeven *et al.*, 2005). This method involves partial dehydration of native membrane on conductive glass surfaces, and controlled rehydration in the presence of an AC electric field to form giant vesicles (Angelova *et al.*, 1992). However, this method do not work for fusion of native membrane.

The other method used for the native membrane fusion to used divalent cations as described by Millar and Racker (1975). Nevertheless, divalent cations do not play a significant role in the membrane fusion and membranes get aggregated. The attempts to fuse inner membranes in the presence of asolectin and 5 mM  $\text{Ca}^{++}$  at pH 8 gave significant levels of fusion. However, we found the major difficult with  $\text{Ca}^{++}$  supported fusion to be an irreversible aggregation of cytoplasmic membranes.

The pH induced membrane fusion procedure is a modified version of the lipid and inner mitochondrial membrane fusion method (Schneider *et al.*, 1980). The pH fusion procedure is technically uncomplicated and does not require the addition of divalent cations. The rate and

quantity of fusion can be controlled by incubation time, temperature, and by changing the pH. When all other conditions were optimal but pH 8.0, no fusion occurs between inner membranes in presence of asolectin. For fusion of membrane, the optimum pH is 6.0 and temperature 32 °C. The recovery of membranes enriched with exogenous lipid was further controlled by selection through sucrose density gradient centrifugation. The pH method is not limited to fusion with asolectin liposomes. The low pH (4.5) method was used for the fusion of liposome with bacterial membrane has been reported elsewhere (Driessen *et al.*, 1985).

The membrane fusion occurred in the presence of asolectin supported by several ultrastructural, compositional, and functional characteristics that were determined: (i) the membrane area increased; (ii) the membranes showed a higher buoyant density. Although real fusion must result in an increase in the membrane lipid-to-protein ratio, it is necessary to assess the possibility that this increase might be due to the loss of membrane protein rather than the enrichment of membrane lipid. In this regard it was determined that the cytochrome *c* oxidase is present, not making any compositional changes in integral protein. In the case of supercomplex topology, the lipid incorporation is not going to make any difference because it is shown that the respiratory complexes exist together in one supercomplex (Stroh *et al.*, 2004).

#### 4.5 Deletion mutant

The supercomplexes were isolated by different type of deletion mutant and confirmed by BN-PAGE (Stroh *et al.* 2005). Based on these result a schematic arrangement of the super complex is shown in Figure 25. The Wild type membrane contains supercomplex consisting of  $[I(III)_2IV_4]$  with a calculated molecular weight of 1.9 MDa. In the Complex III deletion mutant no supercomplex is obtained and no association of Complex I and IV was reported. The Complex I deleted mutant shows the association between Complex III and IV. This result confirms the supercomplex isolated earlier by gel filtration (Berry and Trumpower 1985).

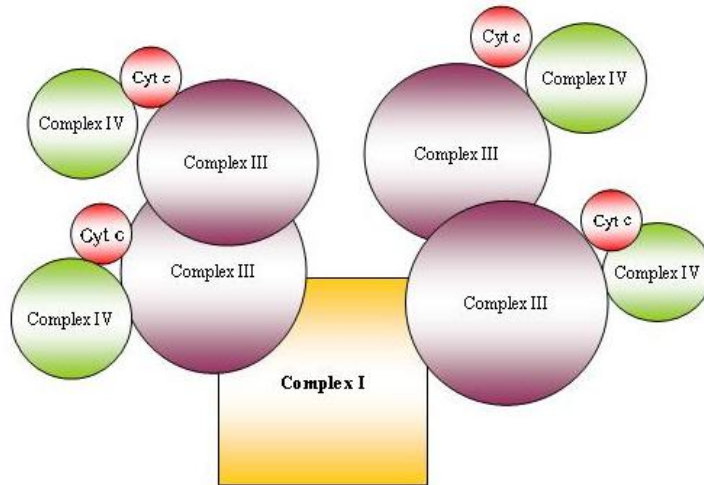


**Figure 26** Highly schematic arrangement of different respiratory complex as 'respirasome'. It consists of monomer Complex I bound to dimer Complex III to Complex IV and unknown copy number of membrane bound cytochrome  $c_{552}$  in the stoichiometric ratio  $I_1(III)_2 IV_4 c_{552}$  (based on Stroh et al., 2004)

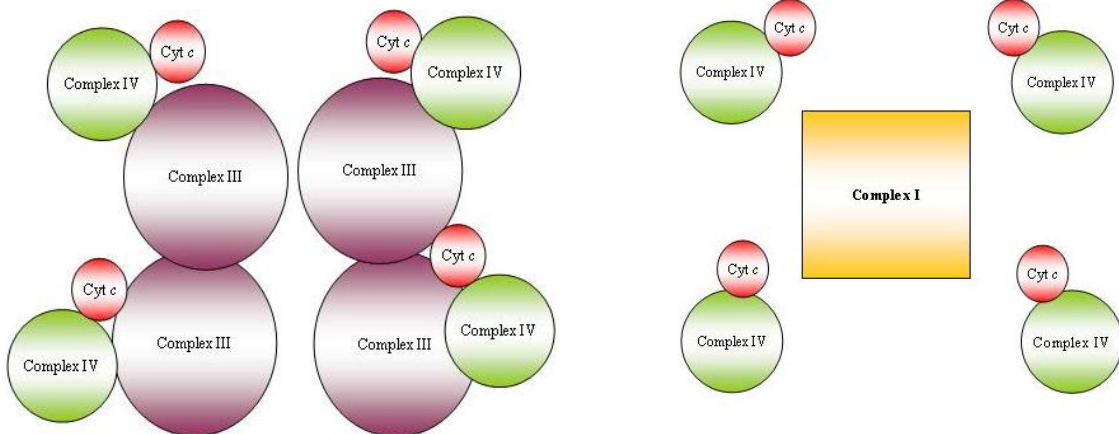


**Figure 27** Complex I deletion mutant supercomplex formed with Complex III and IV

**Figure 28** Complex III deletion mutant: no super complex formed due to deletion of Complex III



#### 4.6 Lateral diffusions experiments

The lateral diffusion experiment was performed to investigate the presence or absence of random mobility of complexes in the native environment. The random diffusion model is based on theoretical assumption and experimental data by FRAP method. The shape and radius of different complexes was assumed because structural detail was not available at that time. Here the experiment carried out in bacterial membrane that gave big advantage of using deletion mutant in the respiratory chain of *P. denitrificans* due to presence of alternative electron transport pathway. There are some disadvantages for bacterial membranes, such as presence of low contents of respiratory complexes compared to inner mitochondrial membrane.

The results and approach for bacterial membrane system for lateral or rotational diffusion are discussed in comparison to mitochondrial inner membrane. The 'fluid mosaic model' of membranes is now observed as more mosaic than fluid part (Engelmann 2005). The mosaic view model supports the presence of membrane protein to form mosaic part due hydrophobic helix, dimer and trimer association for its functional and structural stability.

Present view of the membrane model support larger assemblies of membrane protein due to presence of hydrophobic helices and proteins in cell membranes typically diffuse much more slowly than do proteins in artificial lipid bilayers. Although the simplest hydrodynamic theory predicts that lateral diffusion of proteins in cell membranes should be roughly half as fast as that of lipids (Jacobson *et al.*, 1987). The mitochondrial inner membrane supports a number of rapid macromolecular interactions that draw specific catalytic actions required in the processes of electron transfer. For lateral diffusion to take place, ample space as well as fluidity is required in the membrane lipid bilayer. It was recognized that the mitochondrial inner membrane is composed of 75% protein (Colbeau *et al.*, 1972); while the *P. denitrificans* (Previously name as Micrococcus) has an unusual lipid composition of 15% for *M. denitrificans* (Whiteside *et al.*, 1971). However, it is not known that only one-half of this protein is integral to the mitochondrial membrane bilayer (Hochli and Hackenbrock 1978). The rate and catalytic significance of such diffusion has been determined (Hackenbrock *et al.*, 1980). They developed an *in vitro* method for increasing the surface area of the membrane bilayer with exogenous phospholipids to increase the diffusion distance between

the various interacting membrane components, which catalyze electron transfer in mitochondrial membrane (Hochli *et al.*, 1985). The method was based upon enrichment of the inner membrane lipid bilayer by fusion of sonicated, small unilamellar phospholipids vesicles with the purified inner membrane at pH 6.5 (Schneider *et al.*, 1982). From this fused membrane, Hackenbrock and co-worker conclude that a diffusion-limited step is involved in the transfer of reducing equivalents from the dehydrogenases to cytochrome  $bc_1$  in the native membrane. Several models explain the diffusion-limited step between two complexes. A model, proposed by Ragan and co-workers that electron transfer from NADH to cytochrome  $c$  occurs through specific stoichiometric associations of Complex-III and I (Ragan and Heron, 1978; Heron *et al.*, 1978). Presumably, the Complex I-Complex III unit is necessary for electron transfer from NADH to both ubiquinone and cytochrome  $c$ . The same type of assembly of a plant mitochondrial and mammalian supercomplex was structurally characterized by electron microscopy (EM) (Dudkina *et al.*, 2005; Schäfer *et al.*, 2006).

The random diffusion model was evaluated by physiological functioning of mitochondria. It is important to consider the effects of high protein concentrations in the matrix and intermembrane spaces on the mobilities of membrane bound components. It has been known that the matrix of mitochondria has a very high protein concentration. This protein crowding could hinder lateral and rotational mobility of the integral complexes, resulting in reorganization on a time scale much larger than that of an electron-transfer event. Association and dissociation of the complexes in this period would be compatible with a regulatory function mediated by factors that affect the lifetime of the aggregated state. A resemblance is provided by the studies of Kaback and co-workers (Goldkorn *et al.*, 1984) which indicate that the state of aggregation of a bacterial membrane protein is modulated by the membrane potential. A high membrane potential might a disaggregated state, while at a low-potential aggregated complexes would predominate, giving rise to more efficient electron and energy transfer and its also support the existence of supercomplex in membrane.

The lateral diffusion coefficients of the mitochondrial redox components have been determined experimentally by FRAP (Gupte *et al.*, 1984). The data under the best conditions showed that all the redox component diffuse laterally with same diffusion coefficient and diffuse rapidly in the membrane plane. It supports that the mitochondrial inner membrane is

structurally a fluid rather than a solid-state membrane and that the redox components are physically dispersed randomly rather than organized in a macromolecular or chain-like assembly. Nevertheless, in latest literature conform the membrane have more solid (mosaic) part as compare to fluid part (Engelman 2005).

In our FRAP experiment we want to show that all the redox components diffuse together in the membrane. To do this we started the experiment in the native membrane and compare to the two-deletion mutant (schematic diagram of these mutants is shown in figure 27, 28). Due to smaller size of membrane vesicles compared to bleaching area, we could not perform this experiment yet.

We started the FCS diffusion analysis of fluorescent-labelled molecules in membranes and complex in reconstituted system. These findings might be compared with diffusion coefficient in the mitochondrial membrane. Presently, the lateral diffusion coefficients of the respiratory complex in the native and lipid-enriched membranes are unknown. As described by random diffusion model the inner membrane redox component is a highly mobile, independent lateral diffusion and by every component should be highly rotationally mobile. (see Kawato *et al.*, 1980). Conversely, Kawato and Cherry reported Complex IV to have a relatively low diffusion, and a large rotationally immobile fraction which they attribute to non-specific aggregation of membrane proteins and not to aggregation between Complexes III and IV. Nevertheless, the results of Kawato and coworker have been cited by Hochman *et al.* as physical evidence for functional, multielectron transferring “dynamic aggregates” of redox partners (Hochman *et al.*, 1982). Furthermore, calculations upon which the concept of functional dynamic aggregates was formulated were found to be based on the use of unrealistically low concentrations of redox components. The calculation carried out by Ferguson-Miller *et al.* found their results to be compatible with the random collision model (Ferguson-Miller *et al.*, 1986; Rogers, 1992).

In this previously proposed model (Hochman *et al.*, 1982, 1985) which is consistent with the findings of lateral diffusion in mitochondrial inner membrane and with the results of other investigators. In this model, electron transfer can occur by random diffusion, but more rapid rates are achieved by formation of transitory functional aggregates (dynamic aggregates) among the electron-transfer chain components. In the case of cytochrome *c*, physical association between cytochromes *bc*<sub>1</sub>, and *aa*<sub>3</sub> could create a limited domain in which

cytochrome *c* movement is restricted, thereby increasing the efficiency of electron conductance. These findings also support the formation of supercomplex.

In old literature Erecinska *et al.*, 1979 proposed that the components of the respiratory chain of *Paracoccus denitrificans* including cytochrome *c* appear to be tightly associated, suggesting that even though high rates of electron transfer occur in the system. The highly association in the system was proved by isolation of supercomplex (Stroh *et al.*, 2004). The observations of Cherry and co-workers indicate that the respiratory complexes of mammalian mitochondria are largely immobilized on a short time scale, suggesting a high degree of aggregation in the native membrane (Kawato *et al.*, 1980, 1982). These results suggest that may be this aggregation was a supercomplex in the membrane. The authors attribute this phenomenon to aggregation, but it seems more reasonable from a physiological standpoint that functional aggregates would predominate. Although, the efficiency of electron transfer may be increased by formation of specific associations among the complexes (substrate channelling in the term of supercomplex). It is clear that the structural features of cytochrome *c* are also compatible with two- or three-dimensional diffusion, and this mode of activity may be physiologically important as well.

#### 4.7 Flash photolysis

The other approach was used the flash photolysis experiment to look on the rotational motion of cytochrome *c* oxidase in the native bacterial membrane. The experiment was started in simple system to analyse the photocycle of bacterial cytochrome *c* oxidase in detergent solution and reconstituted system under various conditions. The first aim of this study was to establish a procedure to obtain standardized data based on bacteriorhodopsin (Chizhov *et al.*, 1996). These data should meet the requirement of being applicable for rotational diffusion in membrane.

Photolysis of the fully reduced CO-cytochrome *c* oxidase showed by global analysis of the transient difference spectra gave two apparent lifetimes. This implies at least two kinetic intermediates in addition to the final product, the fully reduced CO complex. The two life time (micro second and millisecond). The millisecond time will be used for our further investigation. The studies on the photo dissociation and recombination dynamics of fully

reduced CO-bound cytochrome oxidase showed that CO binds to Cu<sub>B</sub> following the photolysis of CO from cytochrome (Dyer *et al.*, 1989). By following the CO photodissociation and recombination as a function of CO concentration, also demonstrated that CO binding to cytochrome a<sub>3</sub> involves prior binding of CO to Cu<sub>B</sub> site (Woodruff *et al.*, 1991; Einarsdottir *et al.*, 1993). Based on these results, the two-step model in Scheme to determine the absorption difference spectra between the intermediates and the unphotolyzed fully reduced CO species.

This approach is based upon the results of Kawato *et al.*, 1980. They illustrate that relatively immobile species of cytochrome oxidase in mitochondrial membranes might be either oligomeric cytochrome oxidase or cytochrome oxidase complexed with other membrane proteins. The former possibility is supported by observations of self-association of cytochrome oxidase in reconstituted systems (Kawato *et al.*, 1982) The similar type of experiment we approach to do in the native bacterial membrane system where we have the deletion mutant like Complex-I and complex III. The schematic arrangement of these complexes is shown in the figure 27 and 28. This arrangement is based on the supercomplex isolation and its conformation based on the BN-PAGE (Stroh *et al.*, 2004).

## Outlook

Existence of respiratory supercomplexes from different source has been proved in the presence of detergent by gel filtration and native gel electrophoresis. However, no evidence is provides supercomplex existence in the native membrane. In my studies on supercomplex in native membrane environment, the experiment was carried out in a model system (soluble fragment of the complexes and reconstituted system) due to presence of low content and different type of metal centre of respiratory protein. The ladder type of approach may be used to reach the final destination of supercomplexes in native membrane and various spectroscopic studies shows very promising results. Pulse EPR techniques have been used for the first time successfully to study the structure of a transient protein-protein complex. Electron spin echo measurements of the slower relaxing  $\text{Cu}_A$  paramagnetic centre in the soluble subunit II of cytochrome *c* oxidase in complex with different cytochromes were performed, and allow a clear distinction between binding and non-binding cytochromes. The division method provides pure dipolar relaxation traces was quantitatively analyzed to obtain the structure of the protein-protein complex without the necessity of taking the intrinsic relaxation properties of the observed paramagnetic species into account. The strongly enhanced orientation selection at high magnetic field values gives additional constraints and further improves the structural determination. The second approach to measure the lateral diffusion of respiratory complex in the native membrane is an alterative method to distance determination. The mass difference between monomer complex and supercomplex is around one order of magnitude higher and should be distinguishable by FRAP and FCS experiments. The difference between the lateral diffusion should be comparable to deletion mutants. The initial measurement in reconstituted system was performed and the due to smaller size of native membrane vesicles further experiment was not possible. To overcome this problem, fusion of native membrane was performed to make the giant membrane vesicles. pH induces fusion in the presence of asolectin shows four times larger vesicles than unfused one. Finally the experiment was performed and data analysis and calculation of diffusion coefficients are underway. The other approach to measure the rotational diffusion of oxidase in the native membrane was done with optical absorption spectroscopy. To monitor the reorientation of oxidase in membrane plane, carbon monoxide (CO) used as a probe for this experiment. CO binds to the cytochrome *c* oxidase under reduced conditions to the  $a_3\text{-Cu}_B$  site and the effect was monitored in the Soret region of the spectra. The initial experiment was performed with oxidase in a reconstituted system. The experiment also done with the native membrane but due to low amount of oxidase in the membrane the signal was low. To overcome this problem different membrane preparation were obtained with higher heme contents. The next step would be to use non-polarized and polarized light for measurement to investigate rotational mobility of complex organization in native membranes.

## Abbreviations

|                          |   |
|--------------------------|---|
| % v/v                    | volume percent  |
| Å                        | Angstrom  |
| Ac                       | acetate   |
| Amp                      | ampicilline   |
| AP                       | ammonium persulphate  |
| ATP                      | Adenosine triphosphate                                      |
| BCIP                     | 5-Bromo-4-chloro-3-indolylphosphate                         |
| bp                       | base pair   |
| BSA                      | Bovine serum albumin  |
| Cu <sub>A</sub> fragment | soluble domain of subunit II of cytochrome <i>c</i> oxidase |
| Cys                      | cysteine  |
| Cyt.                     | cytochrome  |
| DEAE                     | diethylaminoethyl   |
| DM                       | n-dodecyl-β-D-maltopyranoside                               |
| DMSO                     | dimethylsulphoxide  |
| DNA                      | deoxyribonucleic acid                                       |
| DTT                      | dithiothreitol  |
| EDTA                     | ethylene diamine tetra acetic acid                          |
| EGTA                     | ethylene bis (oxyethylene nitrilo) tetra-acetic acid        |
| EPR                      | electron paramagnetic resonance                             |
| ET                       | electron transfer   |
| EtOH                     | ethanol   |
| FADH <sub>2</sub>        | flavin Adenine dinucleotide reduced from                    |
| FCS                      | fluorescence correlation spectroscopy                       |
| Fe-S                     | iron-sulphur cluster  |
| FMN                      | flavin mononucleotide                                       |
| FRAP                     | fluorescence recovery after photobleaching                  |
| Fv                       | antibody fragment, variable domain                          |
| GUV                      | giant unilamellar vesicles                                  |
| h                        | hours   |

|                 |   |
|-----------------|---|
| HEPES           | N-2-Hydroxyethyl piperazine-N'-2-ethane sulfonic acid |
| His             | histidine   |
| kb              | kilo base   |
| kDa             | kilo Dalton   |
| Km              | kanamycin   |
| Kpi             | potassium phosphate buffer                            |
| MK6             | Complex III deletion mutant                           |
| MR31            | Complex IV deletion mutant                            |
| MW              | molecular weight                                      |
| MWCO            | molecular weight cut-off                              |
| NMR             | nuclear magnetic resonance                            |
| OD              | optical density                                       |
| OXPHOS          | oxidative phosphorylation                             |
| PAGE            | polyacrylamide gel electrophoresis                    |
| PBS             | phosphate buffered saline                             |
| PCR             | polymerase chain reaction                             |
| PDB             | protein data bank                                     |
| Q               | ubiquinone  |
| QH <sub>2</sub> | ubiquinol   |
| Rif             | rifampicin  |
| rpm             | revolution per minute                                 |
| RT              | room temperature                                      |
| s               | second  |
| SDS             | sodium dodecylsulfat                                  |
| TEMED           | N, N, N' N'- Tetramethylethylendiamin                 |
| Tet             | tetracycline  |
| TNM             | Tris-NaCl- MgCl <sub>2</sub> -buffer                  |
| Tris            | Tris-(hydroxymethyl)-aminomethan                      |
| UV/vis          | ultraviolet/visible                                   |
| WT              | wild type   |
| ε               | extension coefficient                                 |
| τ               | separation time between two pulses                    |



## References

- Abramson** J, Riistama S, Larsson G, Jasaitis A, Svensson-Ek M, Laakkonen L, Puustinen A, Iwata S, and Wikstrom M. 2000. The structure of the ubiquinol oxidase from *Escherichia coli* and its ubiquinone binding site. *Nat. Struct. Biol.* 7 (10): 910-917.
- Ajouz** B, Berrier C, Besnard M, Martinac B, and Ghazi A. 2000. Contributions of the different extramembranous domains of the mechanosensitive ion channel MscL to its response to membrane tension *J. Biol. Chem.* 275 (2): 1015-1022.
- Angelova** MI, and Tsoneva I. 1999. Interactions of DNA with giant liposomes. *Chem. Phys. Lipids* 101 (1): 123-137.
- Antalis** TM, and Palmer G. 1982. Kinetic characterization of the interaction between cytochrome oxidase and cytochrome *c*. *J. Biol. Chem.* 257 (11): 6194-6206.
- Axelrod** D, Koppel DE, Schlessinger J, Elson E, and Webb WW. 1976. Mobility measurement by analysis of fluorescence photobleaching recovery kinetics. *Biophys. J.* 16 (9): 1055-1069.
- Axelrod** HL, Abresch EC, Okamura MY, Yeh AP, Rees DC, and Feher G. 2002. X-ray structure determination of the cytochrome *c*<sub>2</sub>: reaction center electron transfer complex from *Rhodobacter sphaeroides*. *J. Mol. Biol.* 319 (2): 501-515.
- Bacia** K, Scherfeld D, Kahya N, and Schwille P. 2004. Fluorescence correlation spectroscopy relates rafts in model and native membranes. *Biophys. J.* 87 (2): 1034-1043.
- Baker** SC, Ferguson SJ, Ludwig B, Page MD, Richter OM, and Van Spanning RJ. 1998. Molecular genetics of the genus *Paracoccus*: metabolically versatile bacteria with bioenergetic flexibility. *Microbiol. Mol. Biol. Rev.* 62 (4): 1046-1078.
- Banci** L, Bertini I, Rosato A, and Varani G. 1999. Mitochondrial cytochromes *c*: a comparative analysis. *J. Biol. Inorg. Chem.* 4 (6): 824-837.
- Beinert** H. 1997. Copper A of cytochrome *c* oxidase, a novel, long-embattled, biological electron-transfer site *Eur. J. Biochem.* 245 (3): 521-532.
- Berry** EA, and Trumpower BL. 1985. Isolation of ubiquinol oxidase from *Paracoccus denitrificans* and resolution into cytochrome *bc*<sub>1</sub> and cytochrome *c-aa*<sub>3</sub> complexes. *J. Biol. Chem.* 260 (4): 2458-2467.
- Bertini** I, Cavallaro G, and Rosato A. 2005. A structural model for the adduct between cytochrome *c* and cytochrome *c* oxidase. *J. Biol. Inorg. Chem.* 10 (6): 613-624.
- Bianchi** C, Genova ML, Parenti CG, and Lenaz G. 2004. The mitochondrial respiratory chain is partially organized in a supercomplex assembly: kinetic evidence using flux control analysis. *J. Biol. Chem.* 279 (35): 36562-36569.
- Bligh** EG, and Dyer WJ. 1959. A rapid method of total lipid extraction and purification *Can. J. Biochem. Physiol* 37 (8): 911-917.

- Bott** M, and Niebisch A. 2003. The respiratory chain of *Corynebacterium glutamicum*. *J. Biotechnol.* 104 (1-3): 129-153.
- Bottcher** B, Scheide D, Hesterberg M, Nagel-Steger L, and Friedrich T. 2002. A novel, enzymatically active conformation of the *Escherichia coli* NADH:ubiquinone oxidoreductase (complex I). *J. Biol. Chem.* 277 (20): 17970-17977.
- Boumans** H, Grivell LA, and Berden JA. 1998. The respiratory chain in yeast behaves as a single functional unit. *J. Biol. Chem.* 273 (9): 4872-4877.
- Brandt** U, Kerscher S, Droese S, Zwicker K, and Zickermann V. 2003. Proton pumping by NADH:ubiquinone oxidoreductase. A redox driven conformational change mechanism? *FEBS Lett.* 545 (1): 9-17.
- Brautigan** DL, Feinberg BA, Hoffman BM, Margoliash E, Preisach J, and Blumberg WE. 1977. Multiple low spin forms of the cytochrome c ferrihemochrome. EPR spectra of various eukaryotic and prokaryotic cytochromes c. *J. Biol. Chem.* 252 (2): 574-582.
- Bushnell** GW, Louie GV, and Brayer GD. 1990. High-resolution three-dimensional structure of horse heart cytochrome c. *J. Mol. Biol.* 214 (2): 585-595.
- Capaldi** RA. 1982. Arrangement of proteins in the mitochondrial inner membrane. *Biochim. Biophys. Acta* 694 (3): 291-306.
- Chance** B, and Williams GR. 1955. A method for the localization of sites for oxidative phosphorylation. *Nature* 176 (4475): 250-254.
- Chazotte** B, and Hackenbrock CR. 1988. The multicollisional, obstructed, long-range diffusional nature of mitochondrial electron transport. *J. Biol. Chem.* 263 (28): 14359-14367.
- Chazotte** B, Hackenbrock CR. 1989. Lateral diffusion as a rate-limiting step in ubiquinone-mediated mitochondrial electron transport. *J. Biol. Chem.* 264 (9): 4978-4985.
- Chazotte** B, Hackenbrock CR. 1991. Lateral diffusion of redox components in the mitochondrial inner membrane is unaffected by inner membrane folding and matrix density. *J. Biol. Chem.* 266 (9): 5973-5979.
- Chazotte** B, Hackenbrock CR. 1981. Rotation of cytochrome oxidase in phospholipid vesicles. Investigations of interactions between cytochrome oxidases and between cytochrome oxidase and cytochrome *bc*<sub>1</sub> complex. *J. Biol. Chem.* 256 (14): 7518-7527.
- Chazotte** B, Hackenbrock CR. 1988. Multidimensional diffusion modes and collision frequencies of cytochrome c with its redox partners. *J. Biol. Chem.* 263 (11): 5241-5247.
- Cherry** RJ. 1979. Rotational and lateral diffusion of membrane proteins. *Biochim. Biophys. Acta* 559 (4): 289-327.
- Chizhov** I, and Engelhard M. 2001. Temperature and halide dependence of the photocycle of halorhodopsin from *Natronobacterium pharaonis*. *Biophys. J.* 81 (3): 1600-1612.

- Chizhov** I, Chernavskii DS, Engelhard M, Mueller KH, Zubov BV, and Hess B. 1996. Spectrally silent transitions in the bacteriorhodopsin photocycle. *Biophys. J.* 71 (5): 2329-2345.
- Colbeau** A, Vignais PM, and Piette LH. 1972. Biosynthetic synthesis and isolation of phospholipid spin-labels from rat liver microsomes and mitochondria *Biochem. Biophys. Res. Commun.* 48 (6): 1495-1503.
- Criado** M, and Keller BU. 1987. A Membrane-Fusion Strategy for Single-Channel Recordings of Membranes Usually Non-Accessible to Patch-Clamp Pipette Electrodes. *FEBS Letters* 224 (1): 172-176
- Crofts** AR. 2004. The cytochrome *bc*<sub>1</sub> complex: function in the context of structure. *Annu. Rev. Physiol* 66: 689-733.
- Cruciat** CM, Brunner S, Baumann F, Neupert W, and Stuart RA. 2000. The cytochrome *bc*<sub>1</sub> and cytochrome *c* oxidase complexes associate to form a single supracomplex in yeast mitochondria. *J. Biol. Chem.* 275 (24): 18093-18098.
- Darley-Usamr** VM, Capaldi RA, Yakamiya S, Millett F, Wilson MT, Malatesta F & Sarti P: Mitochondria- a Practical approach (*Darley-Usamr VM, Rickwood & Wilson MT, eds*) 1987 pp 143-152. IRL Press Oxford.
- Darszon** A, Vandenberg CA, Schonfeld M, Ellisman MH, Spitzer NC, and Montal M. 1980. Reassembly of protein-lipid complexes into large bilayer vesicles: perspectives for membrane reconstitution. *Proc. Natl. Acad. Sci. U. S. A* 77 (1): 239-243.
- Davies** HC, Smith L, and Nava ME. 1983. Reaction of cytochrome *c* in the electron-transport chain of *Paracoccus denitrificans*. *Biochim. Biophys. Acta* 725 (2): 238-245.
- De Gier** JW, Van Spanning RJ, Oltmann LF, and Stouthamer AH. 1992. Oxidation of methylamine by a *Paracoccus denitrificans* mutant impaired in the synthesis of the *bc*<sub>1</sub> complex and the *aa*<sub>3</sub>-type oxidase. Evidence for the existence of an alternative cytochrome *c* oxidase in this bacterium. *FEBS Lett.* 306 (1): 23-26.
- DeVries** GE, Harms N, Hoogendijk J, Stouthamer AH. 1989 Isolation and characterization of *Paracoccus denitrificans* mutants with increased conjugation frequencies and pleiotropic loss of a n(GATC)n DNA modifying property. *Arch. Microbiol.* (152):52-57
- Doeven** MK, Folgering JH, Krasnikov V, Geertsma ER, van den BG, and Poolman B. 2005. Distribution, lateral mobility and function of membrane proteins incorporated into giant unilamellar vesicles *Biophys. J.* 88 (2): 1134-1142.
- Dopner** S, Hudecek J, Ludwig B, Witt H, and Hildebrandt P. 2000. Structural changes in cytochrome *c* oxidase induced by cytochrome *c* binding. A resonance raman study. *Biochim. Biophys. Acta* 1480 (1-2): 57-64.
- Driessen** AJ, de VW, and Konings WN. 1985. Incorporation of beef heart cytochrome *c* oxidase as a proton-motive force-generating mechanism in bacterial membrane vesicles. *Proc. Natl. Acad. Sci. U. S. A* 82 (22): 7555-7559.

- Driessen** AJ, Hoekstra D, Scherphof G, Kalicharan RD, and Wilschut J. 1985. Low pH-induced fusion of liposomes with membrane vesicles derived from *Bacillus subtilis* J. *Biol. Chem.* 260 (19): 10880-10887.
- Drosou** V, Malatesta F, and Ludwig B. 2002. Mutations in the docking site for cytochrome c on the *Paracoccus* heme *aa*<sub>3</sub> oxidase. Electron entry and kinetic phases of the reaction. *Eur. J. Biochem.* 269 (12): 2980-2988.
- Drosou** V, Reincke B, Schneider M, and Ludwig B. 2002. Specificity of the interaction between the *Paracoccus denitrificans* oxidase and its substrate cytochrome *c*: comparing the mitochondrial to the homologous bacterial cytochrome *c*<sub>552</sub>, and its truncated and site-directed mutants. *Biochemistry* 41 (34): 10629-10634.
- Dudkina** NV, Eubel H, Keegstra W, Boekema EJ, and Braun HP. 2005. Structure of a mitochondrial supercomplex formed by respiratory-chain complexes I and III. *Proc. Natl. Acad. Sci. U. S. A* 102 (9): 3225-3229.
- Eaton** SS, and Eaton GR. 2002. Electron paramagnetic resonance techniques for measuring distances in proteins *Structures and Mechanisms: from Ashes to Enzymes* 827: 321-339.
- Eaton** SS, Eaton GR. 2000 Vol. 19, Biological Magnetic Resonance L.J. Berliner;Eds.; *Kluwer Academic/Plenum Publishers*: New York
- Eichhorn** AC, 2003 Konstruktion und funktionelle Charakterisierung löslicher Fragmente des Cytochrom *c*<sub>1</sub> aus *Paracoccus denitrificans* PhD dissertation Frankfurt University.
- Engelman** DM. 2005. Membranes are more mosaic than fluid. *Nature* 438 (7068): 578-580.
- Erecinska** M, and Wilson DF. 1979. Studies on the orientations of the mitochondrial redox carriers. Orientation of the chromophores of cytochrome *bc*<sub>1</sub> complex with respect to the plane of a cytochrome *bc*<sub>1</sub> complex--lipid model membrane. *Arch. Biochem. Biophys.* 192 (1): 80-85.
- Erecinska** M, Davis JS, and Wilson DF. 1979. Regulation of respiration in *Paracoccus denitrificans*: the dependence on redox state of cytochrome *c* and [ATP]/[ADP][Pi] *Arch. Biochem. Biophys.* 197 (2): 463-469.
- Erecinska** M. 1980. The use of photoaffinity labels in the study of mitochondrial function. *Ann. N. Y. Acad. Sci.* 346: 444-457.
- Eubel** H, Heinemeyer J, and Braun HP. 2004. Identification and characterization of respirasomes in potato mitochondria. *Plant Physiol* 134 (4): 1450-1459.
- Eubel** H, Jansch L, and Braun HP. 2003. New insights into the respiratory chain of plant mitochondria. Supercomplexes and a unique composition of complex II. *Plant Physiol* 133 (1): 274-286.
- Eytan** GD, Matheson MJ, and Racker E. 1976. Incorporation of mitochondrial membrane proteins into liposomes containing acidic phospholipids. *J. Biol. Chem.* 251 (21): 6831-6837.

- Fabian** M, Jancura D, and Palmer G. 2004. Two sites of interaction of anions with cytochrome *a* in oxidized bovine cytochrome *c* oxidase. *J. Biol. Chem.* 279 (16): 16170-16177.
- Fee** JA, Chen Y, Todaro TR, Bren KL, Patel KM, Hill MG, Gomez-Moran E, Loehr TM, Ai J, Thony-Meyer L, Williams PA, Stura E, Sridhar V, and McRee DE. 2000. Integrity of thermus thermophilus cytochrome *c*<sub>552</sub> synthesized by *Escherichia coli* cells expressing the host-specific cytochrome *c* maturation genes, ccmABCDEFGH: biochemical, spectral, and structural characterization of the recombinant protein. *Protein Sci.* 9 (11): 2074-2084.
- Ferguson-Miller** S, Brautigan DL, and Margoliash E. 1976. Correlation of the kinetics of electron transfer activity of various eukaryotic cytochromes *c* with binding to mitochondrial cytochrome *c* oxidase. *J. Biol. Chem.* 251 (4): 1104-1115.
- Finel** M. 1996. Genetic inactivation of the H<sup>+</sup>-translocating NADH:ubiquinone oxidoreductase of *Paracoccus denitrificans* is facilitated by insertion of the *ndh* gene from *Escherichia coli*. *FEBS Lett.* 393 (1): 81-85.
- Flöck** D, and Helms V. 2002. Protein--protein docking of electron transfer complexes: cytochrome *c* oxidase and cytochrome *c*. *Proteins* 47 (1): 75-85.
- Flöck** D, Helms V. 2004. A Brownian dynamics study: the effect of a membrane environment on an electron transfer system. *Biophys. J.* 87 (1): 65-74.
- Fowler** LR, and Hatefi Y. 1961. Reconstitution of the electron transport system. III. Reconstitution of DPNH oxidase, succinic oxidase, and DPNH, succinic oxidase. *Biochem. Biophys. Res. Commun.* 5: 203-208.
- Friedrich** T, and Bottcher B. 2004. The gross structure of the respiratory complex I: a Lego System. *Biochim. Biophys. Acta* 1608 (1): 1-9.
- Friedrich** T. 2001. Complex I: a chimaera of a redox and conformation-driven proton pump *J. Bioenerg. Biomembr.* 33 (3): 169-177.
- Gennis** RB, and Ferguson-Miller S. 1996. Protein structure: proton-pumping oxidases. *Curr. Biol.* 6 (1): 36-38.
- Genova** ML, Bianchi C, and Lenaz G. 2003. Structural organization of the mitochondrial respiratory chain. *Ital. J. Biochem.* 52 (1): 58-61.
- Georgiadis** KE, Jhon NI, and Einarsdottir O. 1994. Time-resolved optical absorption studies of intramolecular electron transfer in cytochrome *c* oxidase. *Biochemistry* 33 (31): 9245-9256.
- Girard** P, Pecreaux J, Lenoir G, Falson P, Rigaud JL, and Bassereau P. 2004. A new method for the reconstitution of membrane proteins into giant unilamellar vesicles. *Biophys. J.* 87 (1): 419-429.
- Goldkorn** T, Rimon G, Kempner ES, and Kaback HR. 1984. Functional molecular weight of the lac carrier protein from *Escherichia coli* as studied by radiation inactivation analysis *Proc. Natl. Acad. Sci. U. S. A* 81 (4): 1021-1025.

- Gonzalez-Rodriguez J**, and Acuna AU. 1987. Probing molecular dynamics of proteins in biological membranes by optical spectroscopy: rotational diffusion. *Revis. Biol. Celular.* 11: 47-74.
- Gray HB**, and Malmstrom BG. 1989. Long-range electron transfer in multisite metalloproteins. *Biochemistry* 28 (19): 7499-7505.
- Grimaldi S**, MacMillan F, Ostermann T, Ludwig B, Michel H, and Prisner T. 2001. QH\*-ubisemiquinone radical in the *bo*<sub>3</sub>-type ubiquinol oxidase studied by pulsed electron paramagnetic resonance and hyperfine sublevel correlation spectroscopy. *Biochemistry* 40 (4): 1037-1043.
- Gupte S**, Wu ES, Hoehli L, Hoehli M, Jacobson K, Sowers AE, and Hackenbrock CR. 1984. Relationship between lateral diffusion, collision frequency, and electron transfer of mitochondrial inner membrane oxidation-reduction components. *Proc. Natl. Acad. Sci. U. S. A* 81 (9): 2606-2610.
- Gupte SS**, and Hackenbrock CR. 1988. The role of cytochrome *c* diffusion in mitochondrial electron transport. *J. Biol. Chem.* 263 (11): 5248-5253.
- Hackenbrock CR**, Chazotte B, and Gupte SS. 1986. The random collision model and a critical assessment of diffusion and collision in mitochondrial electron transport. *J. Bioenerg. Biomembr.* 18 (5): 331-368.
- Hackenbrock CR**, Gupte S, Wu ES, and Jacobson K. 1984. Lateral diffusion, collision and efficiency of oxidation-reduction components in mitochondrial electron transport. *Biochem. Soc. Trans.* 12 (3): 402-403.
- Hackenbrock CR**, Schneider H, Lemasters JJ, and Hochli M. 1980. Relationships between bilayer lipid, motional freedom of oxidoreductase components, and electron transfer in the mitochondrial inner membrane. *Adv. Exp. Med. Biol.* 132: 245-263.
- Hardt SL**. 1980. A measurable consequence of the Mitchell theory of phosphorylation. *J. Theor. Biol.* 87 (1): 1-7.
- Harrenga A**, and Michel H. 1999. The cytochrome *c* oxidase from *Paracoccus denitrificans* does not change the metal center ligation upon reduction. *J. Biol. Chem.* 274 (47): 33296-33299.
- Harrenga A**, Reincke B, Ruterjans H, Ludwig B, and Michel H. 2000. Structure of the soluble domain of cytochrome *c*<sub>552</sub> from *Paracoccus denitrificans* in the oxidized and reduced states. *J. Mol. Biol.* 295 (3): 667-678.
- Hatefi Y**, Haavik AG, and Griffiths DE. 1961. Reconstitution of the electron transport system. I. Preparation and properties of the interacting enzyme complexes. *Biochem. Biophys. Res. Commun.* 4: 441-446.
- Hatefi Y**. 1978. Introduction--preparation and properties of the enzymes and enzymes complexes of the mitochondrial oxidative phosphorylation system. *Methods Enzymol.* 53: 3-4.

- Haustein** E, and Schwille P. 2004. Single-molecule spectroscopic methods. *Curr. Opin. Struct. Biol.* 14 (5): 531-540.
- Helenius** A, and Simons K. 1972. The binding of detergents to lipophilic and hydrophilic proteins *J. Biol. Chem.* 247 (11): 3656-3661.
- Hendler** RW, Pardhasaradhi K, Reynafarje B, and Ludwig B. 1991. Comparison of energy-transducing capabilities of the two- and three-subunit cytochromes *aa<sub>3</sub>* from *Paracoccus denitrificans* and the 13-subunit beef heart enzyme. *Biophys. J.* 60 (2): 415-423.
- Heron** C, Ragan CI, and Trumpower BL. 1978. The interaction between mitochondrial NADH-ubiquinone oxidoreductase and ubiquinol-cytochrome *c* oxidoreductase. Restoration of ubiquinone-pool behaviour. *Biochem. J.* 174 (3): 791-800.
- Hertel** MM, Denysenkov VP, Bennati M, Prisner TF. Pulsed 180 GHz EPR/ENDOR/PELDOR spectroscopy *Mag. Res. Chem.* 2005, (43). 248-255
- Hildebrandt** P, Vanhecke F, Buse G, Soulimane T, and Mauk AG. 1993. Resonance Raman study of the interactions between cytochrome *c* variants and cytochrome *c* oxidase *Biochemistry* 32 (40): 10912-10922.
- Hinchliffe** P, and Sazanov LA. 2005. Organization of iron-sulfur clusters in respiratory complex I. *Science* 309 (5735): 771-774.
- Hirst** J, Carroll J, Fearnley IM, Shannon RJ, and Walker JE. 2003. The nuclear encoded subunits of complex I from bovine heart mitochondria. *Biochim. Biophys. Acta* 1604 (3): 135-150.
- Hochli** M, and Hackenbrock CR. 1979. Lateral translational diffusion of cytochrome *c* oxidase in the mitochondrial energy-transducing membrane. *Proc. Natl. Acad. Sci. U. S. A* 76 (3): 1236-1240.
- Hochli** M, Hochli L, and Hackenbrock CR. 1985. Independent lateral diffusion of cytochrome *bc<sub>1</sub>* complex and cytochrome oxidase in the mitochondrial inner membrane. *Eur. J. Cell Biol.* 38 (1): 1-5.
- Hochman** J, Ferguson-Miller S, and Schindler M. 1985. Mobility in the mitochondrial electron transport chain. *Biochemistry* 24 (10): 2509-2516.
- Hochman** JH, Schindler M, Lee JG, and Ferguson-Miller S. 1982. Lateral mobility of cytochrome *c* on intact mitochondrial membranes as determined by fluorescence redistribution after photobleaching. *Proc. Natl. Acad. Sci. U. S. A* 79 (22): 6866-6870.
- Hollan** S. 1996. Membrane fluidity of blood cells. *Haematologia (Budap.)* 27 (3): 109-127.
- Horvath** LI, Torok M, Hideg K, and Dux L. 1997. Dynamic aspects of the incorporation of proteins into biological membranes. *J. Mol. Recognit.* 10 (4): 188-193.
- Hunte** C, and Michel H. 2002. Crystallisation of membrane proteins mediated by antibody fragments. *Curr. Opin. Struct. Biol.* 12 (4): 503-508.

- Hunte** C, Koepke J, Lange C, Rossmann T, and Michel H. 2000. Structure at 2.3 Å resolution of the cytochrome *bc*<sub>1</sub> complex from the yeast *Saccharomyces cerevisiae* co-crystallized with an antibody Fv fragment. *Structure*. 8 (6): 669-684.
- Hunte** C, Solmaz S, and Lange C. 2002. Electron transfer between yeast cytochrome *bc*<sub>1</sub> complex and cytochrome *c*: a structural analysis. *Biochim. Biophys. Acta* 1555 (1-3): 21-28.
- Iverson** TM, Luna-Chavez C, Cecchini G, and Rees DC. 1999. Structure of the *Escherichia coli* fumarate reductase respiratory complex. *Science* 284 (5422): 1961-1966.
- Iwasaki** T, Matsuura K, and Oshima T. 1995. Resolution of the aerobic respiratory system of the thermoacidophilic archaeon, *Sulfolobus* sp. strain 7. I. The archaeal terminal oxidase supercomplex is a functional fusion of respiratory complexes III and IV with no c-type cytochromes. *J. Biol. Chem.* 270 (52): 30881-30892.
- Iwata** S, Lee JW, Okada K, Lee JK, Iwata M, Rasmussen B, Link TA, Ramaswamy S, and Jap BK. 1998. Complete structure of the 11-subunit bovine mitochondrial cytochrome *bc*<sub>1</sub> complex. *Science* 281 (5373): 64-71.
- Iwata** S, Ostermeier C, Ludwig B, and Michel H. 1995. Structure at 2.8 Å resolution of cytochrome *c* oxidase from *Paracoccus denitrificans*. *Nature* 376 (6542): 660-669.
- John** P, and Whatley FR. 1975. *Paracoccus denitrificans* and the evolutionary origin of the mitochondrion. *Nature* 254 (5500): 495-498.
- Jacobson** K, Ishihara A, and Inman R. 1987. Lateral Diffusion of Proteins in Membranes *Annual Review of Physiology* 49: 163-175.
- Kawato** S, and Kinosita K, Jr. 1981. Time-dependent absorption anisotropy and rotational diffusion of proteins in membranes. *Biophys. J.* 36 (1): 277-296.
- Kawato** S, Lehner C, Muller M, and Cherry RJ. 1982. Protein-protein interactions of cytochrome oxidase in inner mitochondrial membranes. The effect of liposome fusion on protein rotational mobility. *J. Biol. Chem.* 257 (11): 6470-6476.
- Kawato** S, Sigel E, Carafoli E, and Cherry RJ. 1980. Cytochrome oxidase rotates in the inner membrane of intact mitochondria and submitochondrial particles. *J. Biol. Chem.* 255 (12): 5508-5510.
- Kleymann** G, Ostermeier C, Heitmann K, Haase W, and Michel H. 1995. Use of antibody fragments (Fv) in immunocytochemistry. *J. Histochem. Cytochem.* 43 (6): 607-614.
- Koppel** DE, Sheetz MP, and Schindler M. 1980. Lateral diffusion in biological membranes. A normal-mode analysis of diffusion on a spherical surface. *Biophys. J.* 30 (1): 187-192.
- Koppel** DE. 1979. Fluorescence redistribution after photobleaching. A new multipoint analysis of membrane translational dynamics. *Biophys. J.* 28 (2): 281-291.



- Koppenol** WH, and Margoliash E. 1982. The asymmetric distribution of charges on the surface of horse cytochrome *c*. Functional implications. *J. Biol. Chem.* 257 (8): 4426-4437.
- Kornblatt** JA, Theodorakis J, Hoa GH, and Margoliash E. 1992. Cytochrome *c* and cytochrome *c* oxidase interactions: the effects of ionic strength and hydrostatic pressure studied with site-specific modifications of cytochrome *c*. *Biochem. Cell Biol.* 70 (7): 539-547.
- Koutsoupakis** K, Stavrakis S, Pinakoulaki E, Soulimane T, and Varotsis C. 2002. Observation of the equilibrium Cu<sub>B</sub>-CO complex and functional implications of the transient heme *a*<sub>3</sub> propionates in cytochrome *ba*<sub>3</sub>-CO from *Thermus thermophilus*. Fourier transform infrared (FTIR) and time-resolved step-scan FTIR studies. *J. Biol. Chem.* 277 (36): 32860-32866.
- Krause** F, Reifschneider NH, Vocke D, Seelert H, Rexroth S, and Dencher NA. 2004. "Respirasome"-like supercomplexes in green leaf mitochondria of spinach. *J. Biol. Chem.* 279 (46): 48369-48375.
- Kroneck** PM, Antholine WE, Kastrau DH, Buse G, Steffens GC, and Zumft WG. 1990. Multifrequency EPR evidence for a bimetallic center at the Cu<sub>A</sub> site in cytochrome *c* oxidase. *FEBS Lett.* 268 (1): 274-276.
- Laemmli** UK. 1970. Cleavage of structural proteins during the assembly of the head of bacteriophage T4. *Nature* 227 (5259): 680-685.
- Lakshmi** KV, and Brudvig GW. 2001. Pulsed electron paramagnetic resonance methods for macromolecular structure determination. *Curr. Opin. Struct. Biol.* 11 (5): 523-531.
- Lancaster** CR, Kroger A, Auer M, and Michel H. 1999. Structure of fumarate reductase from *Wolinella succinogenes* at 2.2 Å resolution. *Nature* 402 (6760): 377-385.
- Lange** C, Cornvik T, az-Moreno I, and Ubbink M. 2005. The transient complex of poplar plastocyanin with cytochrome *f*: effects of ionic strength and pH. *Biochim. Biophys. Acta* 1707 (2-3): 179-188.
- Lenaz** G, and Fato R. 1986. Is ubiquinone diffusion rate-limiting for electron transfer? *J. Bioenerg. Biomembr.* 18 (5): 369-401.
- Lichtenberg** D. 1985. Characterization of the solubilization of lipid bilayers by surfactants. *Biochim. Biophys. Acta* 821 (3): 470-478.
- Lowry** OH, Rosebrough NJ, Farr AL, and Randall RJ. 1951. Protein measurement with the Folin phenol reagent. *J. Biol. Chem.* 193 (1): 265-275.
- Ludwig** B, and Schatz G. 1980. A two-subunit cytochrome *c* oxidase (cytochrome *aa*<sub>3</sub>) from *Paracoccus denitrificans*. *Proc. Natl. Acad. Sci. U. S. A* 77 (1): 196-200.
- Ludwig** B, Bender E, Arnold S, Huttemann M, Lee I, and Kadenbach B. 2001. Cytochrome *c* oxidase and the regulation of oxidative phosphorylation. *ChemBiochem.* 2 (6): 392-403.

- Ludwig B.** 1986. Cytochrome *c* oxidase from *Paracoccus denitrificans*. *Methods Enzymol.* 126: 153-159.
- Ludwig B.** 1992. Terminal oxidases in *Paracoccus denitrificans*. *Biochim. Biophys. Acta* 1101 (2): 195-197.
- Luisi PL, Walde P, Blocher M, and Liu DJ.** 2000. Research on the origin of life: Membrane-assisted polycondensations of amino acids and peptides. *Chimia* 54 (1-2): 52-53.
- Maneg O,** 2003. Elektronentransfer zwischen Redoxkomplexen aus *Thermus thermophilus* und *Paracoccus denitrificans* PhD dissertation Frankfurt University
- Maneg O, Ludwig B, and Malatesta F.** 2003. Different interaction modes of two cytochrome-*c* oxidase soluble Cu<sub>A</sub> fragments with their substrates. *J. Biol. Chem.* 278 (47): 46734-46740.
- Maneg O, Malatesta F, Ludwig B, and Drosou V.** 2004. Interaction of cytochrome *c* with cytochrome oxidase: two different docking scenarios. *Biochim. Biophys. Acta* 1655 (1-3): 274-281.
- Miller C, and Racker E.** 1976. Ca<sup>++</sup>-induced fusion of fragmented sarcoplasmic reticulum with artificial planar bilayers *J. Membr. Biol.* 30 (3): 283-300.
- Miller C, and Racker E.** 1976. Fusion of phospholipid vesicles reconstituted with cytochrome *c* oxidase and mitochondrial hydrophobic protein *J. Membr. Biol.* 26 (4): 319-333.
- Miller C, Arvan P, Telford JN, and Racker E.** 1976. Ca<sup>++</sup>-induced fusion of proteoliposomes: dependence on transmembrane osmotic gradient *J. Membr. Biol.* 30 (3): 271-282.
- Mitchell P.** 1962. Metabolism, transport, and morphogenesis: which drives which? *J. Gen. Microbiol.* 29: 25-37.
- Musiani F, Dikiy A, Semenov AY, and Ciurli S.** 2005. Structure of the intermolecular complex between plastocyanin and cytochrome *f* from spinach *Journal of Biological Chemistry* 280 (19): 18833-18841.
- Nicolson GL, and Singer SJ.** 1972. Electron microscopic localization of macromolecules on membrane surfaces *Ann. N. Y. Acad. Sci.* 195: 368-375.
- Niebisch A, and Bott M.** 2003. Purification of a cytochrome *bc-aa<sub>3</sub>* supercomplex with quinol oxidase activity from *Corynebacterium glutamicum*. Identification of a fourth subunit of cytochrome *aa<sub>3</sub>* oxidase and mutational analysis of diheme cytochrome *c<sub>1</sub>*. *J. Biol. Chem.* 278 (6): 4339-4346.
- Ohnishi T.** 1998. Iron-sulfur clusters/semiquinones in complex I. *Biochim. Biophys. Acta* 1364 (2): 186-206.
- Ostermeier C, Harrenga A, Ermler U, and Michel H.** 1997. Structure at 2.7 Å resolution of the *Paracoccus denitrificans* two-subunit cytochrome *c* oxidase complexed with an antibody Fv fragment. *Proc. Natl. Acad. Sci. U. S. A* 94 (20): 10547-10553.

- Ostermeier** C, Iwata S, Ludwig B, and Michel H. 1995. Fv fragment-mediated crystallization of the membrane protein bacterial cytochrome *c* oxidase. *Nat. Struct. Biol.* 2 (10): 842-846.
- Otten** MF, Reijnders WN, Bedaux JJ, Westerhoff HV, Krab K, and Van Spanning RJ. 1999. The reduction state of the Q-pool regulates the electron flux through the branched respiratory network of *Paracoccus denitrificans*. *Eur. J. Biochem.* 261 (3): 767-774.
- Otten** MF, van der OJ, Reijnders WN, Westerhoff HV, Ludwig B, and Van Spanning RJ. 2001. Cytochromes *c*<sub>550</sub>, *c*<sub>552</sub>, and *c*<sub>1</sub> in the electron transport network of *Paracoccus denitrificans*: redundant or subtly different in function? *J. Bacteriol.* 183 (24): 7017-7026.
- Page** CC, Moser CC, Chen X, and Dutton PL. 1999. Natural engineering principles of electron tunnelling in biological oxidation-reduction. *Nature* 402 (6757): 47-52.
- Pelletier** H, and Kraut J. 1992. Crystal structure of a complex between electron transfer partners, cytochrome *c* peroxidase and cytochrome *c*. *Science* 258 (5089): 1748-1755.
- Pettigrew** GW, Goodhew CF, Cooper A, Nutley M, Jumel K, and Harding SE. 2003. The electron transfer complexes of cytochrome *c* peroxidase from *Paracoccus denitrificans*. *Biochemistry* 42 (7): 2046-2055.
- Pettigrew** GW, Pauleta SR, Goodhew CF, Cooper A, Nutley M, Jumel K, Harding SE, Costa C, Krippahl L, Moura I, and Moura J. 2003. Electron transfer complexes of cytochrome *c* peroxidase from *Paracoccus denitrificans* containing more than one cytochrome. *Biochemistry* 42 (41): 11968-11981.
- Pettigrew** GW, Prazeres S, Costa C, Palma N, Krippahl L, Moura I, and Moura JJ. 1999. The structure of an electron transfer complex containing a cytochrome *c* and a peroxidase. *J. Biol. Chem.* 274 (16): 11383-11389.
- Pfeiffer** K, Gohil V, Stuart RA, Hunte C, Brandt U, Greenberg ML, and Schagger H. 2003. Cardiolipin stabilizes respiratory chain supercomplexes. *J. Biol. Chem.* 278 (52): 52873-52880.
- Pfitzner** U, Kirichenko A, Konstantinov AA, Mertens M, Wittershagen A, Kolbesen BO, Steffens GC, Harrenga A, Michel H, and Ludwig B. 1999. Mutations in the Ca<sup>2+</sup> binding site of the *Paracoccus denitrificans* cytochrome *c* oxidase. *FEBS Lett.* 456 (3): 365-369.
- Pilet** E, Jasaitis A, Liebl U, and Vos MH. 2004. Electron transfer between hemes in mammalian cytochrome *c* oxidase. *Proc. Natl. Acad. Sci. U. S. A* 101 (46): 16198-16203.
- Prisner** T, Rohrer M, and MacMillan F. 2001. Pulsed EPR spectroscopy: biological applications. *Annu. Rev. Phys. Chem.* 52: 279-313.
- Pristovsek** P, Lucke C, Reincke B, Ludwig B, and Ruterjans H. 2000. Solution structure of the functional domain of *Paracoccus denitrificans* cytochrome *c*<sub>552</sub> in the reduced state. *Eur. J. Biochem.* 267 (13): 4205-4212.

- Puustinen** A, Finel M, Virkki M, and Wikstrom M. 1989. Cytochrome o (bo) is a proton pump in *Paracoccus denitrificans* and *Escherichia coli*. *FEBS Lett.* 249 (2): 163-167.
- Ragan** CI, Heron C:1978. The interaction between mitochondrial NADH-ubiquinone oxidoreductase and ubiquinol-cytochrome *c* oxidoreductase. Evidence for stoichiometric association. *Biochem. J.* 174 (3): 783-790.
- Reichardt** JK, and Gibson QH. 1983. Turnover of cytochrome *c* oxidase from *Paracoccus denitrificans*. *J. Biol. Chem.* 258 (3): 1504-1507.
- Reincke** B, Perez C, Pristovsek P, Lucke C, Ludwig C, Lohr F, Rogov VV, Ludwig B, and Ruterjans H. 2001. Solution structure and dynamics of the functional domain of *Paracoccus denitrificans* cytochrome *c*<sub>552</sub> in both redox states. *Biochemistry* 40 (41): 12312-12320.
- Reincke** B, Thony-Meyer L, Dannehl C, Odenwald A, Aidim M, Witt H, Ruterjans H, and Ludwig B. 1999. Heterologous expression of soluble fragments of cytochrome *c*<sub>552</sub> acting as electron donor to the *Paracoccus denitrificans* cytochrome *c* oxidase. *Biochim. Biophys. Acta* 1411 (1): 114-120.
- Reits** EA, and Neefjes JJ. 2001. From fixed to FRAP: measuring protein mobility and activity in living cells. *Nat. Cell Biol.* 3 (6): 145-147.
- Ribrioux** S, Kleymann G, Haase W, Heitmann K, Ostermeier C, and Michel H. 1996. Use of nano. *J. Histochem. Cytochem.* 44 (3): 207-213.
- Rich** PR. 2003. The molecular machinery of Keilin's respiratory chain. *Biochem. Soc. Trans.* 31: 1095-1105.
- Richter** OM, and Ludwig B. 2003. Cytochrome *c* oxidase--structure, function, and physiology of a redox-driven molecular machine. *Rev. Physiol Biochem. Pharmacol.* 147: 47-74.
- Rigaud** JL, and Levy D. 2003. Reconstitution of membrane proteins into liposomes. *Methods Enzymol.* 372: 65-86.
- Rigaud** JL, Mosser G, Lacapere JJ, Olofsson A, Levy D, and Ranck JL. 1997. Bio-Beads: an efficient strategy for two-dimensional crystallization of membrane proteins. *J. Struct. Biol.* 118 (3): 226-235.
- Rigaud** JL, Pitard B, and Levy D. 1995. Reconstitution of membrane proteins into liposomes: application to energy-transducing membrane proteins. *Biochim. Biophys. Acta* 1231 (3): 223-246.
- Rigaud** JL. 2002. Membrane proteins: functional and structural studies using reconstituted proteoliposomes and 2-D crystals. *Braz. J. Med. Biol. Res.* 35 (7): 753-766.
- Roberts** VA, and Pique ME. 1999. Definition of the interaction domain for cytochrome *c* on cytochrome *c* oxidase. III. Prediction of the docked complex by a complete, systematic search. *J. Biol. Chem.* 274 (53): 38051-38060.

- Rohrer** M; Brüggmann O; Kinzer B; Prisner T F. High-Field/High-Frequency EPR spectrometer operating in pulsed and continuous-wave mode at 180 GHz *Appl. Mag. Res.* 2001, 21, 257-274
- Sampson** V, and Alleyne T. 2001. Cytochrome c/cytochrome c oxidase interaction. Direct structural evidence for conformational changes during enzyme turnover. *Eur. J. Biochem.* 268 (24): 6534-6544.
- Saraste** M. 1999. Oxidative phosphorylation at the fin de siècle. *Science* 283 (5407): 1488-1493.
- Saxton** MJ. 1989. Lateral diffusion in an archipelago. Distance dependence of the diffusion coefficient. *Biophys. J.* 56 (3): 615-622.
- Sazanov** LA, and Hinchliffe P. 2006. Structure of the hydrophilic domain of respiratory complex I from *Thermus thermophilus*. *Science* 311 (5766): 1430-1436
- Schäfer** E, Seelert H, Reifschneider NH, Krause F, Dencher NA, and Vonck J. 2006. Architecture of active mammalian respiratory chain supercomplexes *J. Biol. Chem.* 281 (22): 15370-15375.
- Schägger** H, and Pfeiffer K. 2000. Supercomplexes in the respiratory chains of yeast and mammalian mitochondria. *EMBO J.* 19 (8): 1777-1783.
- Schägger** H, and Pfeiffer K. 2001. The ratio of oxidative phosphorylation complexes I-V in bovine heart mitochondria and the composition of respiratory chain supercomplexes. *J. Biol. Chem.* 276 (41): 37861-37867.
- Schägger** H, de Coo R, Bauer MF, Hofmann S, Godinot C, and Brandt U. 2004. Significance of respirasomes for the assembly/stability of human respiratory chain complex I. *J. Biol. Chem.* 279 (35): 36349-36353.
- Schägger** H. 1995. Native electrophoresis for isolation of mitochondrial oxidative phosphorylation protein complexes. *Methods Enzymol.* 260: 190-202.
- Schägger** H. 2001. Blue-native gels to isolate protein complexes from mitochondria. *Methods Cell Biol.* 65: 231-244.
- Schägger** H. 2001. Respiratory chain supercomplexes. *IUBMB. Life* 52 (3-5): 119-128.
- Schägger** H. 2002. Respiratory chain supercomplexes of mitochondria and bacteria. *Biochim. Biophys. Acta* 1555 (1-3): 154-159.
- Schmidt** B, McCracken J, and Ferguson-Miller S. 2003. A discrete water exit pathway in the membrane protein cytochrome c oxidase. *Proc. Natl. Acad. Sci. U. S. A* 100 (26): 15539-15542.
- Schmidt** TR, Wildman DE, Uddin M, Opazo JC, Goodman M, and Grossman LI. 2005. Rapid electrostatic evolution at the binding site for cytochrome c on cytochrome c oxidase in anthropoid primates. *Proc. Natl. Acad. Sci. U. S. A* 102 (18): 6379-6384.

- Schneider** H, Lemasters JJ, and Hackenbrock CR. 1982. Lateral diffusion of ubiquinone during electron transfer in phospholipid- and ubiquinone-enriched mitochondrial membranes. *J. Biol. Chem.* 257 (18): 10789-10793.
- Schneider** H, Lemasters JJ, Hochli M, and Hackenbrock CR. 1980. Liposome-mitochondrial inner membrane fusion. Lateral diffusion of integral electron transfer components. *J. Biol. Chem.* 255 (8): 3748-3756.
- Scholes** CP, Janakiraman R, Taylor H, and King TE. 1984. Temperature dependence of the electron spin-lattice relaxation rate from pulsed EPR of Cu<sub>A</sub> and heme *a* in cytochrome *c* oxidase. *Biophys. J.* 45 (5): 1027-1030.
- Scholes** PB, and Smith L. 1968. The isolation and properties of the cytoplasmic membrane of *Micrococcus denitrificans*. *Biochim. Biophys. Acta* 153 (2): 350-362.
- Schultz** BE, and Chan SI. 2001. Structures and proton-pumping strategies of mitochondrial respiratory enzymes. *Annu. Rev. Biophys. Biomol. Struct.* 30: 23-65.
- Slutter** CE, Gromov I, Epel B, Pecht I, Richards JH, and Goldfarb D. 2001. Pulsed EPR/ENDOR characterization of perturbations of the Cu<sub>A</sub> center ground state by axial methionine ligand mutations. *J. Am. Chem. Soc.* 123 (22): 5325-5336.
- Smith** L, and Davies HC. 1991. The reactions of the oxidase and reductases of *Paracoccus denitrificans* with cytochromes *c*. *J. Bioenerg. Biomembr.* 23 (2): 303-319.
- Smith** L, Bolgiano B, and Davies HC. 1988. Kinetics of the interaction of cytochrome *c* oxidase of *Paracoccus denitrificans* with *Paracoccus* and mitochondrial cytochrome *c*. *Prog. Clin. Biol. Res.* 274: 619-635.
- Sone** N, Sekimachi M, and Kutoh E. 1987. Identification and Properties of A Quinol Oxidase Super-Complex Composed of A Bc1 Complex and Cytochrome-Oxidase in the Thermophilic Bacterium Ps3. *J. Biol. Chem* 262 (32): 15386-15391.
- Soulimane** T, Buse G, Bourenkov GP, Bartunik HD, Huber R, and Than ME. 2000. Structure and mechanism of the aberrant *ba*<sub>3</sub>-cytochrome *c* oxidase from *Thermus thermophilus*. *EMBO J.* 19 (8): 1766-1776.
- Soulimane** T, von WM, Hof P, Than ME, Huber R, and Buse G. 1997. Cytochrome-*c*<sub>552</sub> from *Thermus thermophilus*: a functional and crystallographic investigation. *Biochem. Biophys. Res. Commun.* 237 (3): 572-576.
- Soulimane** T, vonWalter M, Hof P, Than ME, Huber R, and Buse G. 1997. Cytochrome-*c*<sub>552</sub> from *Thermus thermophilus*: A functional and crystallographic investigation. *Biochemical and Biophysical Research Communications* 237 (3): 572-576.
- Steinrucke** P, and Ludwig B. 1993. Genetics of *Paracoccus denitrificans*. *FEMS Microbiol. Rev.* 10 (1-2): 83-117.
- Stouthamer** AH. 1992. Metabolic pathways in *Paracoccus denitrificans* and closely related bacteria in relation to the phylogeny of prokaryotes. *Antonie Van Leeuwenhoek* 61 (1): 1-33.

- Stroh** A, Anderka O, Pfeiffer K, Yagi T, Finel M, Ludwig B, and Schagger H. 2004. Assembly of respiratory complexes I, III, and IV into NADH oxidase supercomplex stabilizes complex I in *Paracoccus denitrificans*. *J. Biol. Chem.* 279 (6): 5000-5007.
- Svensson-Ek** M, Abramson J, Larsson G, Tornroth S, Brzezinski P, and Iwata S. 2002. The X-ray crystal structures of wild-type and EQ(I-286) mutant cytochrome *c* oxidases from *Rhodobacter sphaeroides*. *J. Mol. Biol.* 321 (2): 329-339.
- Szundi** I, Cappuccio JA, Borovok N, Kotlyar AB, and Einarsdottir O. 2001. Photoinduced electron transfer in the cytochrome *c*/cytochrome *c* oxidase complex using thiouredopyrenetrisulfonate-labeled cytochrome *c*. Optical multichannel detection. *Biochemistry* 40 (7): 2186-2193.
- Trumpower** BL. 1991. The three-subunit cytochrome *bc*<sub>1</sub> complex of *Paracoccus denitrificans*. Its physiological function, structure, and mechanism of electron transfer and energy transduction. *J. Bioenerg. Biomembr.* 23 (2): 241-255.
- Tsukihara** T, Aoyama H, Yamashita E, Tomizaki T, Yamaguchi H, Shinzawa-Itoh K, Nakashima R, Yaono R, and Yoshikawa S. 1996. The whole structure of the 13-subunit oxidized cytochrome *c* oxidase at 2.8 Å. *Science* 272 (5265): 1136-1144.
- Ubbink** M, Ejdeback M, Karlsson BG, and Bendall DS. 1998. The structure of the complex of plastocyanin and cytochrome *f*, determined by paramagnetic NMR and restrained rigid-body molecular dynamics. *Structure.* 6 (3): 323-335.
- Weber** PC, and Tollin G. 1985. Electrostatic interactions during electron transfer reactions between c-type cytochromes and flavodoxin. *J. Biol. Chem.* 260 (9): 5568-5573.
- White** DC, and Sinclair PR. 1971. Branched electron-transport systems in bacteria. *Adv. Microb. Physiol* 5: 173-211.
- Whitesid** TL, Desiervo AJ, and Salton MRJ. 1971. Use of Antibody to Membrane Adenosine Triphosphatase in Study of Bacterial Relationships *Journal of Bacteriology* 105 (3): 957-&.
- Wienk** H, Maneg O, Lucke C, Pristovsek P, Lohr F, Ludwig B, and Ruterjans H. 2003. Interaction of cytochrome *c* with cytochrome *c* oxidase: an NMR study on two soluble fragments derived from *Paracoccus denitrificans*. *Biochemistry* 42 (20): 6005-6012.
- Wilkinson** BJ, Morman MR, and White DC. 1972. Phospholipid composition and metabolism of *Micrococcus denitrificans* *J. Bacteriol.* 112 (3): 1288-1294.
- Williams** PA, Fulop V, Leung YC, Chan C, Moir JW, Howlett G, Ferguson SJ, Radford SE, and Hajdu J. 1995. Pseudospecific docking surfaces on electron transfer proteins as illustrated by pseudoazurin, cytochrome *c*<sub>550</sub> and cytochrome *cd*<sub>1</sub> nitrite reductase *Nat. Struct. Biol.* 2 (11): 975-982.
- Witt** H, and Ludwig B. 1997. Isolation, analysis, and deletion of the gene coding for subunit IV of cytochrome *c* oxidase in *Paracoccus denitrificans*. *J. Biol. Chem.* 272 (9): 5514-5517.

- Witt** H, Malatesta F, Nicoletti F, Brunori M, and Ludwig B. 1998. Cytochrome-c-binding site on cytochrome oxidase in *Paracoccus denitrificans*. *Eur. J. Biochem.* 251 (1-2): 367-373.
- Woodruff** WH, Einarsdottir O, Dyer RB, Bagley KA, Palmer G, Atherton SJ, Goldbeck RA, Dawes TD, and Kliger DS. 1991. Nature and functional implications of the cytochrome  $a_3$  transients after photodissociation of CO-cytochrome oxidase. *Proc. Natl. Acad. Sci. U. S. A* 88 (6): 2588-2592.
- Yagi** T, and Matsuno-Yagi A. 2003. The proton-translocating NADH-quinone oxidoreductase in the respiratory chain: the secret unlocked. *Biochemistry* 42 (8): 2266-2274.
- Yagi** T, Seo BB, Di Bernardo S, Nakamaru-Ogiso E, Kao MC, and Matsuno-Yagi A. 2001. NADH dehydrogenases: from basic science to biomedicine. *J. Bioenerg. Biomembr.* 33 (3): 233-242.
- Yoshikawa** S, Shinzawa-Itoh K, Nakashima R, Yaono R, Yamashita E, Inoue N, Yao M, Fei MJ, Libeu CP, Mizushima T, Yamaguchi H, Tomizaki T, and Tsukihara T. 1998. Redox-coupled crystal structural changes in bovine heart cytochrome  $c$  oxidase. *Science* 280 (5370): 1723-1729.
- Zhang** Z, Huang L, Shulmeister VM, Chi YI, Kim KK, Hung LW, Crofts AR, Berry EA, and Kim SH. 1998. Electron transfer by domain movement in cytochrome  $bc_1$ . *Nature* 392 (6677): 677-684.



## Acknowledgements

*I would like to acknowledge the contributions of all the people who have helped me bring my PhD to fruition.*

*A special thanks to my supervisor, Prof. Dr. Bernd Ludwig, for giving me the opportunity to join the department of molecular genetics, at the institute of biochemistry of Johann Wolfgang Goethe University. I deeply appreciate his support, his profound interest in the project, and for his extremely incisive discussions, crucial advices and generous nature.*

*I am greatly indebted to Prof. Dr. Thomas Prisner for his profound knowledge in the EPR and for showing keen interest in the project. I would like to thank him for his wonderful contributions and for always being positive and enthusiastic about project approach.*

*I would like to thank Sevdalina Lyubenova and Marloes Penning de Vries for conducting the EPR experiments and helping me to learn and interpret the EPR data.*

*Deep appreciation should be made to Prof. Bereiter-Hahn and Prof. Wachtveitl for their academic discussion for translation diffusion approach of the project.*

*I would like to thank Prof. Dr. E. Bamberg for the constructive suggestions during my thesis committee meeting about the native membrane fusion. I thank Prof. Dr. Klaus Fendler who gave me the opportunity to use his instruments for trying the fusion experiment.*

*I am also thankful to Dr. Winfried Haase for measuring the diameter of fused membrane vesicles by electron microscopy.*

*I would also like to thank Dr. R. Naumann, Dr. Ingo Köper for FRAP measurement and Marcel Friedrich for the initial FCS and membrane size measurement, discussion and for his enthusiasm in trying different approaches to conduct experiments.*

*I am grateful to Dr. Igor Chizhov for the flash photolysis experiment, his knowledge and discussions, analysis of kinetic data and all the arrangement, accommodation during the Hannover visit.*

*I would also like to thanks Prof. Dr. B. Brutschy and Drs. Chayan Nandi, Partha Parui for helping in the FCS measurements and wonderful discussion.*

*I am especially grateful to past members Oliver Maneg, Klaus Hoffmeier, Andreas Stocker of my group for being always ready for interesting discussions and for their kindness and generosity.*

*My gratitude goes to Dr. Oliver Richter for his precious knowledge, discussions, and grateful suggestions.*

*I would like to thank Thomas, Alena and Peter for reading my thesis, translating summary (Zusammenfassung) and their helpful suggestions. I thank Bettina, Daniela, Caro, Christian, Andrea for nice working environment. I would like to thank Julia for giving me  $c_1$  fragment and nice discussions.*

*I would like to pay modest gratitude to Oliver Anderka for helping me in understating the different approach for supercomplex in early days of my work and his discussion and suggestion.*

*I appreciate Werner Müller for their excellent technical support and his warm smiling when I came to his lab for asking for technical support.*

*I am thankful to my project collaborators Radhan and Bejoren, for their irreplaceable methods to always help and guide me in my work.*

*I would like to thank the entire Max Planck research school members for providing excellent teaching and practical courses.*

*There are many others that have encouraged me and supported my work. I would like to thank them all. I thank Ravi, my dear old friend, for being there for me in my happy and sad moments. Thanks to Jitendra, for his deep and sincere friendship, modest support, and motivation. I thank Syeed and Annis for their honesty and for their ways to share science and for their sense of humor.*

*A special gratitude goes to Gwen, Mark, Arnab, Sanjeev for being an extremely diverse crowd of people and at the same time being helpful and exciting friends.*

*I would grateful my wonderful parents for their love and support, for being there in my life, and their trust in me. Thanks to my dearest sisters who are my strength and my hope who prayed for my success. I would like to thank Fauziya for her love, encouragement, motivation, support and for her valuable prayers; I would have been nowhere without her.*

*In the end, I acknowledge International Max Planck research school 'structure and function of biological membrane' and SFB 472 for the finance support.*

## Curriculum vitae

Mohd Khalid Siddiqui  
 Am Hang 8,  
 Frankfurt am Main – D 60437,  
 Germany  
 Date of Birth: 07<sup>th</sup> June 1977

### Education

- (Feb 2002-till date)**      **PhD** student of International Max Plank Research School ‘Structure and Function of Biological Membranes’ Frankfurt under the supervision of Professor Dr. Bernd Ludwig, Molecular Genetics Institute of Biochemistry Goethe University Frankfurt.
- (Feb 2001-Feb 2002)**      Research Fellow in Plant Molecular Virology at National Botanical Research Institute (**NBRI**) Lucknow, Uttar Pradesh, India
- (July 1998-Aug 2000)**      **Master of Science in Biotechnology**, H.P.University, Shimla, India

### Research Experience

- |                    |   |
|--------------------|---|
| <b>Topic</b>       | Studies of gemini viruses occurring in weeds  |
| <b>Institution</b> | National Botanical Research Institute (CSIR ) Lucknow India   |
| <b>Period</b>      | One year (2001-2002)  |
|                    |   |
| <b>Topic</b>       | Immobilization of bacterial lipase in different polymeric matrices and its applications                             |
| <b>Institution</b> | Department of Biotechnology, H.P. University, Shimla, India   |
| <b>Period</b>      | One year [June 1999 to August 2000 ]  |
|                    |   |
| <b>Topic</b>       | Development of diagnostic kits for HIV 1&2, synthesis of Hepatitis vaccine and purification of recombinant protein. |
| <b>Institution</b> | Biotechnology Division, Cadila Pharmaceuticals Ltd, Ahmedabad India   |
| <b>Period</b>      | 2 months [Jan 2000 to Feb 2000]   |

## Publications

### **Binding of cytochrome *c* to cytochrome *c* oxidase characterized by multi-frequency Pulse EPR spectroscopy**

S. Lyubenova, **M.K. Siddiqui**, M.J.M. Penning de Vries, B. Ludwig, T.F. Prisner  
Manuscript submitted (2006)

### **Immobilization of lipase on hydrogels: Structural aspects of polymeric matrices as determinants of enzyme activity in different physical environments**

Ghanshyam S. Chauhan, Swati Mahajan, **Khalid M. Siddiqui**, Reena Gupta  
Journal of Applied Polymer Science, Vol. 92, 3135–3143 (2004)

### **The natural occurrence of a begomovirus in sunn hemp (*Crotalaria juncea*) in India**

J. A. Khan, **M.K. Siddiqui** & B. P. Singh  
Plant Pathology, June 2002 Volume 51, No.3, Page 398

## Selected conferences and Symposiums

### **Interaction of cytochrome *c* with oxidase: Distance and orientation studies on soluble fragments by multi-frequency EPR Spectroscopy**

**M. Khalid Siddiqui**, S. Lyubenova, M.J.M. Penning de Vries, T.F. Prisner, B. Ludwig  
Keystone Symposia on Frontier in Structural biology 2006, 29 January to 3 February 2006 in Keystone Colorado USA (**Keystone Scholarship**)

### **Association of Bacterial Respiratory Complexes**

**M. Khalid Siddiqui**, M.J.M. Penning de Vries, S. Lyubenova, T.F. Prisner, and B. Ludwig  
Drug Discovery Technology Europe, 15<sup>th</sup> -16<sup>th</sup> March 2005 in London UK (**Best oral presentation**)

### **Mass spectrometric analyses of integral membrane proteins, solubilized with detergents or reconstituted into artificial phospholipids vesicles**

**B. Meyer, K. Siddiqui**, M. Aivaliotis, B. Ludwig and M. Karas  
53<sup>rd</sup> ASMS Conference (2005), June 5<sup>th</sup>-9<sup>th</sup> in San Antonio, Texas USA

### **Distance and Orientation Studies of the Cu<sub>A</sub> Fragment of Cytochrome *c* Oxidase with different cytochrome *c* by Pulsed EPR Spectroscopy**

**M. Khalid Siddiqui**, S. Lyubenova, M.J.M. Penning de Vries, T.F. Prisner, and B. Ludwig  
13<sup>th</sup> European Bioenergetics Conference (EBEC 2004) August 21<sup>st</sup> - 26<sup>th</sup> in Pisa Italy and abstract is published in BBA bioenergetics Special edition (2004) pp 157

## Workshop

"**Scientific Presentation Skills**" Saarbrücken (IMPRS) and Max-Planck-Society organize a two-day workshop on the improvement of scientific presentation techniques November 12<sup>th</sup> - 13<sup>th</sup> 2004

*Training Courses* **Introduction to FT-EPR: Instrumentation, spectra and to use the FT software** at EPR/Micro Spin Division Bruker BioSpin GmbH. Rheinstetten Germany March 13<sup>th</sup> -17<sup>th</sup> 2003

**Academic Achievements**

- 2006** Director's scholarship for Keystone symposia on 'Frontier in Structural Biology' 2006
- 2005** Scholarship for 'Drug Discovery Technology 2005' London and prize for best oral presentation
- 2002-2006** Max Planck fellowship for International PhD program on 'Structure and function of biological membrane' at (**IMPreS**) Frankfurt am Main
- 2001** Qualified Graduate Aptitude Test In Engineering (**GATE**) life sciences conducted by Indian Institute of Technology (**IIT**) and Indian Institute of Science (**IISc**)
- 2000** National Eligibility Test (**NET**), for the post of a lecturer/assistant professor in university conducted by Council of Scientific & Industrial Research (**CSIR**) government of India and University Grant Commission (**UGC**)
- 1998-2000** Scholarship awarded during the studies of Masters in Biotechnology from Govt. of India
- 1995** Member of Academic Honours Society, Lucknow Christian Degree College, Uttar Pradesh, India.